

ELECTROANALYTICAL ESTIMATION OF HERBICIDES

by

Ana Maria Coelho Ferreira de Oliveira

A thesis submitted

for the

DEGREE OF DOCTOR OF PHILOSOPHY

of the

UNIVERSITY OF LONDON

June, 1980

Department of Chemistry,
Imperial College of Science and Technology,
London SW7.

ABSTRACT

This thesis describes the development of an electroanalytical technique that combines chromatographic separation with electrochemical detection. Eleven urea and carbamate herbicides were identified and analysed quantitatively. Using electrochemical detection it has been possible to reach the detection limit of 30-50 nanograms. This limit could be attained by flow injection analysis or after chromatographic separation. The flow detector was a wall-jet electrode cell where a jet of solution impinges on the electrode surface and the flow pattern can be calculated.

Chromatographic separation was achieved using high pressure liquid chromatography. No prior chemical treatment of the herbicides was necessary and the chromatographic separation and electrochemical detection could be accomplished in 20 minutes. The hydrodynamics of a very small volume flow cell show that only 2% reacts at the electrode so the method is only slightly destructive.

The oxidation mechanism of ureas is complicated: the electrode reaction of chloroxuron has been studied in more detail and a mechanism is proposed. The mechanism follows different routes according to the pH of the medium and several products are formed.

To my Parents and to Chris.

*"We don't know everything
about anything"*

B. Pascal.

ACKNOWLEDGEMENTS

I should like to thank all my friends and my research colleagues at Imperial College who, throughout these three years, have given me their encouragement, help and advice.

I thank Professor W.J. Albery for the opportunity of working in his research group and also for his helpful assistance and supervision, and Dr. B. Fleet for supervision at the beginning of the project

I also thank Fundação Calouste Gulbenkian and Departamento de Química, Universidade de Coimbra for financial support during this project.

Finally, I should like to thank Maria de Carmen Serrano-Widdowson and Moira Shanahan for typing the manuscript.

CONTENTS

<u>CHAPTER I</u>	<u>INTRODUCTION</u>	1
1.	ANODIC OXIDATION	1
1.1.	Electroorganic reactions	2
1.2.	Oxidation of functional groups	2
1.3.	Anodic oxidation at carbon electrodes	8
2.	ELECTRODE AND MECHANISMS OF ELECTRODE REACTIONS	16
2.1.	Working electrode	16
2.2.	The glassy carbon electrode	18
2.2.1.	Material	18
2.2.2.	Effect of double layer	19
2.2.3.	Supporting electrolyte	21
2.2.4.	Reproducibility	25
2.3.	Mechanism of electrode reactions	28
2.3.1.	Electron transfer	28
2.3.2.	Proton transfer	28
2.3.3.	pH dependence	30
3.	ELECTROCHEMISTRY IN FLOW SYSTEMS	32
3.1.	Continuous flow analysis	33
3.2.	Flow injection analysis	34
3.3.	Flow analysis detectors	37
3.4.	Applications of a flow cell as a detector for HPLC	43
4.	CONCLUSIONS	52

<u>CHAPTER II</u>	<u>THEORY</u>	53
1.	INTRODUCTION	53
2.	HPLC SEPARATION	53
2.1	Introduction	53
2.2	Definitions	54
2.3	Theory of HPLC: Thermodynamics	56
2.4	Theory of HPLC: Kinetics	59
2.5	Resolution	60
3.	THEORY OF WALL-JET	62
3.1	Introduction	62
3.2	The wall-jet cell: laminar flow	62
4.	MODES OF OPERATION	68
4.1	Introduction	68
4.2	Differential pulse voltammetry	68
<u>CHAPTER III</u>	<u>EXPERIMENTAL TECHNIQUES</u>	75
1.	INTRODUCTION	75
2.	HIGH PRESSURE LIQUID CHROMATOGRAPHY	75
2.1	Packing materials	75
2.2	Columns	76
2.3	Injection	77
2.4	Pumps	78
3.	ELECTROCHEMISTRY	78
3.1	Instrumentation	78
3.2	Cells	79

4. PROCEDURES	81
4.1 Solution conditions	81
4.2 Experimental conditions	81
4.3 Experimental set-up	88
<u>CHAPTER IV</u> <u>OXIDATION MECHANISM</u>	89
1. INTRODUCTION	89
2. pH MEASUREMENTS	90
3. SCHEME OF SQUARES	96
4. CONCLUSIONS	103
<u>CHAPTER V</u> <u>FLOW SYSTEMS</u>	104
1. INTRODUCTION	104
2. ELECTROANALYTICAL DETECTION WITHOUT PREVIOUS SEPARATION	104
2.1 Continuous flow analysis	104
2.2 Flow injection analysis	107
3. ELECTROANALYTICAL DETECTION AFTER CHROMATOGRAPHIC SEPARATION	112
4. CONCLUSIONS	134
<u>APPENDIX</u>	136
<u>REFERENCES</u>	138

LIST OF TABLES

Table I.1	Oxidation of aromatic compounds	3
I.2	Anodic oxidation mechanisms	4
I.3	Oxidation of organic functional groups	7
I.4	Oxidation at carbon electrodes	9
I.5	Non-aqueous solvents	22
I.6	Response of the GCE and Glass Electrode in pH changes	25
I.7	Electrochemical detectors	41
I.8	Anodic detection at carbon electrodes after chromatographic separation	44
Table III.1	Structures of the herbicides	82
III.2	Supporting electrolytes	85
Table V.1	Results for the electrochemical estimation of the herbicides	132

LIST OF FIGURES

Fig. I.1	Glassy carbon lattice scheme	18
I.2	Electrical double layer	20
I.3	Potential range Pt, GC, Hg	23
I.4	Usable potential range for GCE in various mineral acids	24
I.5	Controller waveform	26
I.6	Cleaning cycle	27
I.7	Oxidation in aprotic solvents	29
I.8	Flow Analysis	33
I.9	Flow Injection Analysis	36
I.10	Electrochemical detectors for HPLC	38
I.11	Hydrodynamic flow pattern	43
Fig. II.1	Parameters for defining retention and peak width	54
II.2	Separation of sulphadiazine (84)	55
II.3	Improvement in resolution A, by increasing peak separation, and B, by reducing peak width. The first peak in each case represents an unretained solute	55
II.4	Diagrammatic illustration of the structure of a packed chromatographic column	56
II.5	Concentration profiles in the mobile and stationary phase with arrested solution	57

Fig. II.6	Concentration profiles during elution chromatography in the mobile and stationary phases	59
II.7	Schematic representation of the velocity and concentration distribution in the laminar wall-jet	63
II.8	Functions of η	66
II.9	Scheme of streamlines	67
II.10	Summary of signal input waveforms and current potential response for a range of voltammetric techniques	69
II.11	Excitation waveform and current behaviour for differential pulse voltammetry	70
Fig. III.1	HPLC column	76
III.2	Injection valve	77
III.3	Cells: A - Stationary cell B - Wall-jet cell	80
III.4	Flow Analysis Experimental Assembly	86
III.5	HPLC Detection Experimental Assembly	87
Fig. IV.1	Inhibition sites and artificial electron donor and acceptor systems in photosynthetic electron flow from water to NADP	89
IV.2	D.P. Voltammogram of chloroxuron	91
IV.3	Successive voltammograms of chloroxuron	92
IV.4	Oxidation of chloroxuron at different pH	93

Fig. IV.5	(a) Variation of half-width, $W_{\frac{1}{2}}$ with pH	
	(b) Variation of peak potential, E_p , with pH	95
IV.6	Plot of $\log k'$ against pH	96
IV.7	Variations in the oxidation of chloroxuron with pH	101
IV.8	Plot of $\log i$ versus pH	102
IV.9	Plot of $\log i$ versus observed E_p	102
Fig. V.1	D.P. voltammogram of fluometuron	105
V.2	Continuous flow voltammogram of diuron	106
V.3	Injection calibration for fluometuron	108
V.4	Injection calibration for diuron	109
V.5	Flow injection analysis calibration plots	110
V.6	Log-log plot for injection of fluometuron	111
V.7	Chromo-amperogram of the mixture of urea and carbamate herbicides	113
V.8	Chromo-amperograms of the carbamate herbicides	115
V.9	Calibration curves of propham and chlor- propham	116
V.10	Chromo-amperograms of urea herbicides group I	117
V.11	Calibration curve of metabromuron	118
V.12	Calibration curve of monolinuron	119
V.13	Calibration curve of linuron	120
V.14	Calibration curve of chlorbromuron	121
V.15	Calibration curve of the mixture of group I	122

Fig. V.16	Chromo-amperograms of urea herbicides group II	123
V.17	Chromo-amperograms of four urea herbicides group II	124
V.18	Calibration curve of fenuron	125
V.19	Calibration curve of fluometuron	126
V.20	Calibration curve of diuron	127
V.21	Calibration curve of chloroxuron	128
V.22	Calibration curve of chlortoluron	129
V.23	Calibration curve of the mixture of group II	130
V.24	Detection limit chromo-amperogram of fenuron	131

CHAPTER I

INTRODUCTION

This thesis is concerned with the use of an electrochemical detector to analyse some urea-type herbicides. The use of these chemicals in crop protection has had disastrous consequences in the biological equilibrium. The urea herbicides are some of the most widely used for the control of weeds and, as for a large number of herbicides, they act as inhibitors of the photosynthetic electron flow by competitive binding. Under the action of these compounds not only pathogens and pests were killed but many other living organisms like birds, fish and other plant species. These side effects are well recognised and it is necessary to control and identify the herbicides quantitatively. Using electrochemical detection it has been possible to analyse quantitatively nanograms of a group of these compounds either in flow analysis or after chromatographic separation. The oxidation of these compounds has been studied and a mechanism is also suggested.

1. ANODIC OXIDATION

As it is possible to oxidise the herbicides studied here and

this was the detection method used, we will now survey the possible electroorganic reactions involving reactive functional groups to give an idea of past work and of present and future prospects. The classification of the electroorganic reactions can be based on the electrode mechanism or on the products formed.

1.1 Electroorganic Reactions

The analysis of the different pathways followed by anodic oxidation of systems containing organic compounds will depend on the supporting electrolyte, on the electrode material and on the potential of the electrode. An example is the oxidation of benzene and toluene (1) in Friedel-Crafts electrophilic substitution (see Table I.1).

When all the variables have been determined there are great advantages in using electrochemical oxidation in synthesis and organic oxidations. An examination of the different types of organic reactions will show what kinds of transformations are possible.

Anodic oxidation reactions are in many cases through a reaction between an organic compound and a nucleophile, as seen in Table I.2. The dimerisation mechanism is not yet clear but in one way or another it is the pathway of oxidation of some aromatics, aromatic amines, phenols and electron-rich olefins and, most important for this work, aromatic urea and carbamate compounds.

1.2 Oxidation of functional groups

Having had a look at the different mechanisms of electrochemical

Table I.1 - Oxidation of Aromatic Compounds


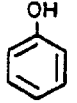
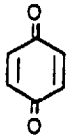
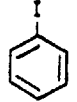
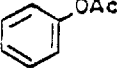
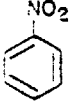
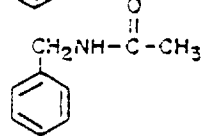
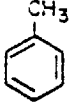
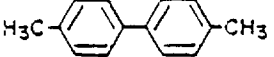
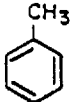
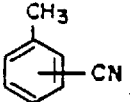
Aromatic Compound	Reaction Conditions		Products
	Electrode	Solution	
	PbO ₂	Aq. H ₂ SO ₄	 → 
	Pt	I ₂ , LiClO ₄ , CH ₃ CN	
	Pt	KOAc, HOAc	
	Graphite	Aq. NaNO ₃	 
	Pt	CH ₃ CN	
	Pt	HCN, NaCN, CH ₃ OH	

Table I.2 - Anodic Oxidation Mechanisms

Type of reaction	Mechanism
<u>Anodic substitution</u>	$Nu^- \longrightarrow Nu^\cdot + e$
	$R-H + Nu^\cdot \longrightarrow R^\cdot + NuH$
	$R^\cdot + Nu^\cdot \longrightarrow R - Nu$
- Acetoxylation	$R-H + CH_3CO^- \xrightarrow{-2e^-} R - COCH_3 + H^+$
- Acetamidation	$R-H + CH_3-C \equiv N \xrightarrow{-2e^-} R - NH - \overset{\overset{O}{ }}{C} - CH_3 + H^+$
- Cyanation	$R-H + CN^- \xrightarrow{-2e^-} R - CN + H^+$
- Alkoxylation	$R-H + CH_3OH \xrightarrow{-e^-} R-OCH_3 + H^+$
- Halogenation	$R-H + X_2 \xrightarrow{-2e^-} R - X + X^\cdot + H^+$
- Kolbe Reaction	$RCO_2^- \xrightarrow{-e^-} R^\cdot + CO_2$ $\begin{matrix} / & \backslash \\ R-R & R^\cdot \end{matrix}$
<u>Anodic addition</u>	$2 Nu^- + \text{>C=C<} \xrightarrow{-e^-} Nu - \text{>C=C<} - Nu$
<u>Anodic elimination</u>	$\begin{matrix} & \\ -C & -Y \\ & \\ X & X \end{matrix} \longrightarrow \text{>C} = Y + 2X^\cdot$
<u>Anodic disproportionation</u>	$R \xrightarrow{-e^-} R^\cdot$
	$2R^\cdot \longrightarrow R + R^\cdot$
<u>Anodic cleavage</u>	
- to a radical cation	$RHX \xrightarrow{-e^-} RHX^\cdot \longrightarrow R^\cdot + X^\cdot$
- to a radical	$R-C-O^- \longrightarrow R-C-O^\cdot \longrightarrow R^\cdot + \text{>C=O}$

Table/continued...

Table I.2/continued...

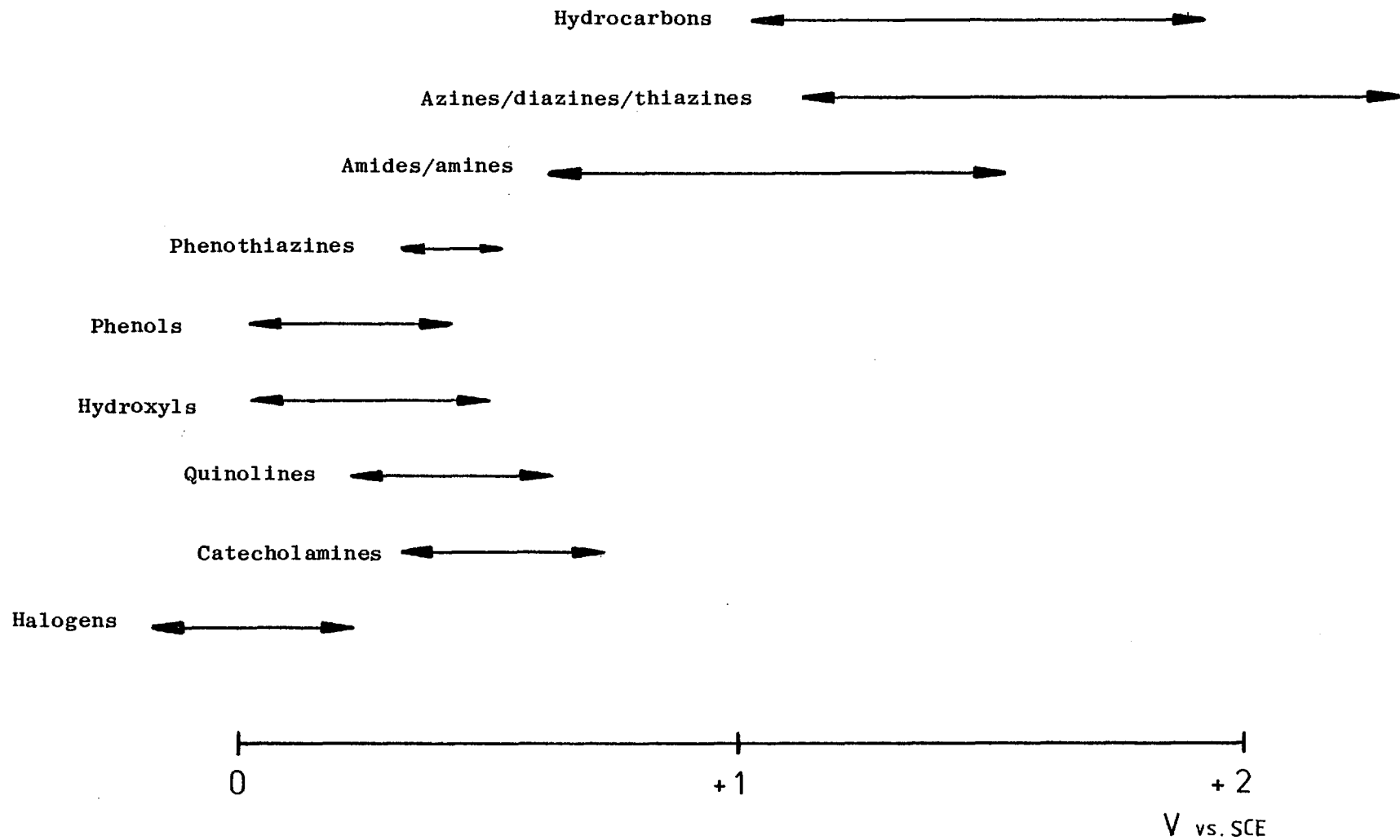
Type of reaction	Mechanism
<u>Anodic dimerization</u>	
— through a radical (like Kolbe reaction)	$2R^- \xrightarrow{-2e^-} 2R^\cdot \longrightarrow R-R$
— through a radical cation	$2RH \xrightarrow{-2e^-} 2RH^{\cdot+} \longrightarrow {}^+HR-RH^+$
	$ \begin{array}{l} \begin{array}{c} \text{R-R} \\ \nearrow \\ {}^+HR-RH^+ \\ \searrow \\ \text{NuHR-RHNu} \end{array} \\ \begin{array}{l} -H^+ \\ +Nu^- \end{array} \end{array} $
<u>Anodic polymerization</u>	
initiation	$R^- \longrightarrow R^\cdot + e$
propagation	$R_n^\cdot + R \longrightarrow R_{n+1}^\cdot$
	$R_{n+1}^\cdot + R' \longrightarrow P$

oxidations of organic species it is important to see, in Table I.3, how the different organic functional groups react.

Unsaturated hydrocarbons either with benzene rings or isolated olefinic double bonds are oxidizable. Carbonyl compounds will follow an addition mechanism similar to that observed in chemical reactions. Under some conditions the carbon-halogen single bond will be electroactive. The electrooxidation of phenols and aromatic amines is very similar. They follow anodic substitution reactions and can also dimerise.

Most of the aliphatic amines cannot be oxidized in hydroxylic solvents because they require high potentials and the solvent will react. The mechanism of oxidation causes the scission of the carbon-nitrogen bond. With the aromatic amines a lot of work has been done with aniline and aniline derivatives because they are easily oxidized in aqueous solutions. The mechanism is almost always through a cation radical. Dimeric products may be formed and a new N-N bond, C-N bond, or C-C bond will appear (2). Two factors make the course of anodic oxidation of aliphatic amines different from that observed with the aromatic amines. First, the aliphatic amines are much stronger bases, and proton transfers are, therefore, facilitated. Second, the primary electrode reaction usually involves transfer of an electron from the lone pair on nitrogen to the anode to form a cation radical as in aromatic amines. The aliphatic amines are much more reactive, as the opportunities for stabilization by electron delocalization are extremely limited. The availability of the π -system in the aromatic amines stabilizing the intermediates makes possible a multiplicity of reaction paths, and the observed final products are both more diverse and more complex.

Table I.3 - Oxidation of Organic Functional Groups (50).



Potential range in which the class of compounds may be oxidised.

Anodic oxidation of amides requires more positive potentials than amines. And although the oxidation of secondary amides requires higher potentials than tertiary amides, it is possible to obtain analogous oxidation products in nucleophilic solvents.

Amino alcohols undergo oxidation at the alcohol function during electrolysis in acid solution to give good yields of the amino acid, while in basic solution the amine function is oxidized. In studies of electrolytic oxidation of amino acids it was noted that some aldehyde along with further oxidation products was formed (3).

Nitroso : compounds follow a cation radical mechanism and always have very high oxidation potentials. Oxidation of organosulphur compounds cleaves the carbon-sulphur bond through the formation of stable cation radicals. The electrochemical oxidation of organometallic compounds involves both the metal atoms and the organic part of the molecule (4).

1.3 Anodic oxidation at carbon electrodes

Although the electrochemistry of organic compounds has been dominated by mercury and platinum electrodes, there is an increasingly large amount of work being done with carbon electrodes and in particular electrodes made of glassy carbon. Only very recently methods based on electrochemical oxidation were used in the investigation of biologically important compounds such as nucleic acids and catecholamines. The parameters of oxidation of some organic compounds on different types of carbon electrodes are summarised in Table I.4.

Table I.4 - Oxidation at carbon electrodes

Compounds	Electrode	pH	$E_{\frac{1}{2}}/V(SCE)$	Products	Techniques	†	Ref.
2-aminopyridine	WIGE	0.1M H ₂ SO ₄	+1.410	-	Differential voltammetry	a	5
3-aminopyridine		0.1M H ₂ SO ₄	+1.235	-			
4-aminopyridine		7	+1.505	-			
7-hydroxychlorpromazine	GPE	2	+0.6	7,8-dioxochlorpromazine	cyclic voltammetry controlled potential coulometry chronoamperometry	b	6
p-tolyl methyl sulphide	HOGP	2% aqueous acetonitrile	+1.1 V/(Ag/AgNO ₃ , 0.1 N)		-	-	7

Table I.4/continued...

Compound	Electrode	pH	$E_{1/2}/V$ (SCE)	Products	Techniques	†	Ref.
9,10-anthraquinone	CPE	2	+0.078-0.083 V/NHE	-	cyclic voltammetry	-	8
chloranil	CPE	2	+0.631-0.641 V/NHE	-	cyclic voltammetry	-	8
2-methyl-1,4-naphtho- quinol-1-phosphate	CPE	1 1-12	+0.6	2-methyl-1,4-naphthoqui- none	cyclic voltammetry, single sweep voltammetry	<i>c</i>	9
Phenylbutazone (R=H) oxyphenbutazone (R=OH)	GCE	-	+0.37 +0.56	-	linear sweep voltammetry, differential pulse volt., cyclic voltammetry	<i>d</i>	10

Table I.4 /continued...

Compound	Electrode	pH	$E_{\frac{1}{2}}/V(SCE)$	Products	Techniques	†	Ref.
ciramadol	GCE	~ 5	+0.87	-	linear sweep voltammetry	e	11
meptazinol			+0.84	-			
dezocine			+0.69	-			
pentazocine			+0.78				
<u>Catecholamines</u> adrenaline	GCE	1M H ₂ SO ₄	+0.55	-	differential pulse voltam.	f	12
adrenaline	CPE	1.0M H ₂ SO ₄	+0.7		cyclic voltammetry chronoamperometry	-	13
		3.0	+0.6				
noradrenaline	CPE	1M H ₂ SO ₄	+0.577		differential double pulse voltammetry (DDPV)	g	14

Table I.4/continued...

Compound	Electrode	pH	$E_{\frac{1}{2}}/V(SCE)$	Products	Techniques	†	Ref.
<u>Nucleic acids</u>							
Polyriboadenylic acid	PGE GCE WISGE	5	+1.2	-	differential pulse voltam.	h	15
adenine	GCE	7.2	+1.2	-	differential pulse voltam.	-	16
		2 - 12	+1.45-0.064 pH	-	linear sweep voltammetry	i	17
		2 - 12	+1.41-0.065 pH	-	linear sweep voltammetry	-	18
guanine	GCE	7.2	+0.9	-	differential pulse voltam.	-	16
		2 - 12	+1.13-0.059 pH	-	linear sweep voltammetry	i	17
		2 - 12	+1.06-0.06 pH	-	linear sweep voltammetry	-	18

Table I.4 /continued.....

Compound	Electrode	pH	$E_{\frac{1}{2}}$ /V (SCE)	Products	Techniques	†	Ref.
adenosine	GCE	2 - 12	+1.49-0.032 pH	-	linear sweep voltammetry	<i>i</i>	17
guanosine	GCE	2 - 12	+1.25-0.046 pH	-	linear sweep voltammetry	<i>i</i>	17
NADH	GCE	7	+0.3	-	single and multiple sweep voltammetry pulse: normal, differential	<i>j</i>	19

Table I.4/continued...

Compound	Electrode	pH	$E_{1/2}$ /V (SCE)	Products	Techniques	†	Ref.
6-aminopurine (adenine)	GCE	0 - 12	1.45-0.064 pH	-	linear sweep voltammetry, coulometry, cyclic voltam.	k	20
6-amino-8-hydroxypurine			1.01-0.067 pH				
6-amino-2-hydroxypurine			1.03-0.057 pH				
6-amino-2,8-dihydroxypurine			0.77-0.072 pH				
2-aminopurine			1.34-0.087 pH				
2-amino-6-hydroxypurine (guanine)			1.13-0.059 pH				
2-amino-8-hydroxypurine			1.11-0.068 pH				
2-amino-6,8-dihydroxypurine			0.79-0.077 pH				
2,6-diaminopurine			1.03-0.054 pH				
2,6-diamino-8-hydroxypurine			0.76-0.074 pH				

/continued...

WIGE = wax-impregnated graphite electrode
 GPE = graphite paste electrode
 HOGE = highly ordered graphite electrode
 CPE = carbon paste electrode
 GCE = glassy carbon electrode
 PGE = pyrolytic graphite electrode

Table I.4/continued...

† *Comments:*

a The graphite electrodes were "special spectroscopic" coated under vacuum with a paraffin film in order to obtain a constant surface. The differential voltammetry technique measures the difference between the current flowing across two cells, with identical geometry, dimensions and working electrodes.

b This oxidation process is associated with several side effects in chlorpromazine therapy.

c The quinol phosphates possess the potential of being phosphorylating agents and have been suggested as being agents for oxidative phosphorylation in biological systems.

d The plot of E_p (peak potentials) vs. $\log V$ (where V is the scan rate) shows the typical exponential increase whereas the plot of peak current (i_p) function $i_p V^{1/2}$ vs. $\log V$ shows a linear relationship which means that the voltammetric oxidation process is essentially diffusion-controlled and is a first-order reaction.

e Determined in their pharmaceutical forms.

f The catecholamines are very important in neurotransmission. Their level in the plasma reflects the activity of the sympathoadrenal system (the sympathetic nervous system is the self-acting, automatic nervous system). A large amount of work has been done with these compounds both in experimental and clinical practice and using HPLC with different electrochemical detectors (see section 3.4).

g They found that the silicone oil carbon paste electrode had somewhat faster electrode kinetics than the nujol paste electrode.

h Absorbs very strongly on GCE.

i The nucleotides, adenosine and guanosine, were oxidised at more positive potentials than their bases, adenine and guanine, and are strongly absorbed on the surface of glassy carbon.

j DNA oxidation takes place in two steps: the first attributed to guanine and the second to adenine.

k The mechanism proposed is similar to enzymatic oxidation.

2. ELECTRODE AND MECHANISMS OF ELECTRODE REACTIONS

In this section we are going to discuss possible working electrodes for oxidation reactions. The glassy carbon electrode will be characterised in more detail. The mechanisms of electrode reaction according to reaction conditions will be analysed.

2.1 Working electrode

The nature of the working electrode will influence the mechanism of electrode reaction and it has to be chosen for the purpose required. The mercury electrodes are the dropping mercury electrode (DME), and the hanging mercury drop electrode (HMDE). They have been used in classical polarography and the DME has the advantage of a new surface on each drop giving very good reproducibility. However, they have a very small oxidation range limited at +0.4 V by the oxidation of mercury itself.

Solid electrodes can be used at high oxidation potentials but have a common disadvantage due to the problems associated with cleaning the electrode surface. It brings very serious problems of reproducibility. Some solid electrodes have been made for specific requirements, such as nickel, iron, manganese and silver electrodes in alkaline solutions.

Platinum and gold are inert to most chemicals with a very good anodic range depending on the supporting electrolyte. They are not as "inert" as one might think. For instance, they form a platinum oxide and a gold oxide film at high anodic potentials. Platinum electrodes

have been used in different forms:

- platinum wire electrode,
- platinum foil electrode,
- platinum rotating disc and rotating ring-disc electrodes,
- platinum tubular electrodes.

Although lead in itself does not make a good anode because it oxidizes too easily, lead dioxide is very stable under anodic conditions. However, it is itself a powerful oxidant which makes it difficult to determine its role in electrolytic oxidation.

Besides all of these, there are all the different kinds of carbon and graphite electrodes. They are very stable and have a very good anodic range. The graphite electrode has been used in the form of wax or polystyrene (21) impregnated graphite electrodes and in some cases pencil leads have been used. Carbon electrodes have been used mainly in three forms:

- carbon paste electrode (CPE) usually made by mixing graphite powder with mineral oil, packing the mixture in the body and smoothing the surface;
- glassy (vitreous) carbon electrode (GCE), appears in rods that can be cut and forms a very shiny surface after polishing;
- carbon fibre electrode, is a new material with a very high surface area.

The electrode chosen for this work was the glassy carbon because it has many advantages for the study of anodic oxidation and in flow detector cells. The properties of glassy carbon are going to be analysed in detail in the next section.

2.2 The glassy carbon electrode

2.2.1 Material

In general, carbons are porous and gas impermeable materials. Nowadays, Tokay Electrodes (22) use a new method to prepare a gas-impermeable, non-impregnated type of carbon. This glassy carbon is amorphous: the atoms are not arranged in the regular shape of a crystal, but small hexagonal planes form crystallites and are packed without orientation between the planes (23) as shown below.

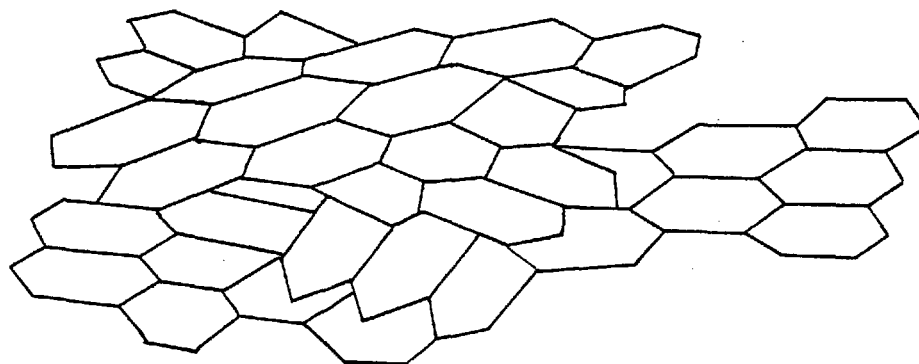


Fig. I.1 - Glassy carbon lattice scheme

Since carbon electrodes are primarily composed of graphite microcrystallites, and since graphite has two kinds of crystal faces, edge and basal, Miller et al. (7) were interested to know if modification and, therefore, asymmetric synthesis was taking place on one or both of these surfaces. This was tested using a highly ordered pyrolytic graphite electrode (HOPG); it has a structure very similar to a single crystal of graphite.

Each piece has well-defined edge surfaces and basal surfaces and

these can be used independently. A perfect basal surface is simply one layer of carbon atoms in the graphitic array. The edge surface is composed of the layer ends and is generally covered with surface oxides. Thus, it is expected that the chiral modifier will be attached at the edge surface via the surface oxides. On one piece the edge surface was covered with silicone rubber and on the second piece the basal surface was covered so that electrochemistry could only occur on one at a time. The oxidation results seem transferable to ordinary carbon and indicate that the activity of modified carbon electrodes results, at least in part, from electrochemistry on the edge surfaces of microcrystallites of graphite and not from modified basal surfaces. Glassy carbon has low porosity, high resistance to chemical attack, is electrically conductive and obtainable in a very pure state (22, 25). The hardness and brittleness of glassy carbon requires that it be shaped by grinding. This produces fresh contamination from the cutting tool that can be removed by polishing.

2.2.2 Effect of double layer

The different adsorption of positive and negative ions causes a charge on the surface of solid particles in solution. The charge on the surface influences the distribution of the neighbouring ions. In a polar medium the ions of opposite charge are attracted to the surface and those of the same charge are repelled. This disposition of the ions leads to the formation of an electrical double layer constituted by a charged surface and an excess of opposite ions over the co-ions in the adjacent solution that neutralize it.

As the electron transfer takes place on the surface of the solid electrode, the understanding of the electrical double layer processes

is very important. Many attempts have been made to explain this quantitatively and the most accepted divides it into an inner double layer of molecules bound so tightly to the surface that they are unaffected by agitation of the bulk of the solutions, and an outer double layer of solvated ions.

The direct electron transfer occurs across the inner double layer and that is where the potential determining species are.

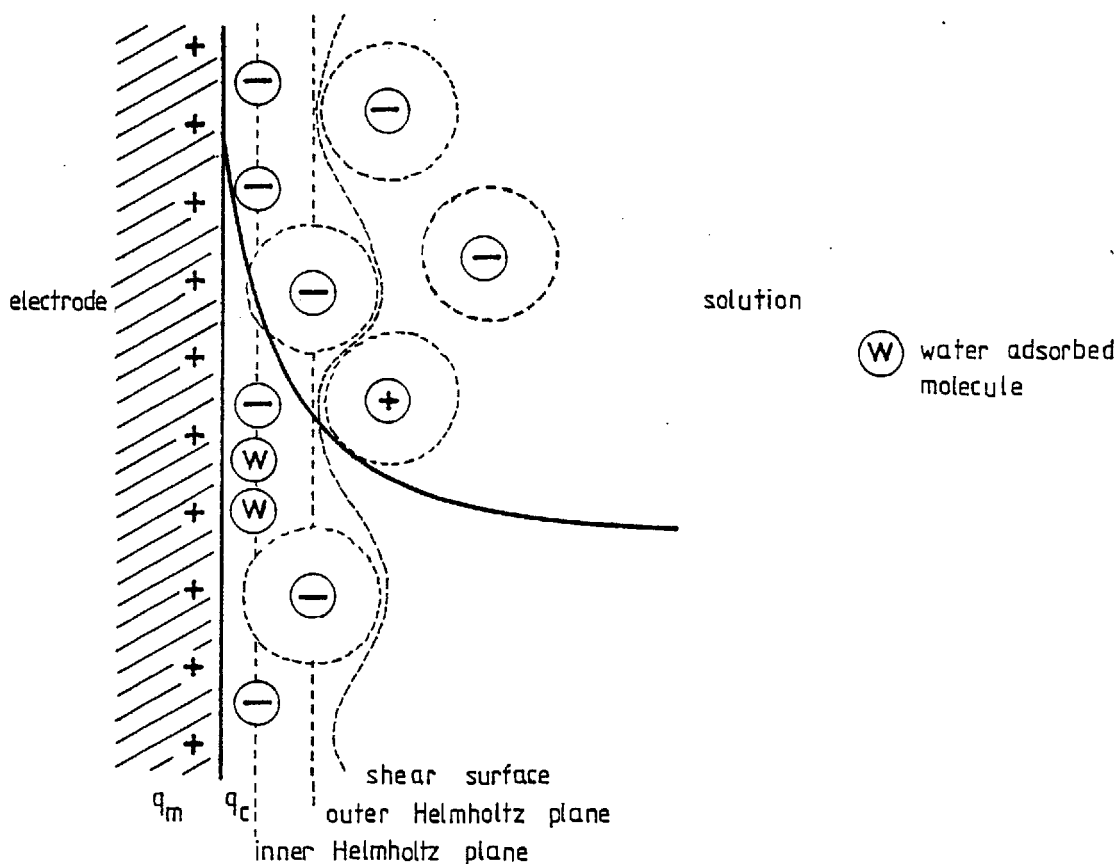


Fig. I.2 - Electrical double layer

Korobanov et al. (26) obtained the potentials of zero charge for the carbon and carbon-black electrode as function of solution pH and they found it is shifting in the cathodic direction with increasing pH.

The capacitance of the double layer at the glassy carbon electrode was studied (27). It was about $200 \mu\text{F cm}^{-2}$ in $1\text{M H}_2\text{SO}_4$ and at a scan

rate of 1 V min^{-1} .

The order of magnitude of the double-layer capacity (28) at Pt is about $20\text{--}40 \mu\text{F/cm}^2$, and the charging current ordinarily is relatively unimportant except at high voltage sweep rates.

2.2.3 Supporting electrolyte

The solutions to be studied electrochemically are composed of the solvent, the supporting electrolyte and the electroactive substance.

For a long time water was the only solvent used, but aprotic organic solvents have been gaining importance recently. The reason is that a number of compounds, which are electrochemically inert in water, can react in other solvents. Nonaqueous polar solvents with high dielectric constant will have the required conductivity. Propylene carbonate, alcohols, dimethylsulfoxide, dimethylformamide, and acetonitrile are all in widespread use. In Table I.5 are listed their potential ranges (1), dielectric constants (29), and viscosities (30). The glassy carbon electrode can be used without major problems either in aqueous or nonaqueous systems, and it is inert to strong acids and oxidizing agents.

The supporting electrolyte is always in excess, reduces the ohmic drop $i.R$ and prevents mass transfer by migration of the electroactive substance.

In Fig. I.3 we compare the potential range of some electrode materials (Hg, GC, Pt). The glassy carbon electrode has a good anodic and a reasonable cathodic range that can be extended by

Table I.5. Non-aqueous Solvents

Solvent	Dielectric Constant (ϵ)	Viscosity (η)	Potential range (vs. SCE)		Electrolytes
			cathodic	anodic	
Acetonitrile (CH_3CN)	37.45	0.33	-3.5 V	+2.4V	tetraalkylammonium halides, perchlorates, and tetrafluoroborates, sodium perchlorate, lithium halides.
Dimethylformamide [DMF, $\text{HCON}(\text{CH}_3)_2$]	36.7	0.80	-3.0V	+1.6V	tetraalkylammonium halides, perchlorates, and fluoroborates, sodium perchlorate, lithium chloride.
Pyridine ($\text{C}_5\text{H}_5\text{N}$)	13.2	0.88	-2.3V	+1.4V (vs. Ag/AgCl)	lithium salts, tetraalkylammonium salts, sodium iodide, potassium thiocyanate, tetraphenylborate.
Dimethylsulphoxide [DMSO, $(\text{CH}_3)_2\text{SO}$]	46.7	1.10	-3.0V	+0.7V	lithium and sodium salts, potassium perchlorate, tetraalkylammonium salts.
Methylene Chloride (CH_2Cl_2)	8.9	.393	-1.9V	+1.8V	tetrabutylammonium perchlorate, chloride, and iodide.
Propylene carbonate ($\text{C}_4\text{H}_6\text{O}_3$)	69.0	1.71	-1.9V	+1.7V	tetraethylammonium perchlorate
Acetic acid (CH_3COOH)	6.2	1.05	-1.7V	+2.0V	sodium and ammonium acetates, hydrochloric and sulphuric acids, alkali halides and perchlorates.

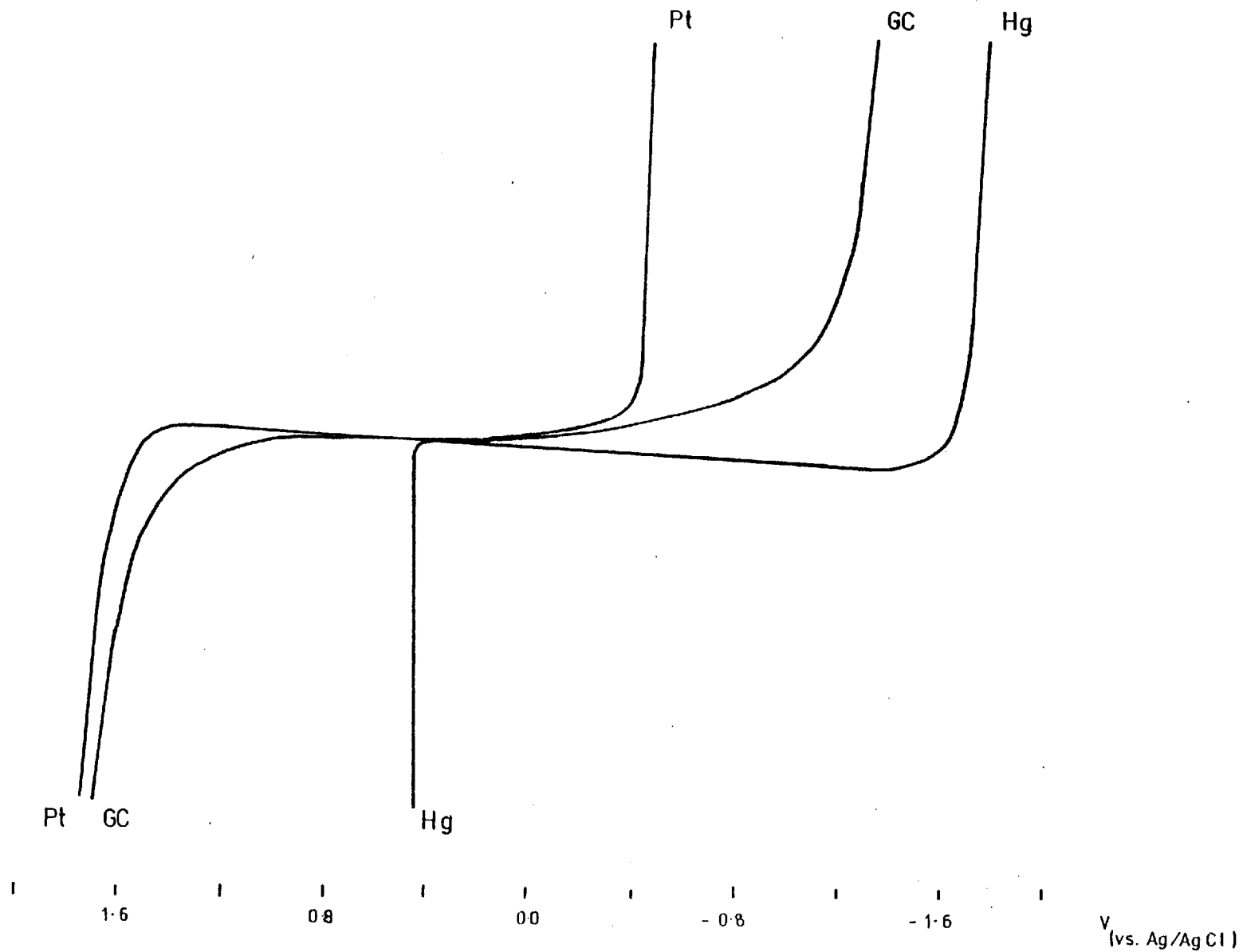


Fig. I.3 - Potential Range Pt, GC and Hg.

plating a thin film of mercury on the working electrode surface. The usable potential range of glassy carbon has been studied (27),

Fig. I.4.

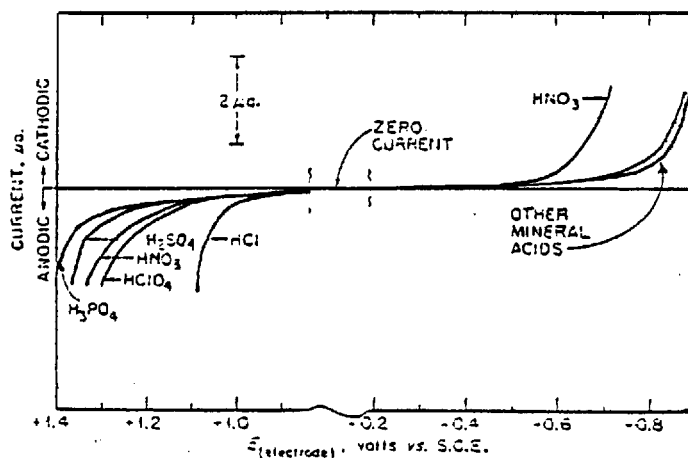


Fig. I.4 - Usable potential range for GCE in various mineral acids

The response of the GCE to change in pH has also been studied. The data in Table I.6 show that the GCE is relatively insensitive to changes in pH.

Steady state potentiostatic polarization curves of vitreous carbon recorded at potentials where oxygen, carbon monoxide, and carbon dioxide are evolved, are reported (31) for acidic and alkaline solutions with and without additives - methanol or sodium, cadmium, and chloride ions. There is practically no change in the slope of the polarization curves in the presence of the additives. The conclusions are that the effect of added surfactants on oxygen evolution at vitreous carbon is insignificant and this is independent of the medium.

Table I.6 - Response of the GCE and Glass Electrode in pH changes (27)

Measuring instrument, Beckman research pH meter^a

Glass electrode, Beckman glass electrode (standard 1199-30)

Reference electrode, Beckman calomel reference electrode (standard 1199-31)

Test solution		Electrode response			
		Glass electrode		GCE	
Identity	pH	mV	pH	mV	pH
HCl, 1M		+407.6	0.082	+93.4	5.385
Buffer	4.00	+174.7	4.011	+13.4	6.746
Buffer	6.86	+6.5	6.860	+7.0	6.850
Buffer	10.00	-176.1	9.945	+0.6	6.968
NaOH, 1M		-344.1	12.808	-71.1	8.181

^a Meter standardized with pH-6.86 buffer and glass electrode.

2.2.4 Reproducibility

Adsorption of products of electrode processes decreases the active surface area of the electrode and the peaks are not reproducible. The surface adsorption is a major practical problem with solid electrodes, namely glassy carbon. An adequate pre-treatment of the electrode can improve precision.

There are some techniques for elimination-minimisation of surface adsorption effects: (a) use of low concentrations, when possible;

- (b) chemical cleaning - not recommended, e.g. chromic/sulphuric acid mixture will form a film on the electrode surface;
- (c) mechanical abrasion - various abrasive techniques have been employed, for example addition of carborundum chips to an agitated cell (even sand in one case), rotating abrasive drums or removal of electrode from cell to polish with Al_2O_3 or diamond paste. Generally, these methods are elaborate and do not give a reproducible surface.
- (d) Electrochemical cleaning by potential cycling.

Electrochemical methods were also tried based on potential cycling techniques, e.g., where alternate measurement and cleaning voltage pulses were applied to the cell.

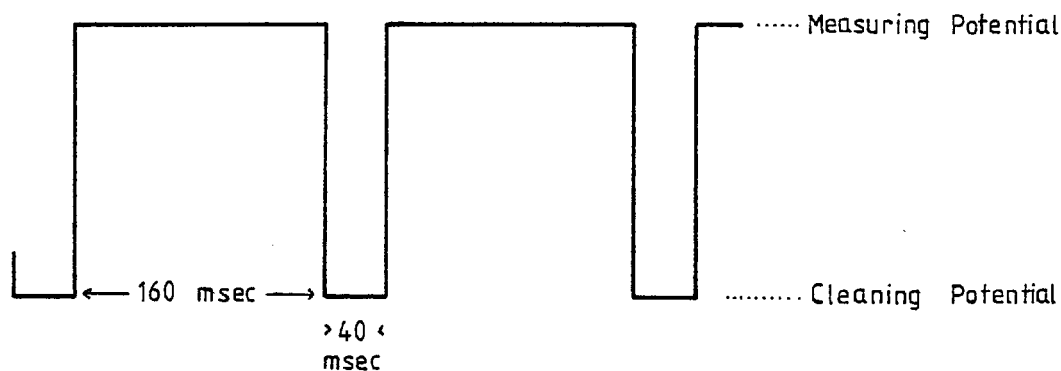
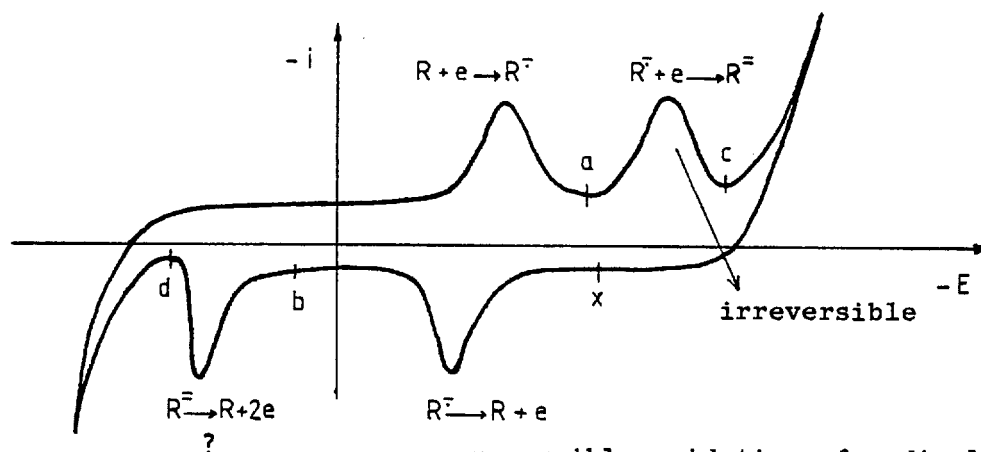
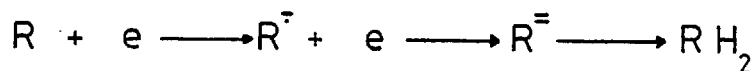


Fig. I.5 - Controller waveform

Also d.c. operation with occasional cleaning pulses may be used but choice of operating and cleaning potentials is critical. Fig. I.6 shows a cyclic voltammogram for the electrode process. Measuring or cleaning must not be either at more positive or at more negative potentials than the potential limits. If measured at c then "clean" would have to be at d which is dangerously close to the anodic limit.



possibly see an irreversible oxidation wave?

reversible oxidation of radical formed during scan from x $\Delta E_p = 60$ mV. i.e., reversible.

Fig. I.6 - Cleaning cycle

- set "measure" at a volts
- set "clean" at b volts

There is not enough real experimental work to conclusively prove the utility of electrochemical cleaning but the approach is promising unless the products are polymers, in which case an irreversible film will be formed on the surface of the electrode.

2.3 Mechanism of electrode reactions

In studying the mechanism of organic reactions it is important to consider the electron as another reagent, very versatile, able to initiate substitution, addition, cleavage and polymerisation reactions and the products can follow very different reaction pathways. It is

rare, if ever possible, to have complete information about the course of a chemical reaction. There are many factors involved. An electron transfer in organic reactions is one step in the whole reaction, preceding and/or following chemical reactions, a second electron transfer and adsorption-desorption phenomena.

2.3.1 Electron transfer

After dissolution of a sample in an appropriate supporting electrolyte the current-voltage curve obtained corresponds to an electron transfer from the highest filled molecular orbital of the neutral substrate to the anode. This oxidation process yields a radical cation as an intermediate product.

2.3.2 Proton transfer

The preceding or following proton transfer is one of the most common chemical reactions associated with electrode processes. To study some organic electrode reactions it is necessary to use aprotic solvents and supporting electrolytes to avoid the protonation reactions (Fig I.7).

The use of aprotic media proved to be the key to study the anodic behaviour of hydrocarbons (3). Studies of oxidations of aromatic and alkyl-aromatic hydrocarbons in water containing electrolytes under constant current conditions lead to very complex mixtures. The oxidation of aromatic hydrocarbons in acetonitrile-sodium perchlorate has aimed at elucidation of anodic hydrocarbon oxidation processes.

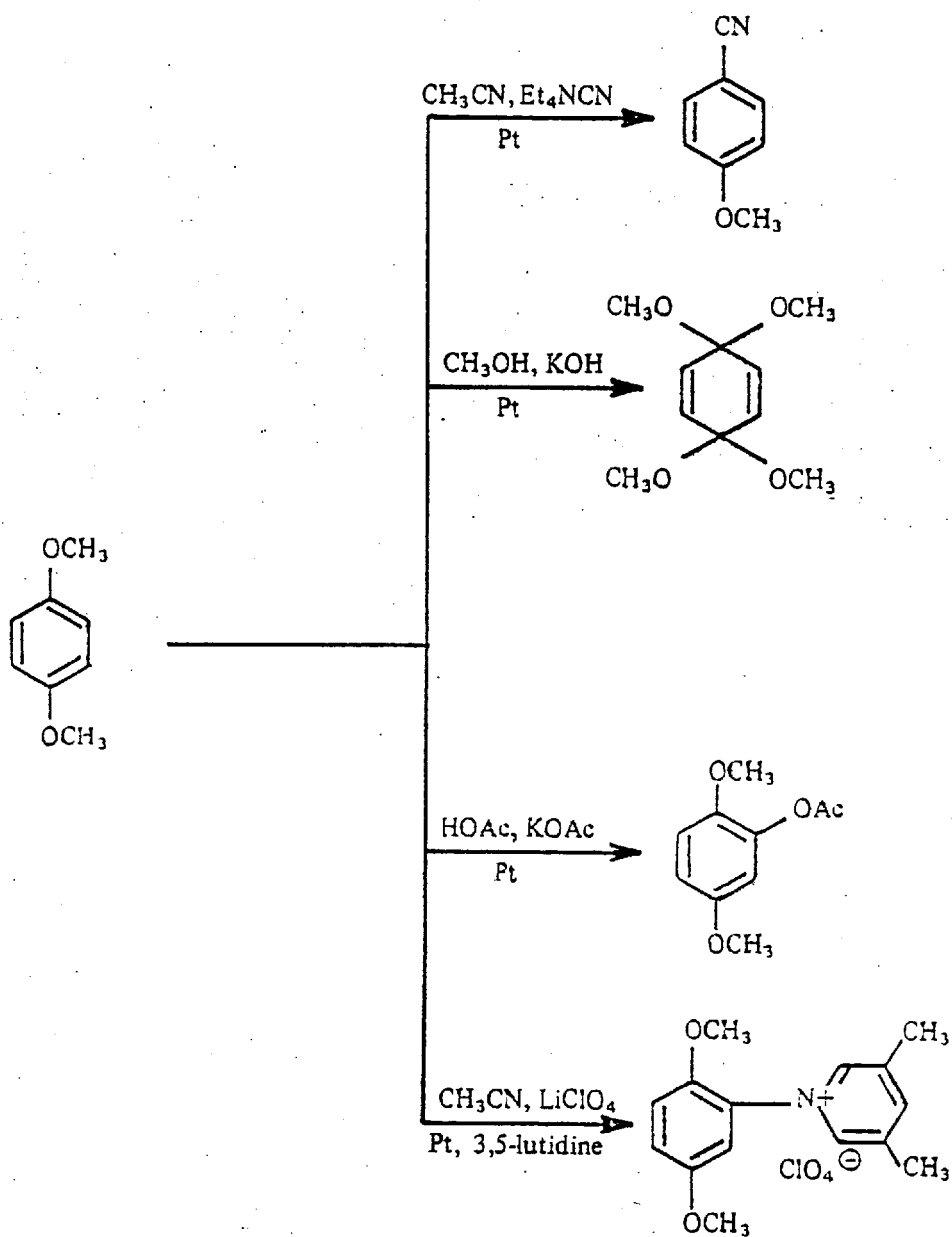
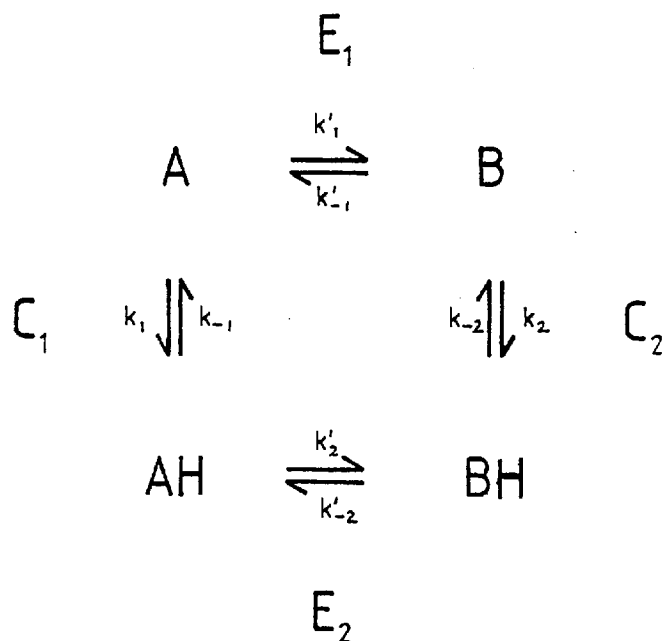


Fig. I.7 - Oxidation in aprotic solvents (32)

2.3.3 pH Dependence

Organic electrode reactions are very complex. Usually they involve more than one electron transfer and some chemical reactions as have been mentioned before (section 1.1).

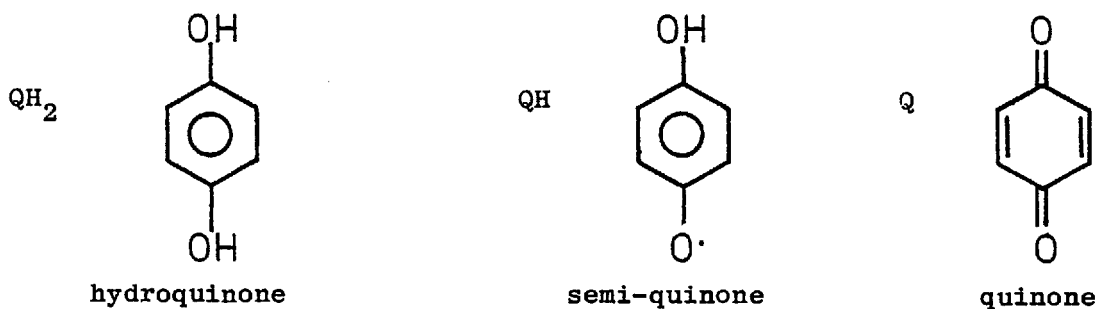
For the compounds studied in this work, the chemical reaction is a protonation and the "scheme of squares" (33) will be used to explain the oxidation mechanism. Considering a reaction involving only one square



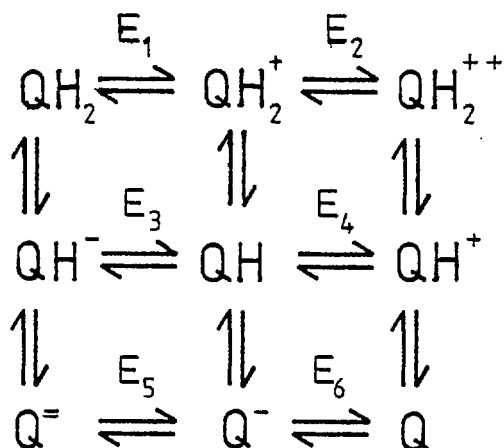
E_1 and E_2 represent electron transfer and are written horizontally; C_1 and C_2 represent proton transfer and are written vertically and it is assumed that proton and electron transfer take place separately.

The followed pathway around a square will be $E_1 C_2$ or $C_1 E_2$ depending on which transition state is rate-determining. In buffered solutions the proton transfer is a rapid equilibrium and the electron transfers are rate-determining.

If we consider, for instance, a two electron transfer reaction,
e.g. hydroquinone,



the complete oxidation scheme will be:



To simplify the resolution of this scheme we have to assume that the proton transfers are rapid and that they will influence the pK's of the various species that are likely to be found. The possible mechanisms will be

E	E	C	C
E	C	E	C
E	C	C	E
C	E	E	C
C	E	C	E
C	C	E	E

and each route is now reduced to a two-electron reaction.

Another mathematical formulation (35) is used to explain an ECE protonation mechanism using controlled potential voltammetry. Using the $E_{1/2}/\text{pH}$ diagrams it is possible to theoretically determine the equilibrium and rate constants of the chemical equilibrium and the standard potentials of the electrode reactions.

3. ELECTROCHEMISTRY IN FLOW SYSTEMS

Nowadays the chemical quality control in clinical, agricultural pharmaceutical and industrial levels asks for rapid methods of analysis, which possess high precision, are not expensive and use small volumes of samples and reagents. Different methods of analysis have been developed and some of them are for automated analysis. But the two main groups for analysis of a large number of individual sample solutions are:

(a) Batch analysers - each sample is placed in its individual container in which it remains for at least most of the analytical procedure. The analytical method includes discrete additions of buffers and other reagents at various points until the sample reaches the detector;

(b) Flow analysers - in one way or another using different processes, the sample becomes part of a continuously moving stream, into which the reagents and buffers are added at fixed flow rates until it flows through the detector cell. The detector cell is very important and one has to choose the best cell for each specific task. The purpose of the present work is to apply the electrochemical principles in a detector for flow

analysis, with or without chromatographic separation.

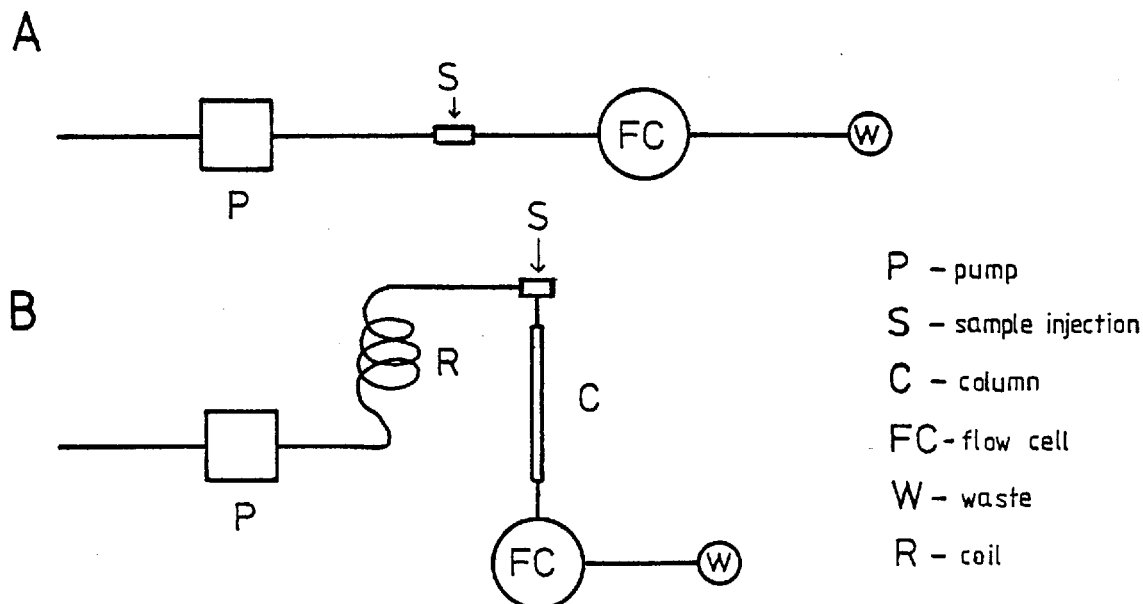


Fig. 1.8 - Flow analysis

A - Flow injection analysis.

B - Detection after chromatographic separation.

3.1 Continuous flow analysis (CFA)

In continuous flow analysis the samples are aspirated from their individual containers into a tube through which they move towards the detector. The reagents are added into the moving stream and all the liquid movement is controlled by a peristaltic pump. Although very versatile, samples can follow a whole chain of chemical treatment before analysis, the contamination of a sample from the previous one is very possible. One is unable to increase the rate of sampling as contamination will increase with closer spaced samples. The cross-contamination

can be suppressed in a continuously moving stream by alternate aspiration of sample solution and distilled water.

The attainment of a "steady state" signal is an essential part of continuous flow analysis. The peaks recorded consist of rising and falling curves which represent the transition between different steady-state conditions. The electronic and mechanistic improvements of this method permit the use of computing techniques and lead to much more expensive instrumentation.

3.2 Flow injection analysis (FIA)

Flow injection analysis is a continuous flow technique. The sample is introduced via a valve or syringe and mixes by a diffusion-controlled process. The signal is a sharp peak and no steady-state is attained. The dispersion of the sample is controlled by the flow rate, tube diameter, distance from injection port to the detector, and volume injected.

The flow injection analysis (FIA) system was invented by J. Ruzicka and E.H. Hansen (36), "who believe that the concept of controlled dispersion will have the same impact on analytical chemistry of solutions as the discovery of the transistor on electronics has had".

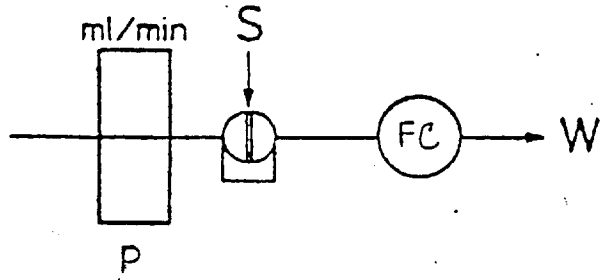
Ruzicka et al. tested the flow injection analysis with different systems such as:

- determination of phosphorus in plant digests (37), very important in agricultural and environmental research;
- rapid determination of the total nitrogen content in plant digest (38), with a rate of 250 samples per hour;

- determination of the concentration of chloride in the Amazon River, estuary and sea water samples (39). (Because it has the largest drainage basin and the greatest discharge volume of all the rivers of the world, 1/5 of all the river water discharged into oceans, it is very important to study the contamination of the environment at the mouth of the river);
- rapid determination of nitrogen and phosphorus in a single acid digest of plant material (40);
- rapid determination of chloride and inorganic phosphate in blood serum as dialysis can be performed on serum samples without distorting the sample zones formed in the flow injection procedure (41);
- method for the determination of nitrate and potassium in soil extracts, and sodium and potassium in blood serum (42), with an ion-selective electrode detector;
- enzymatic determination of glucose in blood serum with glucose dehydrogenase (43).

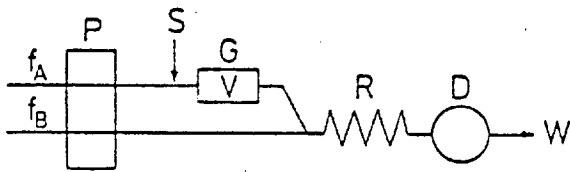
After the development of simple flow injection analysis (Fig. I.9a) they used this technique for flow injection titrations (Fig. I.9b) (44), and designed the Stopped Flow Injection Method (Fig. I.9c) as well as the Merging Zones Flow Injection Method (Fig. I.9d) (45).

The stopped flow injection method exploits the concentration profiles formed along the sample zone in order to obtain the optimum degree of dispersion. The merging-zone principle is based on the simultaneous injection of the sample and the reagent into two separate carrier streams which then meet in a controlled manner.



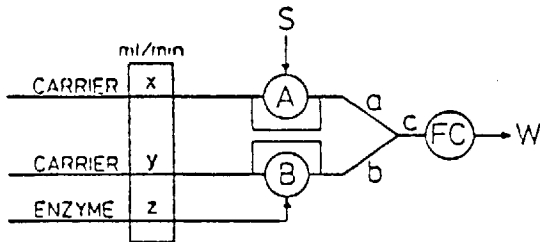
(a) Flow Injection Analysis

P - pump; S - sample injection;
FC - flow cell; W - waste.



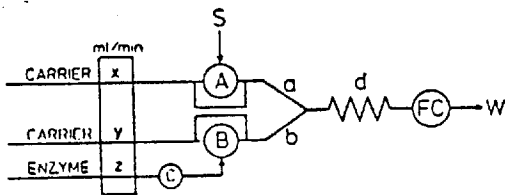
(b) Flow Injection Titration

P - pump; f_A - diluent;
 f_B - reagent; G - gradient;
V - chamber volume; R - coil;
D - detector; W - waste.



(c) Stopped-Flow Injection Method

S - sample injection; A, B - enzyme injection; FC - flow cell; W - waste.



(d) Merging Zones Method

S - sample injection, A;
B - enzyme injection;
FC - flow cell; W - waste;
C - valve for blank experiments.

Fig. I.9 - Flow Injection Analysis.

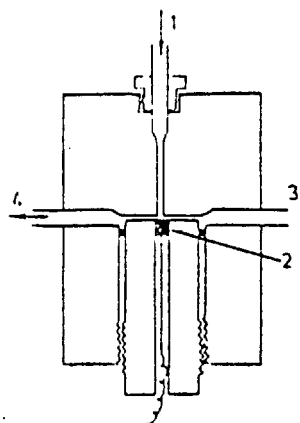
3.3 Flow analysis detectors

Several types of flow cells have been used as detectors such as:

- spectrophotometer cell used to detect the sample peak colour development, as used by Ruzicka (36-41);
- ion-selective electrodes in a tubular container: the effluent flows onto the indicator electrode and then onto the reference electrode (42);
- potentiometric detector with one electrode in the carrier stream before injection point (46);
- potentiometric/refractometric detectors and dielectric detectors are being studied by Betteridge (47);
- other non-electrochemical detectors (48, 49).

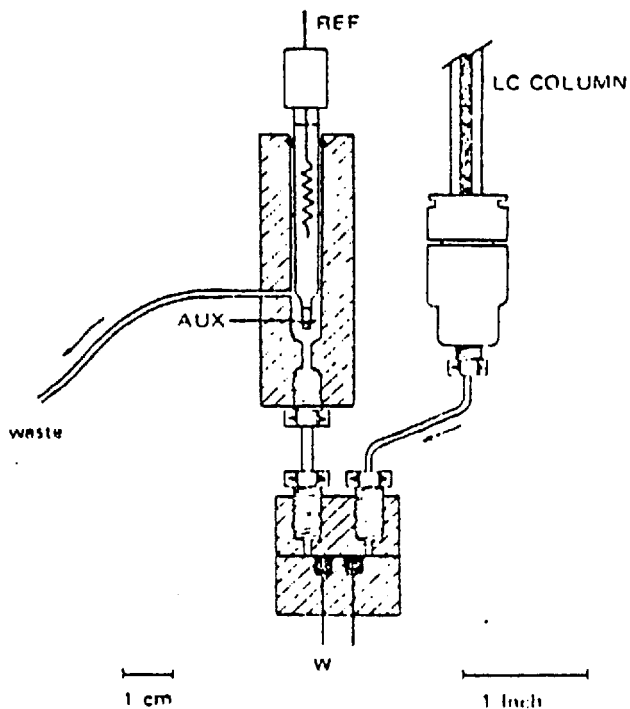
Some of these detectors have been used after separation of the compounds by high pressure liquid chromatography (HPLC) but none of them can become a universal detector. Selective detectors have great importance. In Fig. I.10 are illustrated some electrochemical detectors using glassy carbon, carbon paste, platinum and mercury electrodes. Additional information is shown in Table I.7.

The purpose of this work is to investigate the possibility of electrochemical detection of some urea and carbamate type herbicides. The flow cell used is the wall-jet cell that was first developed by Fleet (50). The flow follows the wall-jet hydrodynamics principle described by Yamada and Matsuda Fig I.11 (63). It is called the wall-jet cell detector and uses glassy carbon as the working electrode. This cell is going to be used in flow injection analysis and after chromatographic (HPLC) separation.



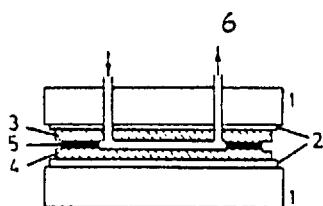
1. Wall-jet detector (50)

- 1 - Inlet; 2 - working electrode;
3 - reference electrode;
4 - outlet.



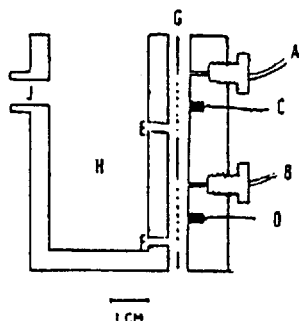
2. Thin layer cell as an Amperometric chromatography detector (51, 52).

- REF - reference electrode
AUX - auxiliary electrode
W - working electrode



3. Coulometric detector (53)

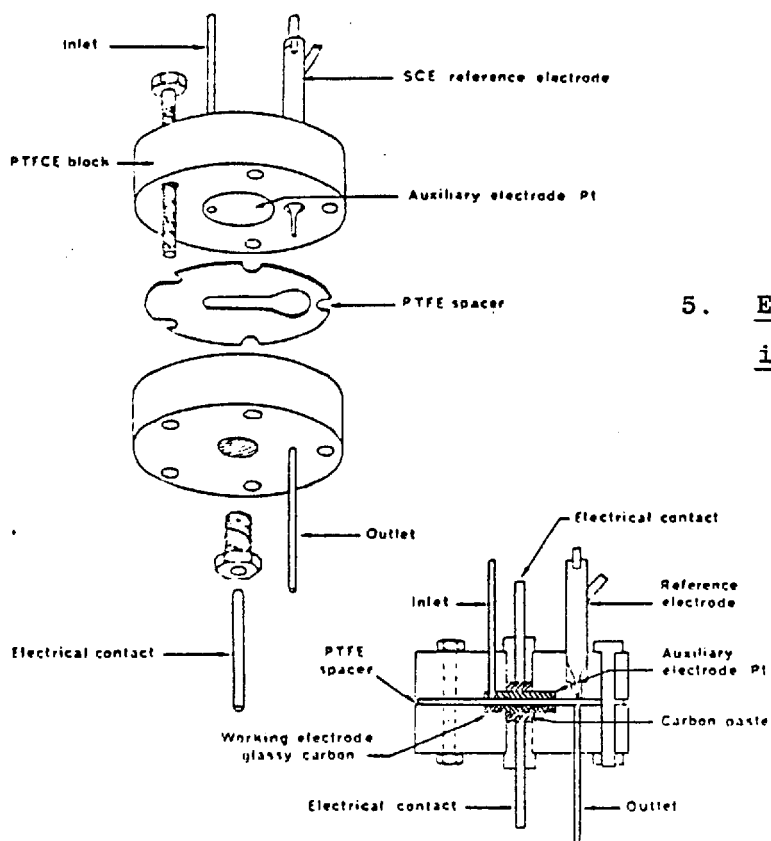
- 1 - steel plates; 2 - teflon isolation;
3 - aux. electrode; 4 - working electrode;
5 - teflon spacer; 6 - ref. electrode.



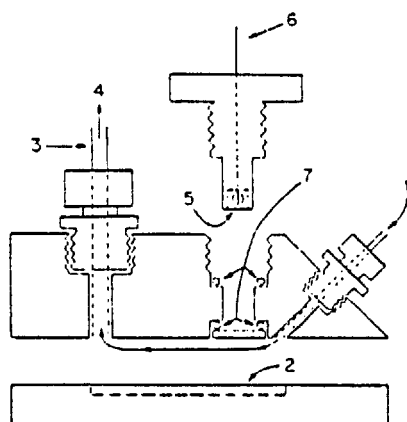
4. Thin-layer flow cell of the differential amperometric detector (54).

- A - inlet sample cell; B - inlet ref. cell;
C - working electrode (sample cell);
D - WE (ref. cell); E - sample outlet;
F - ref. cell outlet; G - spacer (100 μ m thick); H - compartment for ref. and aux. electrodes; J - overflow to waste.

Fig. I.10.— Electrochemical detectors for HPLC.

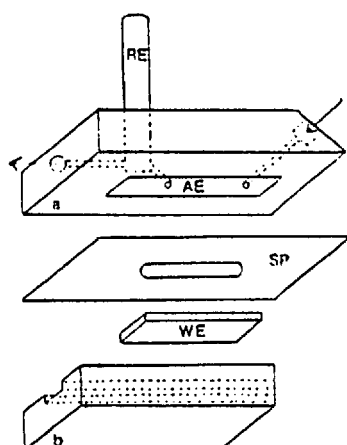


5. Electrolysis Electrochemical detector (55)



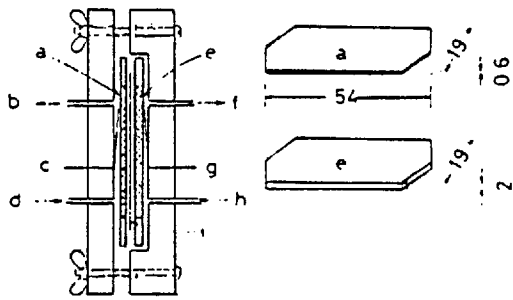
6. Electrochemical cell (56)

- 1 - inlet from chromatography;
- 2 - flow channel in spacer;
- 3 - 1/8 in. outlet tube and aux. electrode;
- 4 - flow to reference electrode;
- 5 - cavity for working electrode;
- 6 - platinum wire contact;
- 7 - O-ring seals.



7. Electrochemical cells (57)

- RE - reference electrode;
- AE - auxiliary electrode;
- WE - working electrode;
- a and b - lucite
- SP - spacer (125 μ m thick).

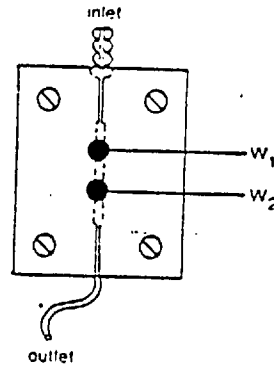
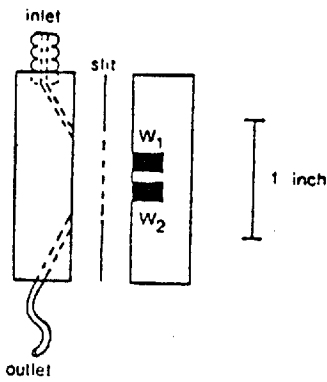


8. Detector cell (58)

a - working electrode; b - sample solution outlet; c-WE - lead; d - sample solution inlet; e - auxiliary electrode; f - electrolyte outlet; g-AE - lead; h - electrode inlet; i - diaphragm (ion-exchange membrane).

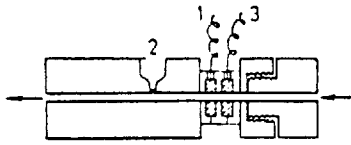
A

B



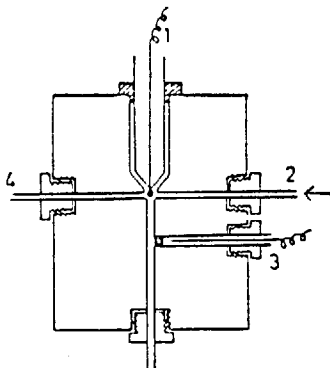
9. Dual electrode detector (59)

W_1, W_2 - working electrodes.



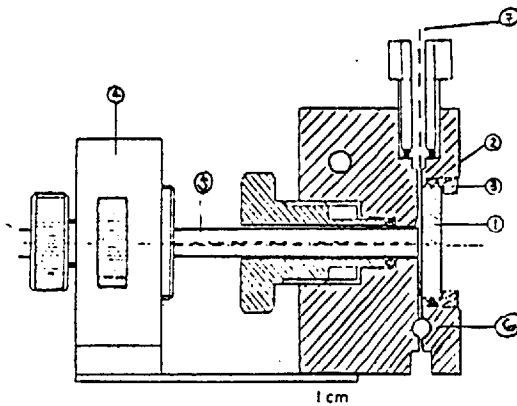
10. Voltammetric tubular detector(60,61)

1 - working electrode; 2 - reference electrode; 3 - auxiliary electrode.



11. Dropping mercury electrode detector (50)

1 - conical DME; 2 - column inlet; 3 - reference electrode; 4 - auxiliary electrode.



12. Dropping mercury electrode detector (62)

1 - round glass plate; 2 - O-ring; 3 - metallic ring; 4 - screw mechanism; 5 - DME; 6 - ref. electrode; 7 - inlet from column.

Fig. I.10 /cont...

Table I.7. Electrochemical Detectors

Detector	Electrodes		Flow	Detection Limits	Cell Volume	Date	Fig. I.10	Ref.	
	working	ref. auxiliary							
Wall-jet cell	glassy carbon	Ag/AgCl	Pt (tube)	turbulent	10 pg	0.5 μ l	1974	1	50
Thin-layer cell	carbon paste	Ag/AgCl	Pt (wire)	laminar	50-100 pg	< 1 μ l	1973 1976	2	51 52
Coulometric	glassy carbon	Ag(tube)	glassy carbon	laminar	picogram	variable	1976	3	53
Thin-layer cell	glassy carbon	SCE	Pt (wire)	-	5 ng	-	1978	4	54
Partial electro-lysis cell	glassy carbon	SCE	Pt (disc)	laminar	10^{-14} moles	variable	1977	5	55
Thin-layer cell	carbon paste	SCE	Pt (tube)	laminar	5 pg	-	1976	6	56
Thin-layer cell	pyrolytic graphite	SCE	Pt (foil)	laminar	1 pmol	variable	1978	7	57

/continued...

Table I.7/continued...

Detector	Electrodes			Flow	Detection Limits	Cell Volume	Date	Fig. I.10	Ref.
	working	ref.	auxiliary						
Coulometric	carbon cloth	-	Ag/AgI net	-	5.10^{-8} mol	-	1975	8	58
Dual electrochemical cell	carbon paste	SCE	Pt (wire)	-	0.03 pmol	-	1976	9	59
Tubular cell	Pt	SCE	Pt	turbulent	-	0.2 ml	1976 1979	10	60 61
DME cell	DME	Ag/AgCl	Pt (tube) or Ti (tube)	turbulent	10^{-7} M	2-5 μ l	1974	11	50
DME cell	DME horizontal capillary	Ag/AgCl	-	turbulent	4.4 ng	< 1 μ l	1979	12	62

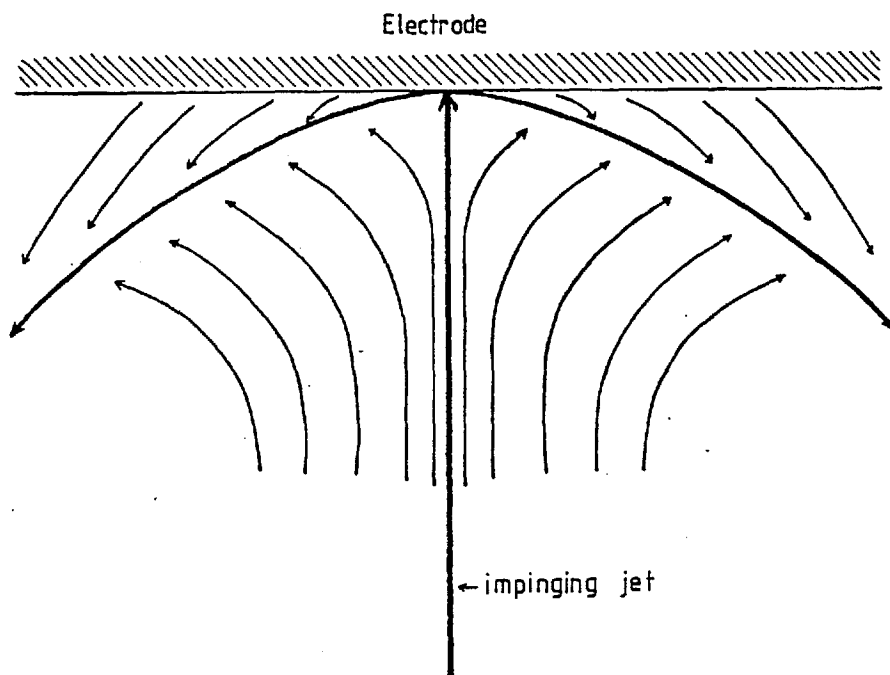


Fig. I.11 - Hydrodynamic flow pattern

3.4 Applications of a flow cell as a detector for HPLC

This technique combines the high resolution of high pressure liquid chromatography with sensitive electrochemical detection. In the last couple of years an increasing amount of work with organic compounds separated by HPLC and identified with an electrochemical detector, has been done. Most of the work done is in the detection of pollutants or in biological determinations. This work is summarised in Table I.8.

Table I.8 Anodic detection at carbon electrodes after chromatographic separation

Type of Compound	Type of Column	Eluent	Detector	Applied Potential V vs. Ag/AgCl	Limit of Detection	†	Ref.
STEROIDS							
estrone	-	-	WJCD	+0.8	< 0.1 ng	-	50
AMINO ACIDS							
arginine	Meter SCX	methanol borate 0.5M (1 : 9)	WJCD	+0.8	0.1 mg/ml	<i>a</i>	50
CATECHOLAMINES							
norepinephrine	cation exchange	0.1M per-	Kissinger	+0.8	nanogram	<i>c</i>	51
dopamine	resin, SCX (Du Pont)	chloric acid					64
norepinephrine	strong cation	citrate	Kissinger	+0.65	17 pg	<i>d</i>	65
epinephrine	exchange, resin,	Buffer			18 pg		
dopamine	corasil CX				20 pg		
α-methyldopamine	(waters Ass.)				-		
serotonin					-		
noradrenaline	strong cation	acetate-	Kissinger	+0.6	-	<i>e</i>	66
adrenaline	exchange resin	citrate					
dopamine	Vydac CX	buffer					
α-methyldopamine	(Separation Group)	pH=5.2					

/continued...

Table I.8/continued...

Type of Compound	Type of Column	Eluant	Detector	Applied Potential V vs. Ag/AgCl	Limit of Detection	†	Ref.
noradrenaline adrenaline dopamine	Nucleosil 10 SA	acetate- citrate buffer pH = 5.2	Kissinger	+0.72	1.7 pg 0.9 pg	<i>f</i>	67
α -methyldopa dihydroxybenzyl- amine dopamine norepinephrine α -methyldopamine	cation exchange resin, Vydec SCX (Altex) 30-44 μ m	20 mM ammonium dihydrogen phosphate +0.1 mM EDTA pH = 2.55	Kissinger	+0.54	0.05 μ g/ml	<i>g</i>	68
2-S-Cysteinyldopa 5-S-Cysteinyldopa 2,5-S,S-dicystein- yldopa dopamine dopa noradrenaline adrenaline	Nucleosil C ₁₈ 5 or 10 μ m Spherisorb ODS Lichrosorb RP-18 Partisil ODS 10 μ m	sodium sulphate and phosphoric acid	Kissinger	+0.75	- 5 pg	<i>h</i>	69

continued...

Table I.8/continued...

Type of Compound	Type of Column	Eluent	Detector	Applied Potential V vs. Ag/AgCl	Limit of Detection	†	Ref.
norepinephrine dopamine epinephrine serotonin 5-hydroxyindole acetic acid	strong cation exchange resin (Du Pont)	0.1 M perchloric acid with hydrogen sulphide	thin layer	+0.80	100-150 pg 500 pg	<i>i</i>	70
norepinephrine hydrochloride dopamine hydrochloride Serotonin creat- inine sulphate	strong cation exchange, Zipax SCX Vydac SCX	citrate- acetate Buffer pH = 5.1	Kissinger	+0.60	sub pico mole	<i>j</i>	71
5-hydroxy- ptamine (serotonin, 5-HT)	Nucleosil C18	phosphoric acid, methane sulphoric acid	Kissinger	+0.75	25 pg	<i>l</i>	72
norepinephrine 6-hydroxydopamine dopamine	strong cation exchange resin, Zipax SCX (Du Pont)	0.1 M HClO ₄	Dual detector	+0.4 +0.8	0.03 pmol 0.07 0.08	<i>m</i>	59

/continued...

Table I.8/continued...

Type of Compound	Type of Column	Eluent	Detector	Applied Potential V. vs. Ag/AgCl	Limit of Detection	†	Ref.
epinephrine norepinephrine L-dopa dopamine	Zipax SCX (Du Pont)	0.4M Sodium acetate Buffer pH = 4.0	Thin layer	+0.8 V vs. SCE	0.2-0.3 pmol	n	73
8-HYDROXYCARTEOLOL	Partisil 10 SCX	sodium sulphate, 2-propanol, sodium dihydrogen phosphate, phosphoric acid	Kissinger	+0.65	0.22 ng	o	74
METHYLYXANTHINES							
theophylline (1,3-dimethyl- xanthine) theobromine caffeine 8-chlorotheo- phylline	LiChrosorb C ₈ 10 µm	sodium acetate- acetic acid buffer pH = 4.0/ ethanol (92:8)	Electrochemical flow cell	+1.24 V vs. SCE	0.5 mg/l	p	75

/continued...

Table I.8/continued...

Type of Compound	Type of Column	Eluent	Detector	Applied Potential V vs Ag/AgCl	Limit of Detection	†	Ref.
theophylline 7-methylxanthine 3-methylxanthine 1-methylxanthine theobromine caffeine	μ Bondepak C ₁₈	sodium monohydrogen phosphate, sodium dihydrogen phosphate monohydrate	Coulometric	+1.4 V vs. SCE	2 ng	-	76
TRYPTOPHAN METABOLITES	ODS-Hypersil 5 μm	potassium- phosphate buffer pH = 5.2	WJCD	+1.24 vs. SCE	2 pmol	-	77
CYSTEINE GLUTATHIONE	strong cation exchange resin Vydac CX	0.02 M H ₃ PO ₄ pH = 2.1	Kissinger	+1.0	5 pmol	-	78
ACETAMINOPHEN	Pellidon 37 μm	0.04 M NaH ₂ PO ₄ pH = 7.4 5% methanol	Kissinger	+0.7	0.2 μg/mol	-	79

/continued...

Table I.8/continued...

Types of Compounds	Type of Column	Eluent	Detector	Applied potential V vs. Ag/AgCl	Limit of Detection	†	
p-AMINOHIPURIC ACID	strong anion exchange resin Zypax	acetate buffer pH = 5.25	Kissinger	+1.0	100 pg	-	80
PHENOLS	strong cation exchange resin Partisil ODS-2	water aceto- nitrile +0.05N H_3PO_4	Tubular	+1.2	- - 0.83 ppb 1.6 1.5 1.4 1.6 2.1 2.2 - 1.2	q	81
hydroquinone							
phenol							
o-chlorophenol							
2,6-dichlorophenol							
2,4-dichlorophenol							
2,4,6-trichloro- phenol							
2,4,5-trichloro- phenol							
2,3,4,6-tetra- chlorophenol							
pentachlorophenol							
p-chlorophenol							

/continued...

Table I.8/continued...

Type of Compound	Type of Column	Eluent	Detector	Applied potential V vs. Ag/AgCl	Limit of Detection	†	Ref.
ANILINES							
aniline	Zorbax-C18	0.15M	Kissinger	+1.1	0.23 ng	-	82
2-amine-4-chloro-phenol		phosphate			0.28		
o-chlorophenol		Buffer			-		
p-bromoaniline		pH = 2.1			0.38 ng		
m-chloroaniline					0.27		
p-chloroaniline					0.33		
3,4-dichloro-aniline					0.38		

†

- a) The amino-acids can not be measured with UV detection. Due to the electroactivity of the amino group they can be detected with the WJCD;
- b) The catecholamines have been studied in blood, plasma, urine and brain tissue in particular;
- c) This separation has become the basis of a rapid, routine determination of the catecholamines in mouse and rat brain tissue;
- d) Measurement of Dopamine in hypophysical stalk blood of rats;
- e) Assay of plasma catecholamines;
- f) i.s. dihydroxybenzylamine (i.s. = internal standard);

/continued...

Table I.8/continued...

- g) Using EDTA in the eluent to suppress erratic fluctuations in the background current;
- h) i.s. isoprenaline;
- l) i.s. 2,4-dihydroxybenzylamine;
- j) i.s. 3,4-dihydroxybenzylamine hydrobromide;
- l) i.s. 5-hydroxy-N ω -methyltryptamine oxalate;
- m) i.s. 3,4-dihydroxybenxylamine;
- n) Uses a four electrode detector;
- r) Analysis in plasma and urine;
- o) Methylxanthines have numerous pharmacological actions and are used for their effects on cardiac muscle and the cardiovascular system, the central nervous system, the kidneys and smooth muscles;
- p) The halogenated phenolic compounds are of concern in the environment because of their toxicity to fish and other aquatic life and their adverse effect on water and fish taste;
- q) The halogenated anilines may enter the environment from a variety of sources, including metabolism of insecticides, herbicides and fungicides.

1.4 CONCLUSIONS

This thesis, as said before, is concerned with the use of an electrochemical detector, either in flow analysis or after chromatographic separation to analyse some herbicides. Chapter two is going to deal with the theoretical principles of the HPLC separation, of the electrochemical hydrodynamic detection and of the waveform applied. Chapter three explains the experimental techniques used in this work. Chapter four gives an approach for the oxidation mechanism using the scheme of squares. Finally, in Chapter five we analyse the results obtained in flow systems: continuous flow analysis, flow injection analysis and after HPLC separation.

CHAPTER II

THEORY

1. INTRODUCTION

In this chapter we are going to review the theory of each part of the analytical procedure. The next section deals with the chromatographic separation, the third with the electrochemical detection, and the fourth with the differential pulse waveform used in the mechanistic studies.

2. HPLC SEPARATION

2.1 Introduction

The word chromatography was used for the first time by the Russian botanist Tswett in 1906 to describe the technique used to separate leaf pigments. This thesis is concerned with high pressure liquid chromatography where a dilute solution of the sample is pumped through a column packed with small diameter, high surface area particles, using pressures of 1000 p.s.i. and higher; this is done in order to speed the separation.

2.2 Definitions

The parameters of the chromatographic peak must be defined before proceeding further (83, 84, 85). Fig. II.1 is a schematic representation of a chromatogram.

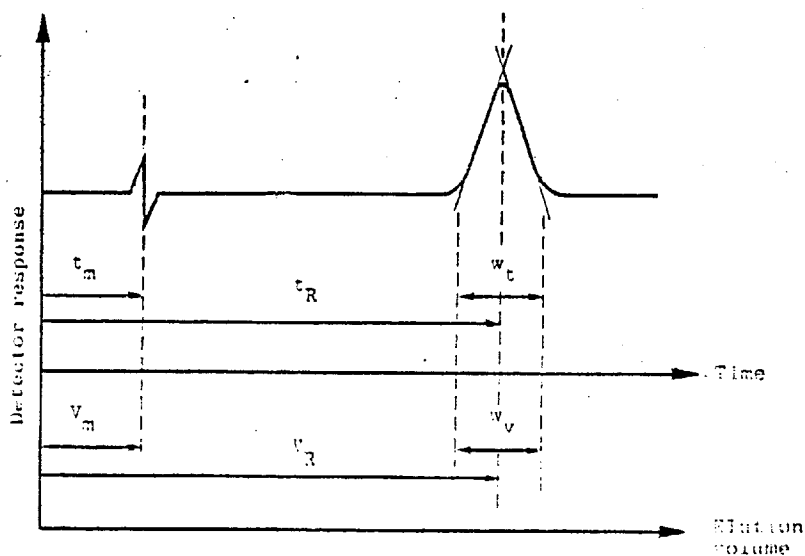


Fig. II.1 - Parameters for defining retention and peak width.

The time that elapses between injection and elution of a solute is called the retention time or elution time, t_R , and the volume of eluent passed into the column during this time is called the retention or elution volume of the solute, V_R . Elution time and volume are connected via the volumetric flow rate, f_V

$$V_R = t_R \cdot f_V$$

The peak width at the base of the peak is denoted by W_t when measured in time units and as a distance within the column by W_z . Both

theory and practice agree that the width of a band within the column W_z increases as the square root of the distance migrated, Fig. II.2.

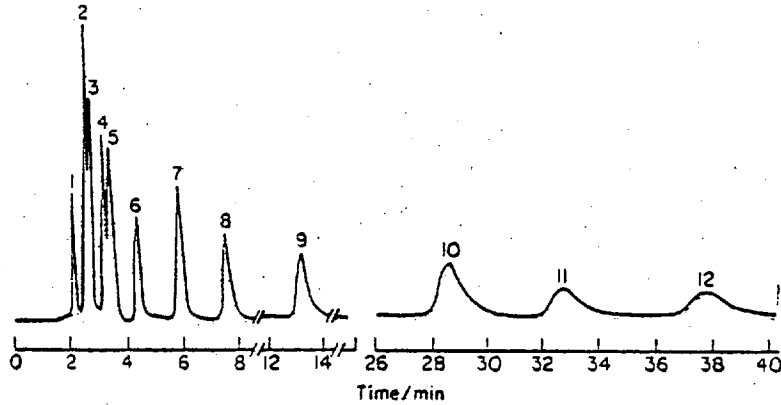


Fig. II.2.- Separation of sulphadiazine (84)

The separation between two adjacent bands is called resolution, R_s , and is defined by the distance between the band centres divided by the average band widths - in time units,

$$R_s = \frac{t_{R_2} - t_{R_1}}{\frac{1}{2}(W_{t_1} + W_{t_2})}$$

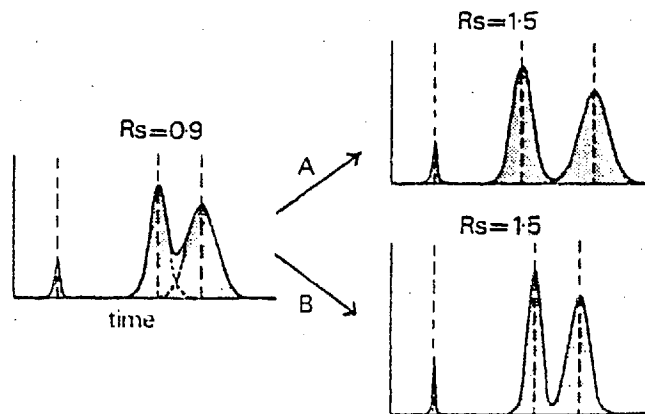


Fig. II.3 - Improvement in resolution A, by increasing peak separation, and B, by reducing peak width. The first peak in each case represents an unretained solute.

In chromatography the elution time of a solute relative to that of an unretained compound is determined entirely by thermodynamic considerations, while the peak width relative to the retention time is determined by kinetic considerations. Thus change of resolution by method A of Fig. II.3 involves changing the thermodynamic aspects of the chromatography, while changing resolution by method B involves improving the kinetics. These two aspects of chromatography are independent and we therefore consider them separately.

2.3 Theory of HPLC - Thermodynamics

In a chromatographic column there are the stationary and the mobile zones, Fig. II.4. The stationary zone consists of a micro-porous material, coated with a stationary phase.

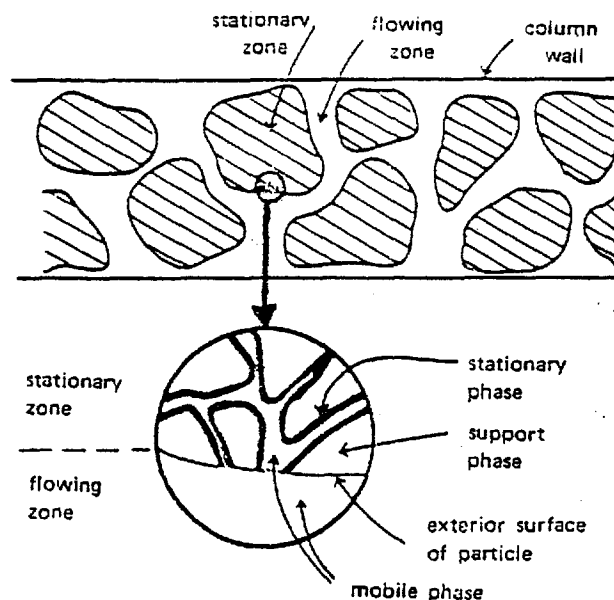


Fig. II.4 - Diagrammatic illustration of the structure of a packed chromatographic column.

Consider a simple idealised experiment. A band of solute is eluted part way down a column and the solute flow arrested so that complete equilibration can take place between the solute and the mobile and stationary phases, Fig. II.5. The concentration profile of the solute band in the mobile phase is mirrored, apart from scale, by the profile in the stationary phase, which for simplicity we take to be a liquid.

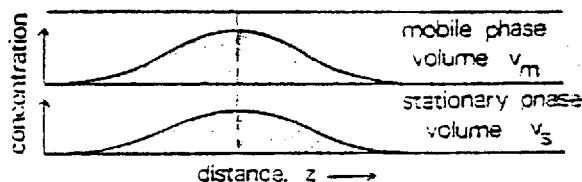


Fig. II.5 - Concentration profiles in the mobile and stationary phase with arrested elution.

Since the system is at equilibrium, the concentration ratio is the equilibrium partition ratio, k , for the solute between the two phases which we assume is independent of the absolute values of the concentrations:

$$k = \frac{C_s}{C_m}$$

where C_s and C_m are the concentrations (moles/unit volume) of solute in the stationary and mobile phases. The column capacity ratio, k' , is a measure of the degree of retention of a solute in the two phases, q_s and q_m ,

$$k' = \frac{q_s}{q_m} = \frac{C_s V_s}{C_m V_m} = k \frac{V_s}{V_m} = \frac{t_s}{t_m}$$

V_s and V_m are the volumes of stationary and mobile phases in the column. Since all equilibria are dynamically maintained, k' is also equal within statistical limits to the ratio of the times t_s and t_m , spent by typical molecules in the stationary and mobile phases. Therefore,

$$\text{mean fraction of time spent by molecules in mobile phase} = \frac{\bar{t}_m}{\bar{t}_m + \bar{t}_s} = \frac{1}{1 + k'}$$

when the mobile phase starts moving at a linear velocity u , and the molecule finds itself in the mobile phase it will move along at a speed u , whereas when it is in the stationary phase it is of course motionless. This movement cannot alter the average proportion of time spent by a typical molecule in the mobile phase. The linear velocity of a solute band is

$$u_{\text{band}} = u \times \frac{\text{fraction of time spent by typical molecule in the mobile phase}}{1} = \frac{u}{1 + k'}$$

The fraction of solute in the mobile zone at equilibrium is the relative migration rate R ,

$$R = \frac{u_{\text{band}}}{u} = \frac{1}{1 + k'} = \frac{t_0}{t}$$

because the band velocities are inversely proportional to their elution times, t and t_0 for retained and unretained bands. Hence,

$$k' = \frac{t - t_0}{t_0}$$

and k' is immediately obtained from an elution chromatogram.

The variation of k' with temperature depends upon the heat of transfer of the solute from the mobile to the stationary phase and follows the

Van't Hoff equation,

$$\frac{d \ln k'}{dT} = \frac{\Delta H_{(m \rightarrow s)}}{RT^2}$$

Since $\Delta H_{m \rightarrow s}$ is very small in liquid chromatography, temperature has very little effect on the degree of retention.

2.4 Theory of HPLC - Kinetics

When the flow is restarted after arresting elution and allowing the system to equilibrate we note, Fig. II.6, that the concentration band in the mobile phase must inevitably move slightly ahead of the associated band in the stationary phase thereby producing a slight displacement, Δz ,

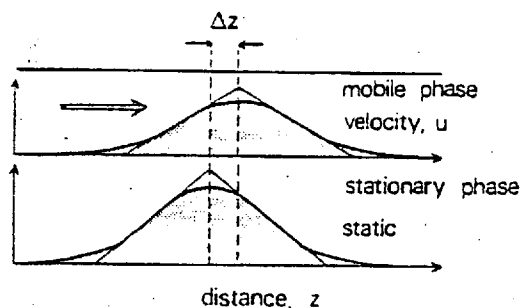


Fig. II.6 - Concentration profiles during elution chromatography in the mobile and stationary phases.

which is related to the relaxation time for equilibrium, τ , and the mean flow rate of the mobile phase, u , by

$$\Delta z = \tau u$$

When the band is Gaussian the width of it will be proportional to the

square root of the distance moved:

$$w_t = 4 \sigma_t = 4 \sqrt{Hz}$$

where σ^2 is the variance of the peak, H is the height equivalent to a theoretical plate and is equal to the differentiation of the ratio between the increase of peak variation and distance migrated $\partial\sigma_z^2/\partial z$.

It has the dimensions of a length within the column

$$H = \frac{\partial\sigma_z^2}{\partial z} = \frac{\sigma_L^2}{L} = \left(\frac{\sigma_t}{t_R}\right)^2 L = \frac{1}{16} \left(\frac{w_t}{t_R}\right)^2 L$$

and the last is the formula used to calculate the plate height in elution chromatography. The number of plates, N, in a column measures the efficiency of the column and is given by,

$$N = \frac{L}{H} = 16 \left(\frac{t_R}{w_t}\right)^2$$

and a separation requires minimum column efficiency in terms of the number of theoretical plates. Number N is associated with kinetic "parameters" in chromatography.

2.5 Resolution

The objective of an HPLC run is to separate the components of a mixture as under the correct conditions different components in a mixture migrate along the column at different rates. As the theoretical factors influencing the resolution of these bands are:

Resolution = f(Thermodynamics x Kinetics)

$$\text{base width of bands} \quad w = (16H)^{\frac{1}{2}} \sqrt{z} \quad (\text{II.1})$$

$$\text{separation of bands} \quad \Delta z = z \cdot \frac{\Delta k'}{1 + k'} \quad (\text{II.2})$$

and resolution R_s of band is defined as

$$R_s = \frac{\Delta z}{w} \quad (\text{II.3})$$

combining (II.1), (II.2) and (II.3)

$$R_s = \frac{1}{4} \cdot \frac{\Delta k'}{1 + k'} \cdot \left(\frac{z}{H}\right)^{\frac{1}{2}}$$

Z/H is the number of theoretical plates to which the length Z of column is equivalent, N . If we introduce the separation factor α ,

$$\alpha = \frac{k'_2}{k'_1}$$

and

$$\frac{\Delta k'}{k'} = \frac{\alpha - 1}{1 + \alpha}$$

resolution may be expressed as

$$R_s = \frac{1}{4} \cdot \left(\frac{\alpha - 1}{1 + \alpha}\right) \cdot \left(\frac{k'}{1 + k'}\right) \cdot N^{\frac{1}{2}}$$

(a) (b) (c)

where the three factors are:

(a) relative partition factor ($\alpha \neq 1$), separation of compounds requires them to have different partition ratios between the

two phases;

(b) retention factor ($k' \neq 0$), separation of components requires them to be retained;

(c) column efficiency factor, separation requires a minimum column efficiency in terms of the number of theoretical plates.

The first two factors in the resolution equation are essentially thermodynamic, whereas the plate number N is mainly associated with the kinetic features of chromatography.

3. THEORY OF WALL-JET

3.1 Introduction

The rate of an electrode process depends on the electron transfer at the electrode, on the transfer of species from the bulk solution towards the electrode and on the removal of the reaction products from the electrode surface. The transfer of species from the bulk solution to the electrode is called the mass transfer process and it can be accomplished in three ways: diffusion under the effect of a concentration gradient; convection due to an external force; and migration of charged ions in an electric field.

3.2 The Wall-jet cell: laminar flow

"When a jet of air strikes a surface at right angles and spreads out radially over it, it forms what will be termed a wall-jet". This is the definition of a wall-jet introduced by Glauert (86). In this paper he studies the theory of the wall-jet, radial or planar, laminar or turbulent,

velocity distribution using appropriate boundary layer equations.

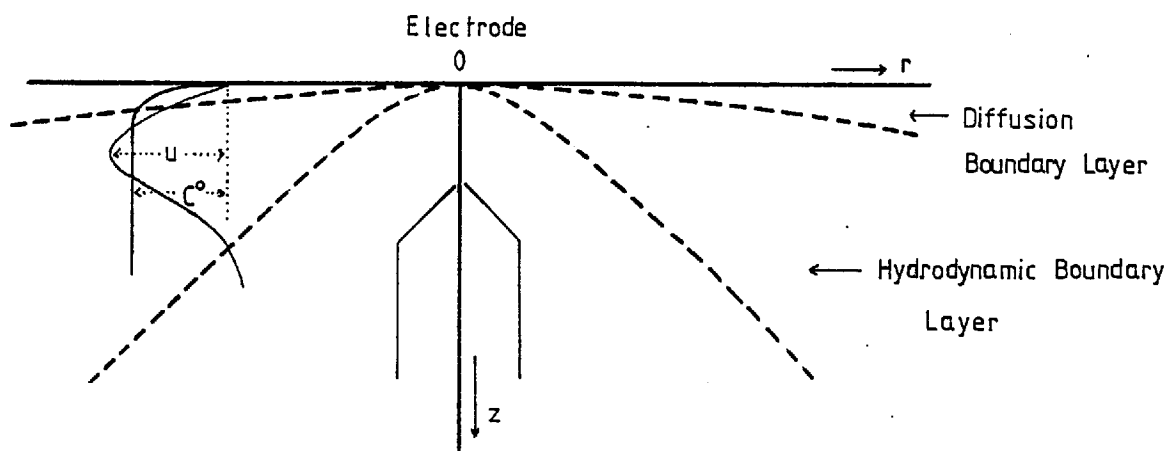


Fig. II.7 - Schematic representation of the velocity and concentration distribution in the laminar wall-jet (63)

Based on Glauert's correlations for a laminar wall-jet, Yamada and Matsuda (63) introduced the term wall-jet in electrochemistry and derived the limiting current expression for a disc electrode. Albery and Brett have studied the velocity distribution for a wall-jet in some detail (87). The radial velocity component, u , in a laminar wall-jet is expressed by

$$u = \frac{1}{r} \cdot \frac{\partial \Psi}{\partial z}$$

and the axial velocity component by

$$v = \frac{-1}{r} \cdot \frac{\partial \Psi}{\partial r} \quad (\text{II.4})$$

where Ψ is a stream function

$$\psi = \left(\frac{40 M \nu r^3}{3} \right)^{\frac{1}{4}} f(\eta) \quad (\text{II.5})$$

$$u = \left(\frac{15 M}{2 \nu r^3} \right)^{\frac{1}{2}} f'(\eta)$$

$$\eta = \left(\frac{135 M}{32 \nu^3 r^5} \right)^{\frac{1}{4}} z$$

M is flux of exterior momentum flux given by

$$\begin{aligned} M &\sim \frac{1}{2} (\text{typical velocity})(\text{volume flow/radian})^2 \\ &= \frac{k^4 V_f^3}{2 \pi^3 a^2} \end{aligned}$$

$f(\eta)$ is mass flux, $f'(\eta)$ is velocity, x and z denote distances along and normal to the disc wall (x being measured from the centre of the disc), η is the normalized distance from the wall, ν is the kinematic viscosity (viscosity/density), k is a proportional factor, V_f is the volume flow rate.

Substituting (II.5) in (II.4) gives,

$$\nu = \frac{3}{4} \left(\frac{40 M \nu}{3 r^5} \right)^{\frac{1}{4}} \left\{ \frac{5}{3} \eta f'(\eta) - f(\eta) \right\}$$

η , $f(\eta)$ and $f'(\eta)$ are related by a dimensionless variable g , where $0 < g < 1$.

$$f(\eta) = g^2$$

$$f'(\eta) = \frac{2}{3} g (1 + g^3)$$

$$\eta = \ln \left(\frac{\sqrt{1+g} + g^2}{1-g} \right) + \sqrt{3} \tan^{-1} \frac{\sqrt{3} g}{2+g}$$

Fig. II.8 is a plot of $f(\eta)$, $f'(\eta)$ and $h(\eta) = \left\{ \frac{5}{3} \eta f'(\eta) - f(\eta) \right\}$ as functions of η , which represent the behaviour of Ψ , u and v respectively. It can be seen that $f'(\eta)$ (or u) passes through a maximum then through zero and becomes negative - this shows that at large distances from the electrode, solution is drawn towards it and at small distances it is drawn away.

Taking into account the fact that η has a radial dependence ($\eta \propto r^{-5/4} z$; eqn II.5) the schematic streamlines shown in Fig. II.9 can be drawn. A point to note is that some recirculation of solution must occur in the practical wall-jet cell in order for the solution to be drawn towards the electrode at large η . However, because v is away from the electrode at η (or z) = 0 then this will not reach the electrode again, which will thus always receive fresh solution. This has been tested experimentally (88).

The limiting current found to be

$$i_L = (1.60 k) n F C^0 D^{2/3} \nu^{-5/12} V_f^{3/4} a^{-1/2} r^{3/4}$$

where k is a numerical coefficient, n is the number of electrons involved in the electrode reaction, F is the Faraday, C^0 is the bulk concentration of the sample, D the diffusion coefficient of the sample, ν the kinematic viscosity of the sample, and r the radius of the disc electrode. This equation has been verified experimentally for the wall-jet electrode cell. The dependence of current on nozzle distance, bulk concentration, volume flow rate, disc radius was tested and the numerical coefficient, k , has been found to be 0.86 (63).

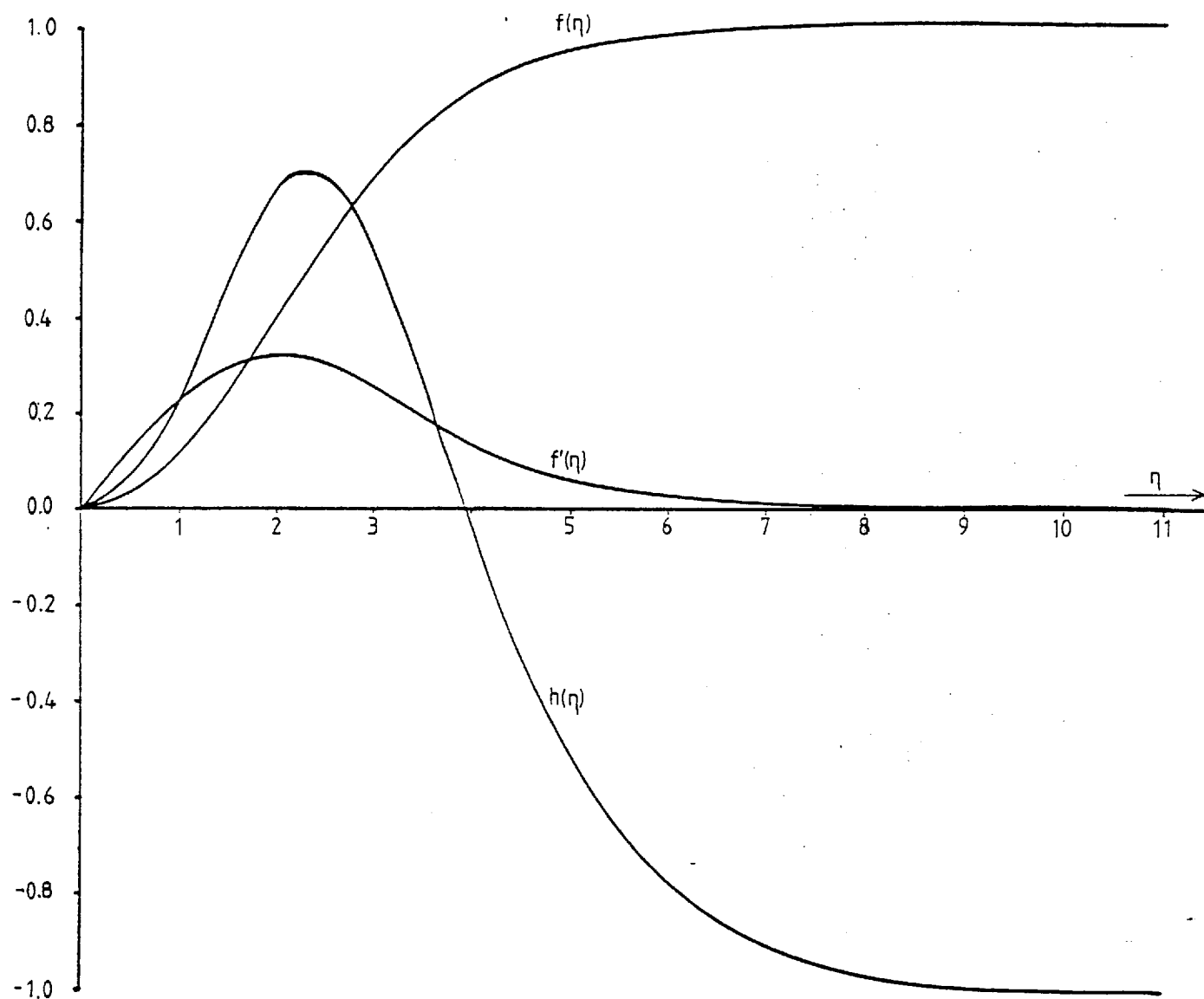


Fig. II.8 - Functions of η .

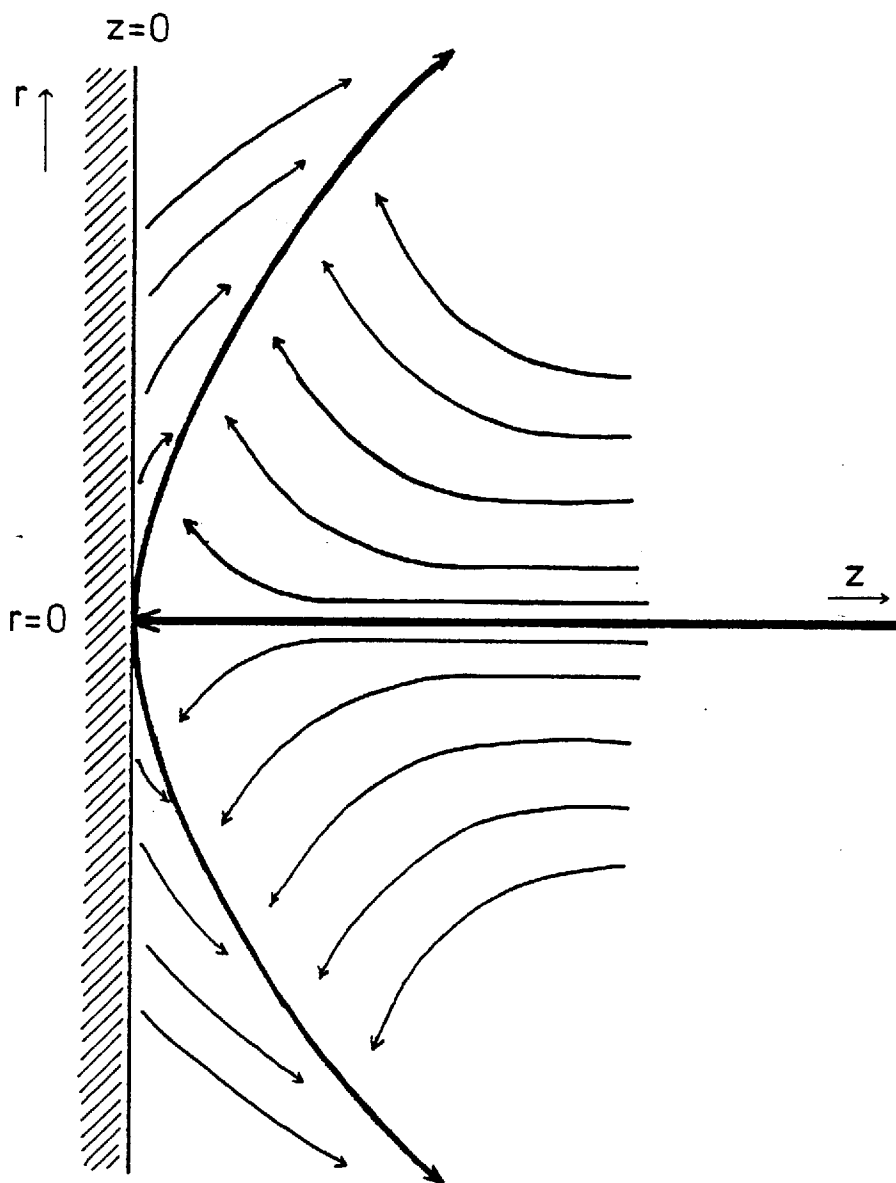


Fig. II.9 - Scheme of Streamlines.

4. MODES OF OPERATION

4.1 Introduction

More sophisticated waveforms than the simply varying d.c. potential, normally used in classical polarography, allow the possibility of trace analysis. There are various modes of processing the signal obtained, each of them designed to overcome one or more specific problems. As shown in Fig. II.10, different input waveforms give different output signals and have different detection limits.

We use the differential pulse voltammetry. It consists of superimposing a fixed height potential pulse at regular intervals on the slowly varying potential associated with dc voltammetry and sampling the current at two intervals: on the ramp prior to the imposition of the pulse and at the end of the pulse. In the next section the theory of the waveform is going to be discussed.

4.2 Differential pulse voltammetry (DPV)

The differential pulse voltammetry technique started being developed in the 1950's and the principle is that the capacitative current which flows at an electrode in response to a potential pulse decays exponentially, while the faradaic current decays at a much slower rate, Fig. II.11. The current can be measured at some time after pulse application which is long enough so that the capacitive current is negligible while the faradaic current is still appreciable (89). Thus, the measured current is much more nearly a pure faradaic current, and hence proportional to the

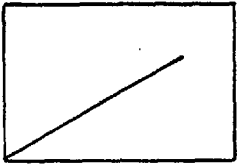

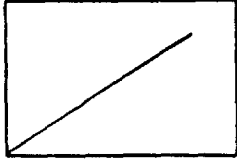

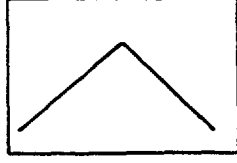
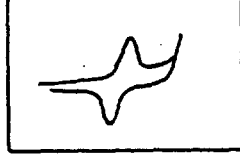
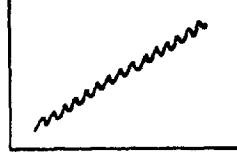
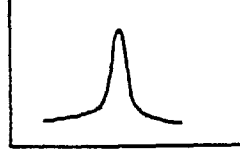
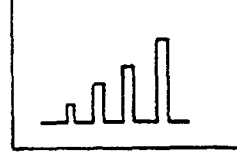

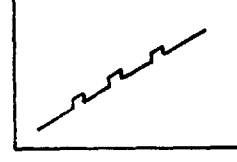
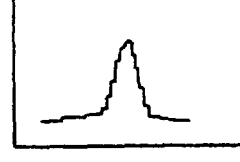

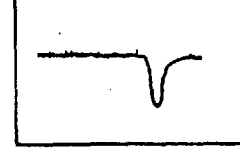

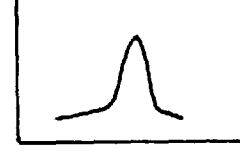
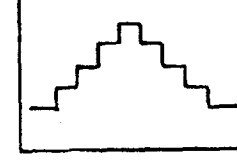

Technique	Input waveform	Output signal	Limit of Detection (M)
	E-t	i-E	
DC voltammetry			10^{-4}
Linear sweep voltammetry			10^{-6}
Cyclic voltammetry			
AC polarography			$10^{-5} - 10^{-6}$
Pulse			$10^{-6} - 10^{-7}$
Differential pulse			$10^{-7} - 10^{-8}$
Stripping voltammetry			10^{-10}
Double differential pulse			10^{-7}
Cyclic staircase voltammetry			10^{-6}

Fig. II.10 - Summary of signal input waveforms and current potential response for a range of voltammetric techniques.

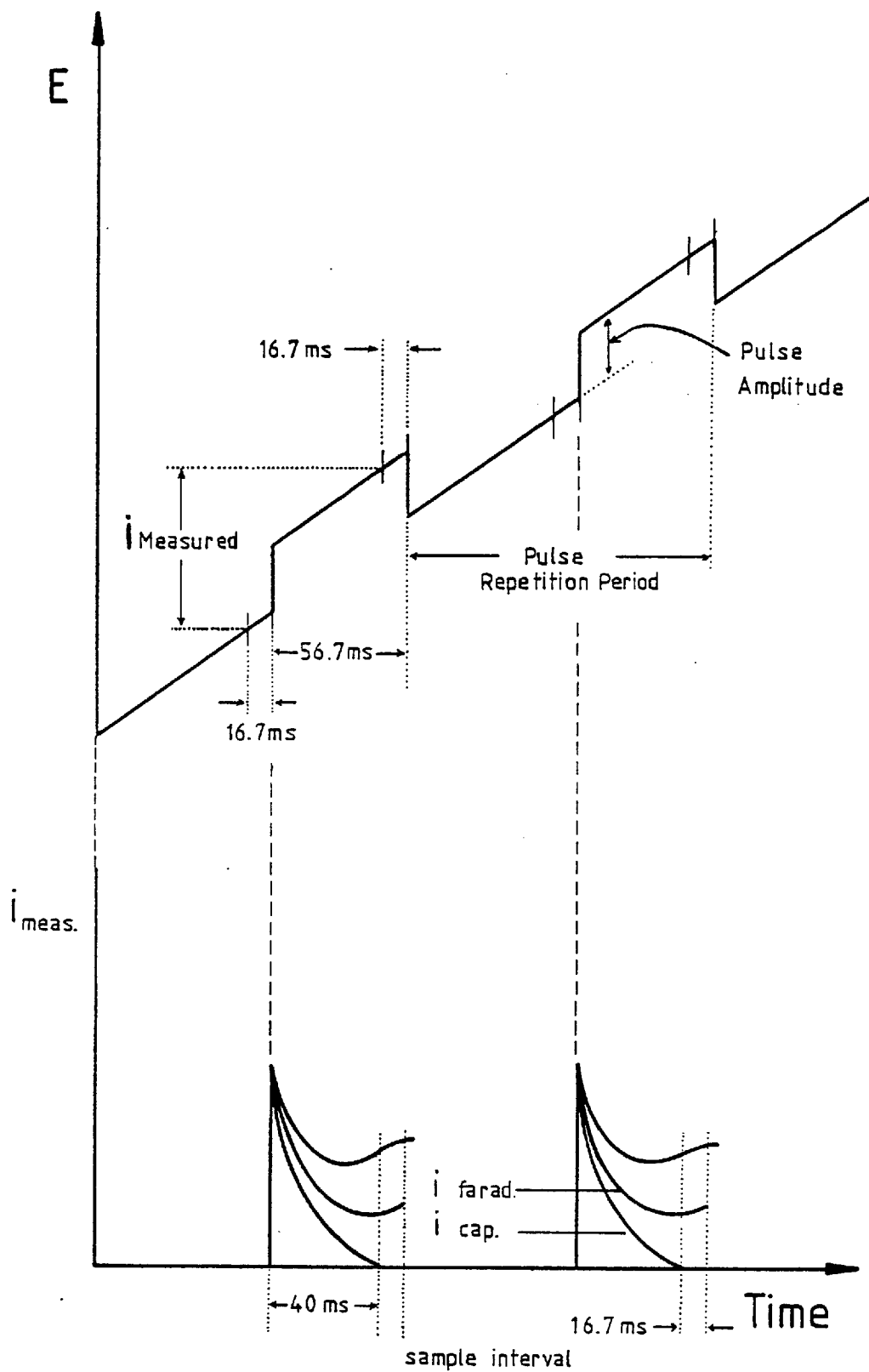
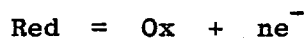


Fig. II.11 - Excitation waveform and current behaviour for differential pulse voltammetry.

concentration of depolarizer, than is the case with dc voltammetry. In differential pulse voltammetry, we are measuring not a constant current on a plateau, but rather the rate at which the current increases to that plateau value as the potential is changed. We start with the Nernst equation,*

$$\begin{aligned} E &= E_{\frac{1}{2}} - \frac{RT}{nF} \ln \left(\frac{\text{Red}}{\text{Ox}} \right) \\ &= E_{\frac{1}{2}} - \frac{RT}{nF} \ln \left(\frac{i}{i_d - i} \right) \end{aligned}$$

where E is the potential and $E_{\frac{1}{2}}$ is the half-wave potential for the reaction



where F is the Faraday, R is the gas constant ($8.314 \text{ J mol}^{-1} \text{ K}^{-1}$) and T the absolute temperature (K), i is the current at E and i_d is the diffusion current. Therefore

$$\frac{i}{i_d} = \frac{1}{1 + \epsilon} \quad (\text{II.6})$$

where

$$\epsilon = e^{+\frac{nF}{RT} (E - E_{\frac{1}{2}})}$$

and the difference current

$$i(E + \Delta E) - i(E) = \Delta i(E)$$

will be

$$\frac{\Delta i(E)}{i_d} = \frac{\epsilon (\sigma^2 - 1)}{(\sigma^2 + \epsilon)(1 + \epsilon)} \quad (\text{II.7})$$

* This assumes that the diffusion coefficients of the oxidised and reduced species are equal.

where

$$\sigma = \exp \left(- \frac{nF}{RT} \cdot \frac{\Delta E}{2} \right)$$

and ΔE is a signed quantity, anodic going pulses having a positive sign.

The maximum value of $\Delta_i(E)$, $\Delta_i(E_p) = i_p$, is found by differentiating eq. (II.7) and is given by

$$\frac{i_p}{i_d} = \frac{\sigma - 1}{\sigma + 1} \quad (\text{II.8})$$

$$E_p = E_{1/2} - \frac{\Delta E}{2}$$

Eq. (II.7), actually gives the derivative currents whereas the DPV experiment employs a differential current measurement. Agreement of theory with experiment arises from the fact that the dc current contribution is small. If we call the peak difference current in differential pulse i_{DPV} and the diffusion current in normal pulse i_{NPV} , we can rewrite eq. (II.7)

$$i_{\text{DPV}} = i_{\text{NPV}} \cdot \frac{\sigma - 1}{\sigma + 1}$$

and the normal pulse current on the diffusion plateau is

$$i_{\text{NPV}} = nF AD^{\frac{1}{2}} \cdot \frac{C_b}{(\pi t_m)^{\frac{1}{2}}}$$

where A is the electrode area in cm^2 , D the diffusion coefficient of the reaction sample in cm^2/s , C_b the bulk concentration in mM, and t_m the time in seconds, measured from pulse application, at which the

current is measured. The peak height in DPV, while proportional to sample concentration, also depends on the electrochemical oxidation rate. The ratio

$$\frac{\sigma - 1}{\sigma + 1}$$

depends only on the number of electrons transferred and on pulse amplitude, ΔE , and is always less than one. For small values of the pulse amplitude, the ratio in eq. (II.8) can be approximated to

$$\frac{\sigma - 1}{\sigma + 1} = \frac{nF}{RT} \cdot \frac{\Delta E}{4} \quad (\text{II.9})$$

The peak shape can be described for small pulse amplitudes by differentiating eq. (II.6)

$$\frac{i(E)}{i_d} = \frac{nF}{RT} \cdot \frac{\Delta E}{(1 + \epsilon)^2} \quad (\text{II.10})$$

To define the peak half width, $W_{\frac{1}{2}}$, we wish to find the potentials at which the current is equal to half the peak current. To do this, we set half of the rhs of eq. (II.9) equal to the rhs of eq. (II.10)

$$\frac{nF}{RT} \cdot \frac{\Delta E}{2.4} = \frac{nF}{RT} \cdot \frac{\epsilon \Delta E}{(1 + \epsilon)^2}$$

The solution is

$$\epsilon = 3 \pm \sqrt{2}$$

or

$$W_{\frac{1}{2}} = E_+ - E_- = 3.52 \cdot \frac{RT}{nF} \quad (\text{II.11})$$

From eq. (II.11) we can conclude that for small pulse amplitudes the

peak width is independent of pulse amplitude and inversely proportional to the number of electrons transferred. $W_{\frac{1}{2}}$ is equal to about 90, 45, and 30 mV for $n = 1, 2$ and 3 respectively, at room temperature.

CHAPTER III

EXPERIMENTAL TECHNIQUES

1. INTRODUCTION

This chapter is a description of all the techniques necessary to perform one experiment. First, all the different apparatus used in HPLC, second, the electrochemical equipment and third, the actual procedure.

2. HIGH PRESSURE LIQUID CHROMATOGRAPHY

2.1 Packing Material

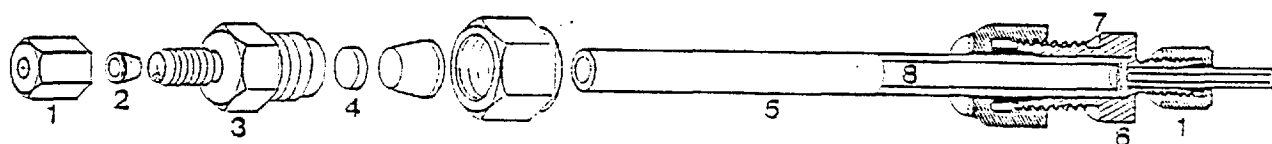
The column packing material is directly related to the type of eluent polarity. It is necessary here to use a highly polar eluent because it has to be at the same time the supporting electrolyte. The packing material for water-insoluble non-polar compounds is a non-polar stationary phase chemically bonded to the support material. This form of liquid chromatography is termed "bonded reverse phase chromatography".

In this work a LiChrosorb 10 RP 8 packing material was used. This is a totally porous chemically bonded reverse phase packing material irregularly shaped with 10 μm particle size. The functional group is

C_8 ($-(CH_2)_7-CH_3$) and the chemical bond is C-Si-O-Si; the pore diameter is 100 Å. The retention time in C_8 packing materials is less than with C_{18} , so an optimum reverse phase effect can be attained.

2.2 Columns

The column construction, the hardware used and the way the column is packed influence the optimal separation. In Fig. III.1 is shown the HPLC column used;



- 1 : 1/16" nut SS
- 2 : 1/16" ferrule SS
- 3 : Snubber injector side.
- 4 : Removable frit injector side.
- 5 : Handy and Harman LiChroma tubing.
- 6 : Removable frit detector side.
- 7 : Snubber detector side.
- 8 : Packing material.

Fig. III.1 - HPLC Column

the column is of a symmetrical design. Both ends are terminated by snubbers with a removable frit. All snubbers terminate on both sides in 1/16" Swagelok male connections, that seal off the column against pressures up to 12,000 psi. The tubing has a precision bore internal diameter with a smooth and polished wall, and the frits prevent loss of packing material and any damage on the packing bed. Connecting this column with the injector and the detector by means of low internal volume capillary tubing, with both tubings touching the first, all dead volume is eliminated. Any dead volume will act as a dilution

vessel and will mix up the sample with the mobile phase which broadens the peak so giving poorer efficiencies and less sample detectability.

There is a limited length of the column with a maximum number of theoretical plates. As column length depends on the internal diameter, on the particle size of the packing material, and on the packing method, there is an optimum length for each case. The column used has the optimum length of 25 cm for 10 μm particle size and 4.6 mm i.d. and the frit's pore diameter is 2.0 μm .

2.3 Injection

The sample valve injection uses a simple principle. An external sample loop is filled at atmospheric pressure with the sample; then, by switching of the rotator the sample loop or cavity is placed in the flow lines and the sample is swept onto the column by the eluent.

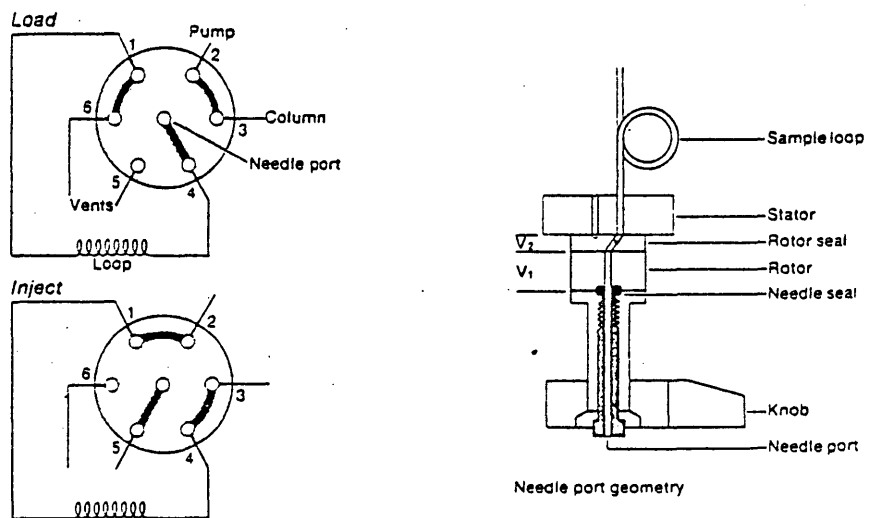


Fig. III.2 - Injection valve

After injection, the rotator is switched back and the sample loop or cavity can be filled with the next sample.

The valve, Fig. III.2, used is the Rheodyne model 7120, with 20 μ l or 200 μ l capacity. The stator and rotor are Type 316 stainless steel. The rotor seal is a disc of Vespel, a high-performance inert polyimide which has chemical inertness and sufficient mechanical strength to hold 7000 psi pressure.

2.4 Pumps

The pressure used for the HPLC separation was 1000 psi and was obtained using a Model 396 Milton Roy Instrument Mini Pump. The Mini Pump has a low internal dead volume and a constant volume delivery is obtained through the use of a positive displacement reciprocating plunger assembly.

For flow injection analysis a LKB-Varioperpex peristaltic pump was used.

3. ELECTROCHEMISTRY

3.1 Instrumentation

During this work the apparatus used was the Polarographic Analyzer, model 174, manufactured by Princeton Applied Research Corporation (PAR), capable of performing normal and sampled DC polarography, pulse polarography, differential pulse polarography, linear sweep voltammetry at a stationary electrode, and anodic stripping analysis. The modes

of operation used were differential pulse (sec. 4.3, Ch. II) and controlled potential voltammetry. The constant potential applied during flow injection was chosen higher than the oxidation potential of the species injected.

The recorder used was a Servoscribe RE511.20 and 20 nA was the maximum full-scale current readout.

3.2 Cells

Two different types of cells have been used for this work. A typical polarographic cell has been used in stationary solution measurements, Fig. III.3 A, and the wall-jet cell has been used in flow systems, Fig. III.3 B. This cell is a practical application of the wall-jet principle. The main parts are:

- (1) the body, made of KEL-F plastic, resistant to organic solvents;
- (2) the working electrode, a disc of glassy carbon embedded in a KEL-F body and connected to a copper wire with silver epoxy araldite;
- (3) the counter electrode, a platinum tube downstream of the working electrode and at the same time acting as outlet of the cell;
- (4) the reference electrode, a silver/silver chloride electrode.

To coat the silver electrode with AgCl the silver wire is first cleaned with 3M nitric acid, washed thoroughly with water, and put in a cell. The silver is coated with the silver chloride at a current density of $\sim 0.4 \text{ mA cm}^{-2}$ for about 30 min, using 0.1 M HCl as the electrolyte. The electrode is washed and allowed to age for one to two days in 1M KCl.

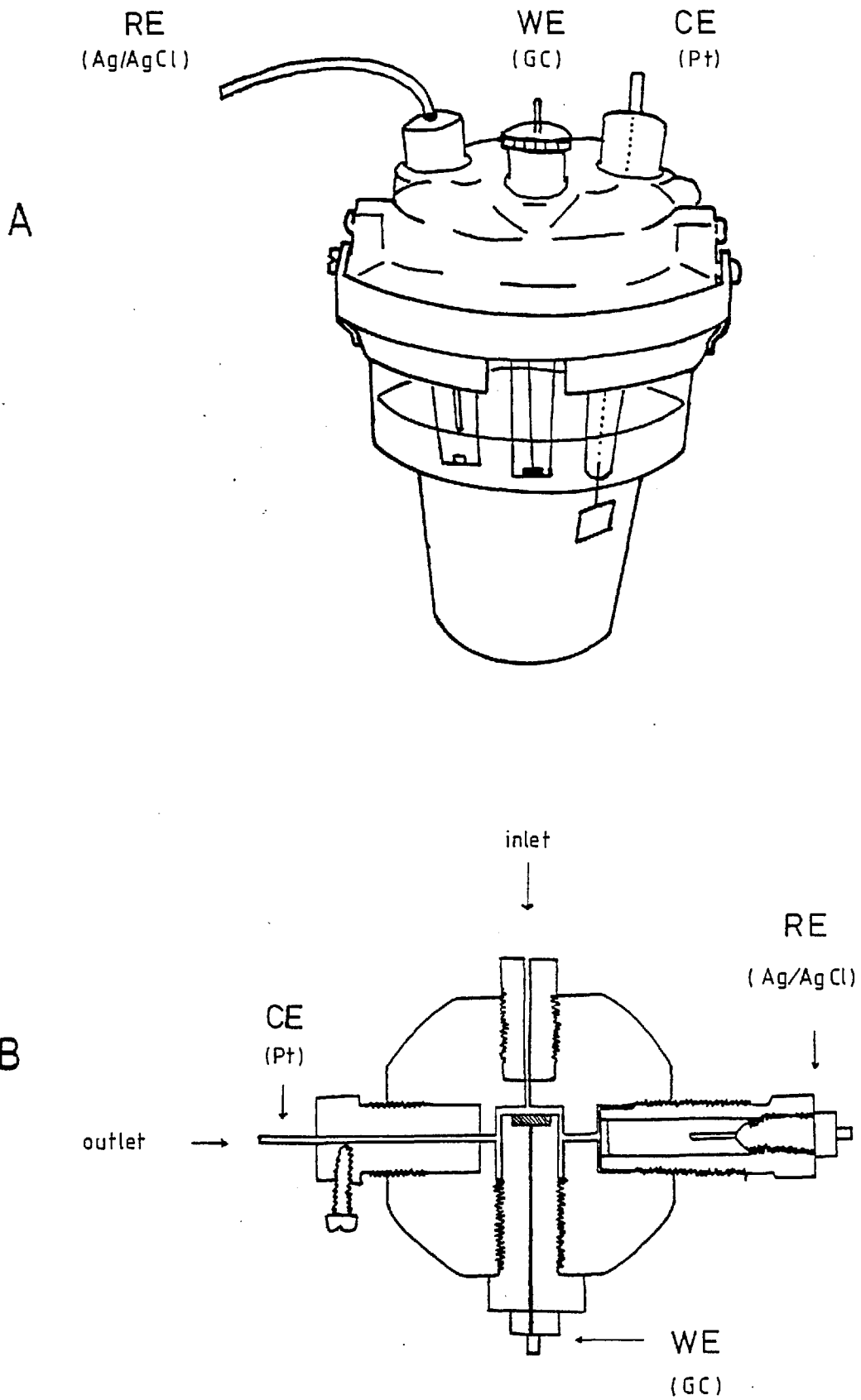


Fig.III.3 - Cells: A - Stationary Cell.

B - Wall-jet Cell.

4. PROCEDURES

4.1 Solution Conditions

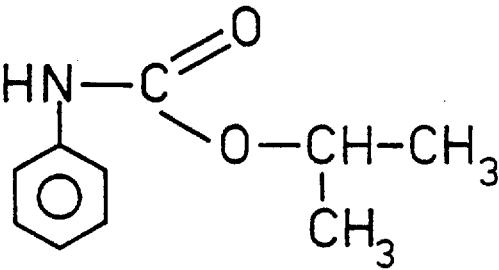
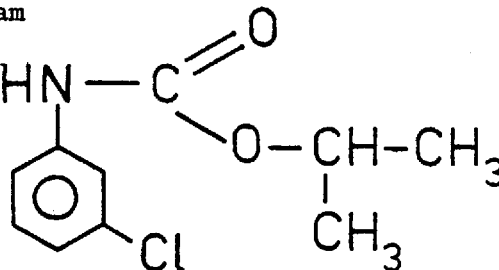
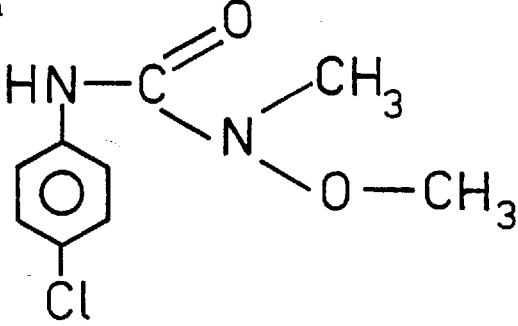
The chemicals used were AnalaR grade and all the aqueous solutions were made using deionised, double distilled water. The samples, Table III.1, were supplied by Murphy Chemical Ltd., and they are divided into two groups: ureas and carbamates. All samples were soluble in ethanol: aqueous solution, 1 : 1. The buffers used are tabulated in Table III.2.

4.2 Experimental Conditions

All the experiments have been carried out at room temperature and the solutions were not deoxygenated:

- (a) In the stationary solution measurements the supporting electrolytes were a 1 : 1 solution of Ethanol : Buffer and the concentration of Chloroxuron was 10^{-5} M.
- (b) In continuous flow analysis the supporting electrolyte was 1 : 1, Ethanol : Acetate Buffer, pH 4.75 and the concentration of Diuron was 10^{-4} M or 10^{-5} M, and the flow rate $0.01 \text{ cm}^3 \text{ S}^{-1}$;
- (c) In flow injection analysis the same supporting electrolyte and flow rate as above were used and 20 μl of the sample, with concentrations from 10^{-5} M \rightarrow 10^{-3} M, were injected with the Rheodyne valve, at a constant potential of + 1.4 V vs. (Ag/AgCl).
- (d) In HPLC detection as (c) except that the volume injected was 200 μl .

Table III.1 - Structures of the herbicides

COMPOUND	PURITY
<u>CARBAMATES</u>	
Propham 	—
Chlorpropham 	—
<u>UREAS</u>	
Monolinuron 	—

/continued...

Table III.1/continued...

COMPOUND	PURITY
UREAS Linuron	Tech. grade
Metabromuron	Tech. 83.8%
Chlorbromuron	Tech. 96.5%
Fenuron	—
Diuron	Tech. 98%

/continued...

Table III.1/continued...

COMPOUND	PURITY
<u>UREAS</u>	
Chlortoluron	
	—
Fluometuron	
	Tech. 97.8%
Chloroxuron	
	Tech. 98.5%

Table III.2 - Supporting Electrolytes

BUFFER (diluted to 100 ml)	Supporting Electrolyte pH
0.2 M KCl (25 ml) + 0.2 M HCl (42.5 ml)	1.2
0.2 M KCl (25 ml) + 0.2 M HCl (6.5 ml)	2.02
0.2 M NaAcO (3.7 ml) + 0.2 M HAcO (46.3 ml)	3.4
0.2 M NaAcO (13.2 ml) + 0.2 M HAcO (36.8 ml)	4.3
1 M NaAcO (7.2 ml) + 1 M HAcO (12.5 ml)	4.5
0.2 M NaAcO (41.2 ml) + 0.2 M HAcO (8.8 ml)	5.4
0.2 M Na ₂ HPO ₄ (6.15 ml) + 0.2 M NaH ₂ PO ₄ (43.85 ml)	6.08
0.2 M Na ₂ HPO ₄ (30.5 ml) + 0.2 M NaH ₂ PO ₄ (19.5 ml)	6.9
0.2 M Na ₂ HPO ₄ (47.35 ml) + 0.2 M NaH ₂ PO ₄ (2.65 ml)	8.05
0.025M Na ₂ B ₄ O ₇ ·10H ₂ O (50 ml) + 0.1M NaOH (3.0 ml)	9.25
0.2 M KCl (25 ml) + 0.2 M NaOH (6.0 ml)	12.04
0.2 M KCl (25 ml) + 0.2 M NaOH (42.0 ml)	12.85

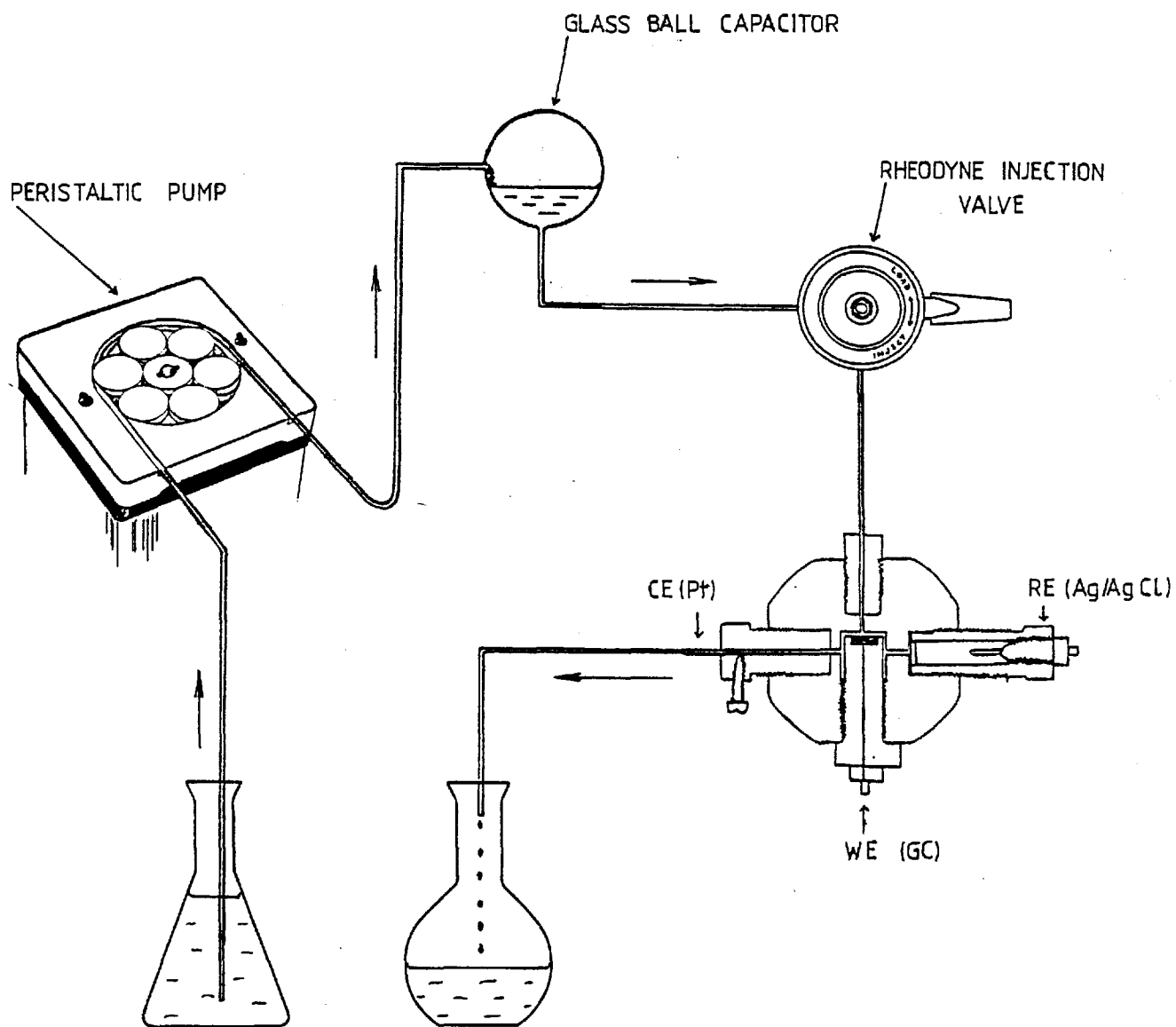


Fig. III.4 - Flow Analysis Experimental Assembly.

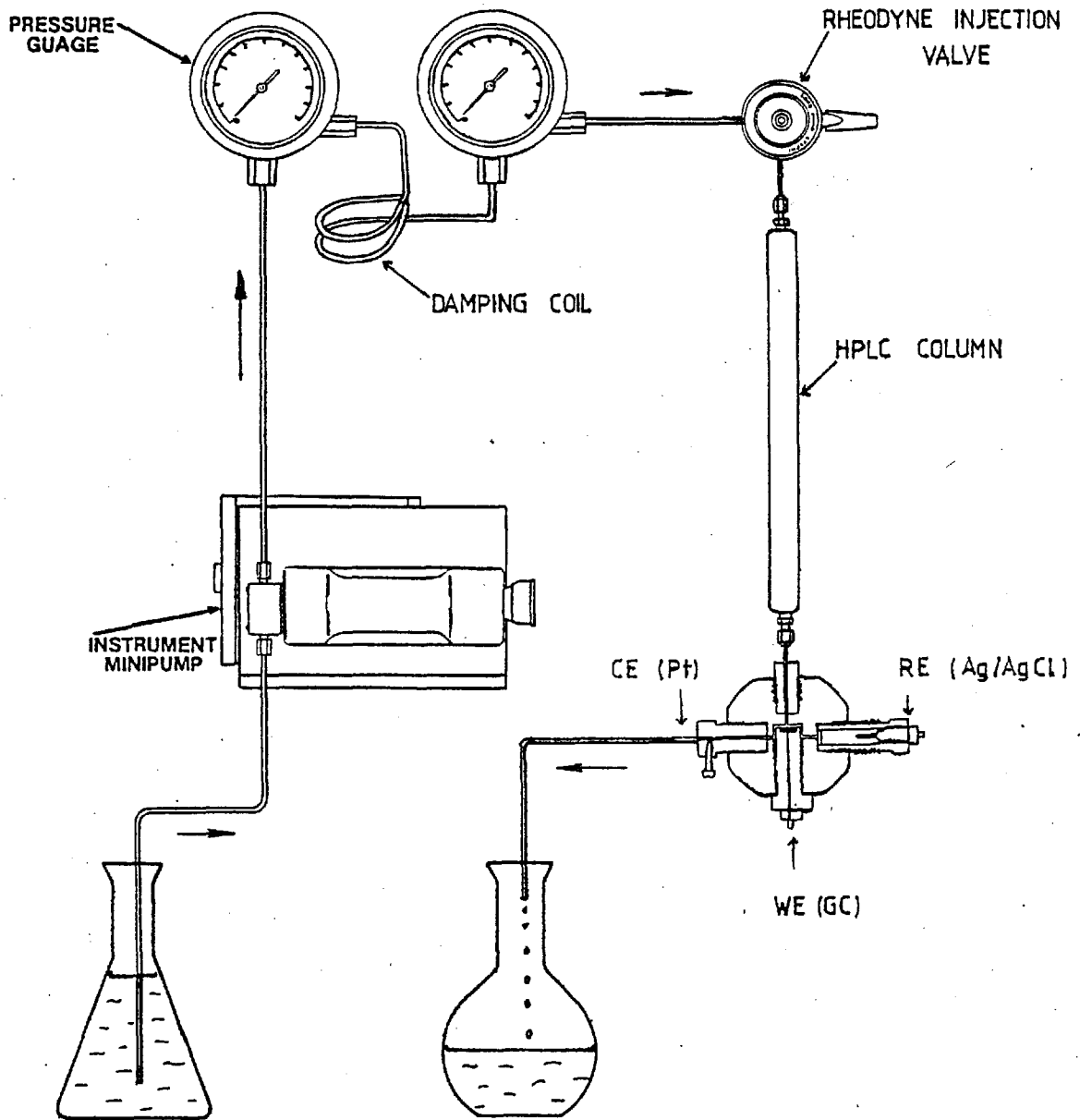


Fig. III.5 - HPLC Detection Experimental Assembly.

4.3 Experimental set up

In flow analysis the supporting electrolyte is pumped from an Erlenmeyer, Fig. III.4 , passes through a glass ball capacitor, to minimise the pump pulses, through the injector valve, the wall-jet cell and then to waste. In continuous flow analysis the sample is pumped with the supporting electrolyte. In flow injection analysis the sample is injected into the flow stream.

For HPLC detection the supporting electrolyte is pumped from an Erlenmeyer, Fig.III.5 , passes through the pressures gauges and a damping coil , to avoid the pump pulses, through the injector valve, the HPLC column, the wall-jet cell and then to waste. The sample is injected into the flow stream.

CHAPTER IV

OXIDATION MECHANISM

I. INTRODUCTION

The herbicidal families of urea and carbamates act as inhibition sites in photosynthetic electron flow (24). A common basic chemical element essential for inhibition became apparent as a sp^2 hybrid -C-N- bound to a lipophilic "carrier" (say phenyl) for inhibition, (see structure of chloroxuron). The photosynthetic flow system is localised in the inner thylakoid membrane of the chloroplast.

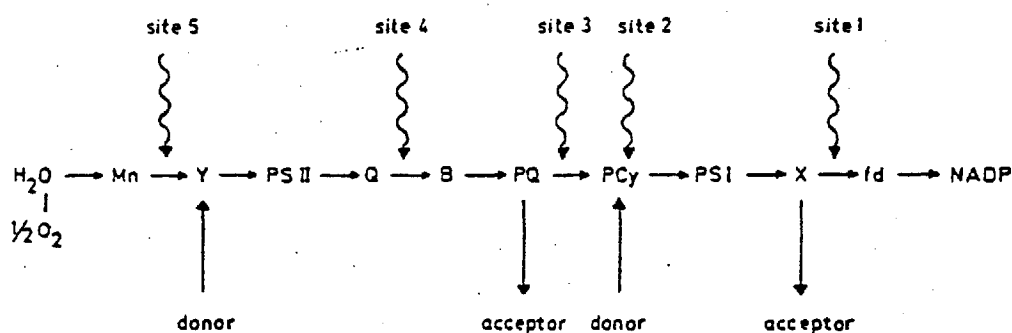
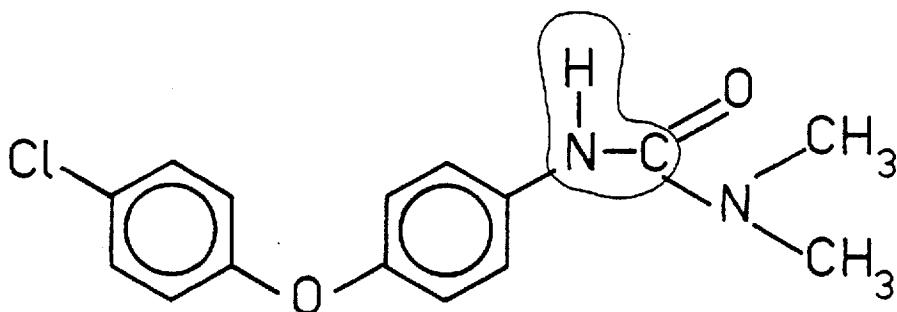


Fig. IV.1 - Inhibition sites and artificial electron donor and acceptor systems in photosynthetic electron flow from water to NADP.

PS = photosystems; Mn = manganese in the oxygen evolution system; Q and B = primary and secondary acceptor of PS II = quenchers of chlorophyll fluorescence = special forms of plastoquinone; PQ = plastoquinone; PCy = plastocyanin; X = primary acceptor of PS I; fd = ferredoxin.

There are, so far, five possible areas of attack of inhibitors on components along the photosynthetic electron flow system. The urea herbicides are acting at site 4 (see Fig. IV.1).

The electrochemical detection of the herbicides made us interested in explaining the possible oxidation mechanism of this type of compound. As it is necessary to have a very clear, well defined peak to enable us to study the mechanism, we selected chloroxuron: this compound oxidizes at less positive potentials and has very well defined voltammograms, Fig. IV.2. The molecular structure of chloroxuron is



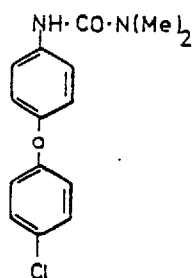
In the oxidation of chloroxuron we are interested to know the degradation mechanism.

2. pH MEASUREMENTS

The experimental technique has already been described (Chapter III, Sections 3 and 4) and the results are plotted in Fig. IV.3 to IV.8.

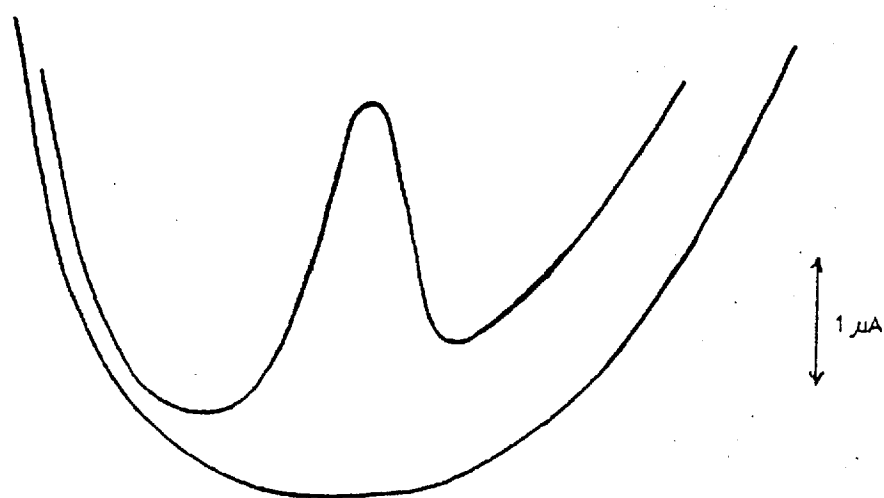
The results shown in Fig. IV.3 may suggest that the electrode process involves several reactions. The oxidation of chloroxuron

CHLOROXYURON

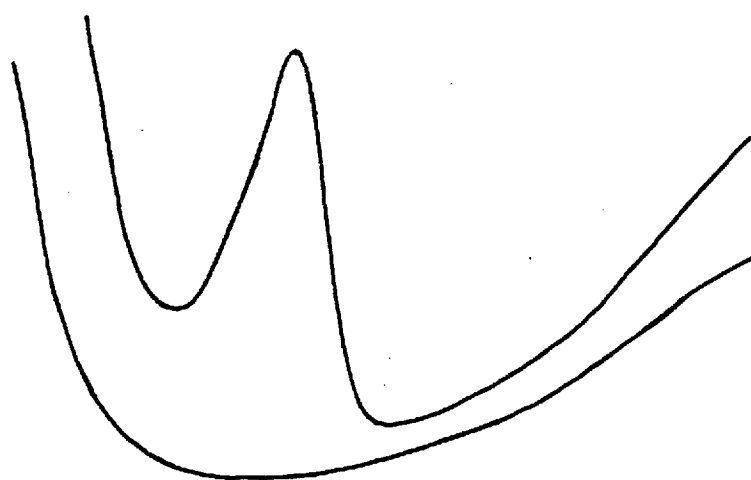
 10^{-5} M
 I | 5% Ethanol
 | 10^{-2} M KOH

 II | 5% Ethanol
 | 10^{-2} M KCl

II



I

V
(vs. Ag/AgCl)

0.9

.0.1

Fig. IV.2 - D.P. Voltammogram of Chloroxuron.

CHLOROXYURON

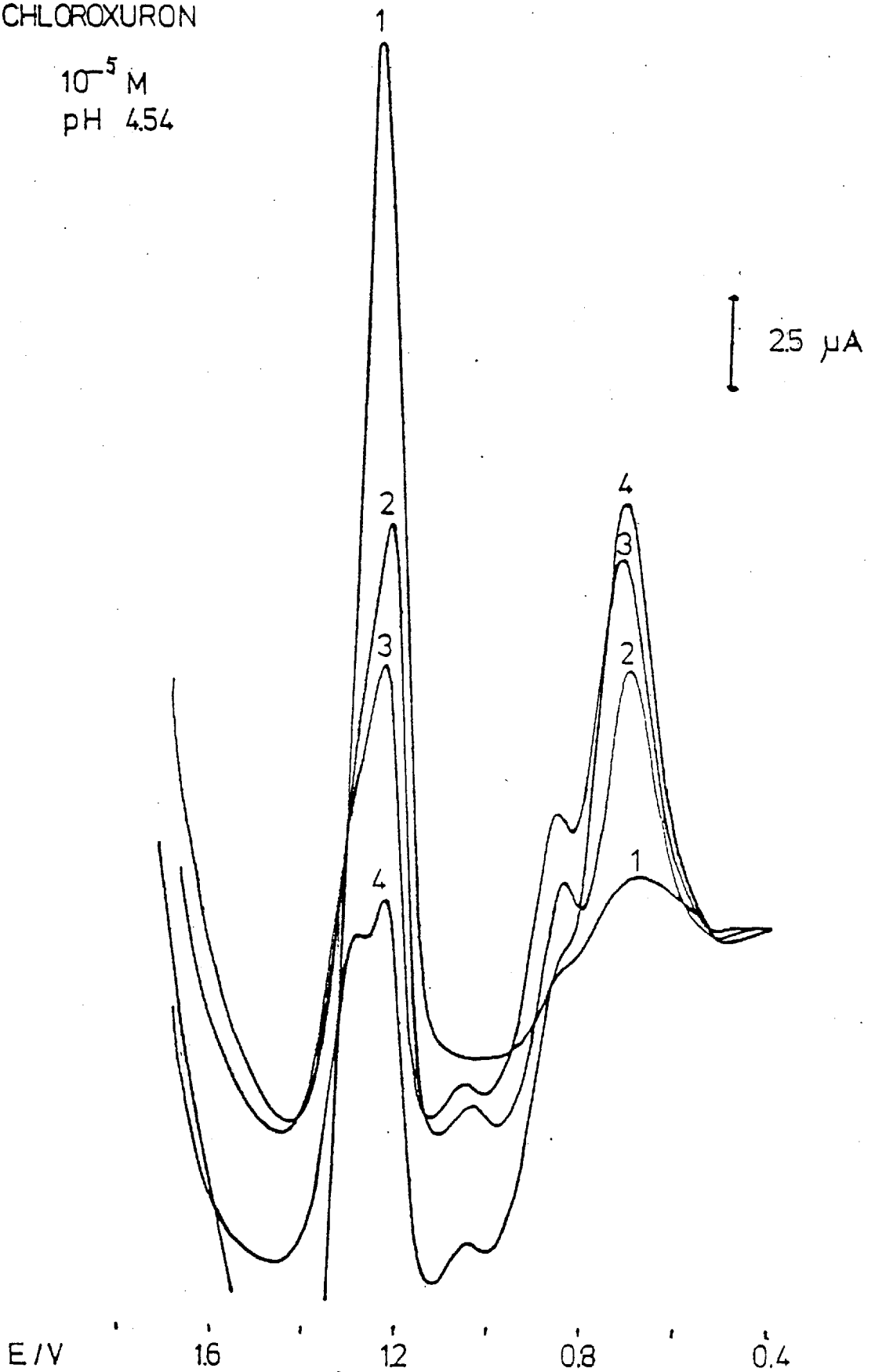
 10^{-5} M
pH 4.54

Fig. IV.3 - Successive Voltammograms of Chloroxyuron.

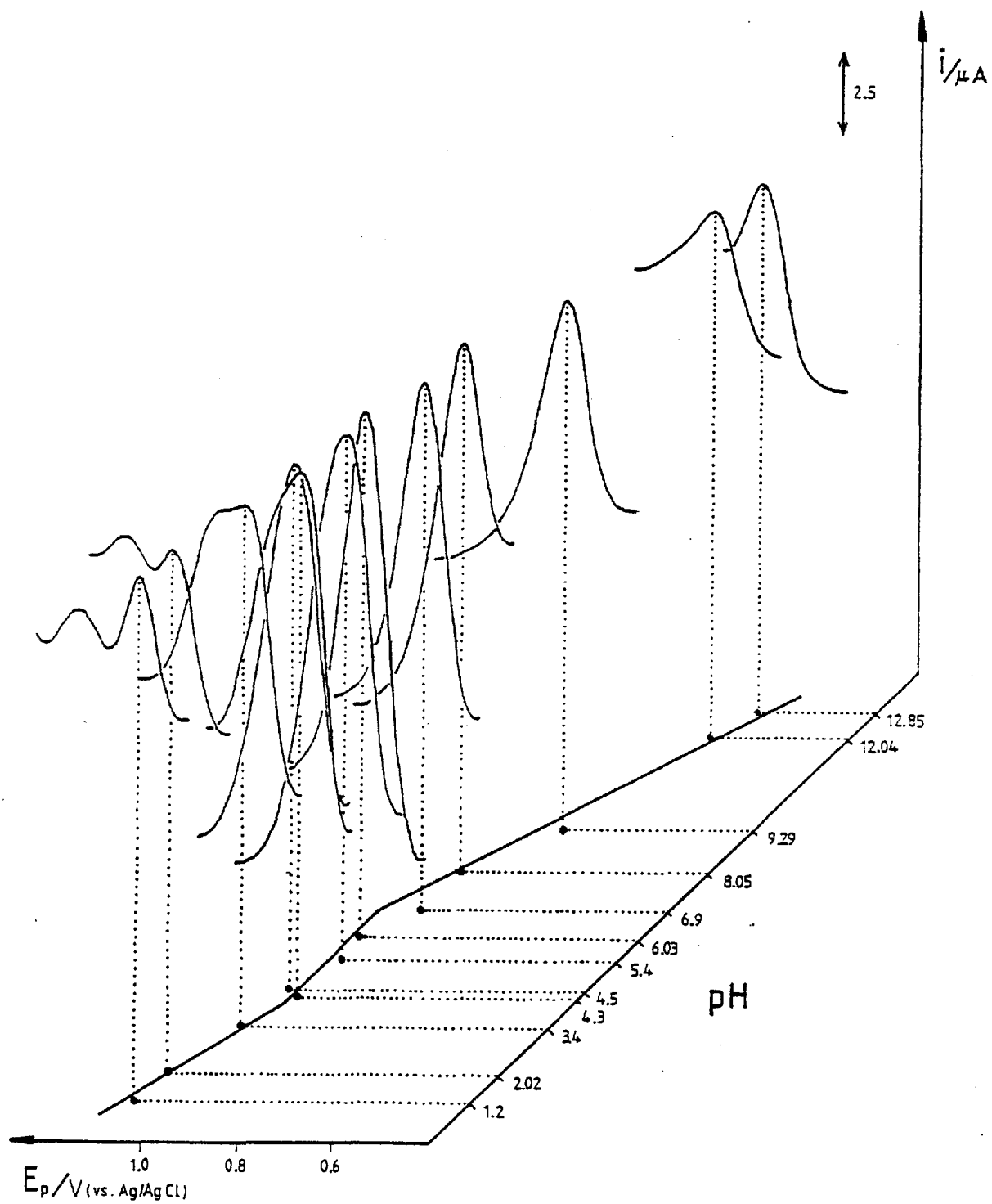


Fig. IV.4 - Oxidation of Chloroxuron at different pH.

(peak A) causes the depletion of the compound at the surface of the electrode but the products adsorbed to the surface of the electrode will themselves be oxidised (peaks B, C and D).

The oxidation potentials have been measured over a wide range of pH. The three dimensional plot in Fig. IV.4 shows progressive change in the oxidation peak with pH. In this plot we can see that the peak potential changes to less positive values when the pH is increased. On the y axis is drawn the peak observed at each different pH and we measured the peak current. The value of the half width of each peak remains approximately constant and is plotted against pH in Fig. IV.5(a).

According to Osteryoung's differential pulse theory (89) the values of 100 mV for the half width of the peaks implies that the number of electrons transferred $n = 1$. The first step is a one electron transfer followed by subsequent oxidation of the products.

In Fig. IV.5 (b) is plotted the variation of the oxidation potentials of chloroxuron and oxidation products with pH. The results for the products are designated by B, C and D in agreement with Fig. IV.3's notation of the peaks. The dotted line corresponds to 59 mV per unit of pH. We are going to examine in detail the results corresponding to peak A. For low and high values of pH we have good lines parallel to the dotted line and between pH 4.3 and 7.5 there is no change in the potential with pH.

In acid media the E_p is higher so the rate constant, k' , is smaller, i.e. it is more difficult to oxidise the compound. If we now (from Fig. IV.4) plot $\log k'$ against pH it will look like Fig. IV.6:

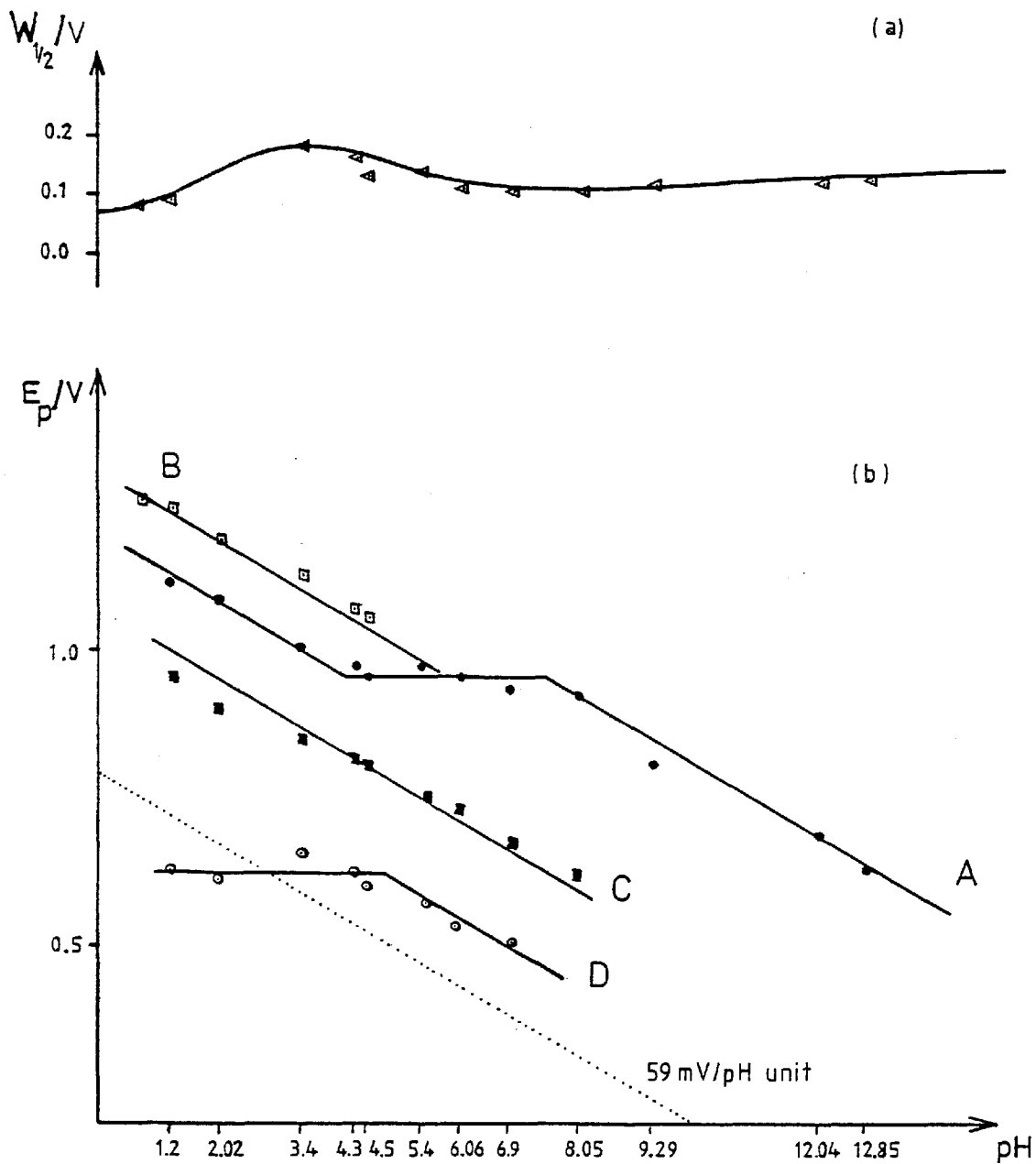


Fig. IV.5 — (a) Variation of half-width, $W_{1/2}$, with pH.

(b) Variation of peak potential, E_p , with pH.

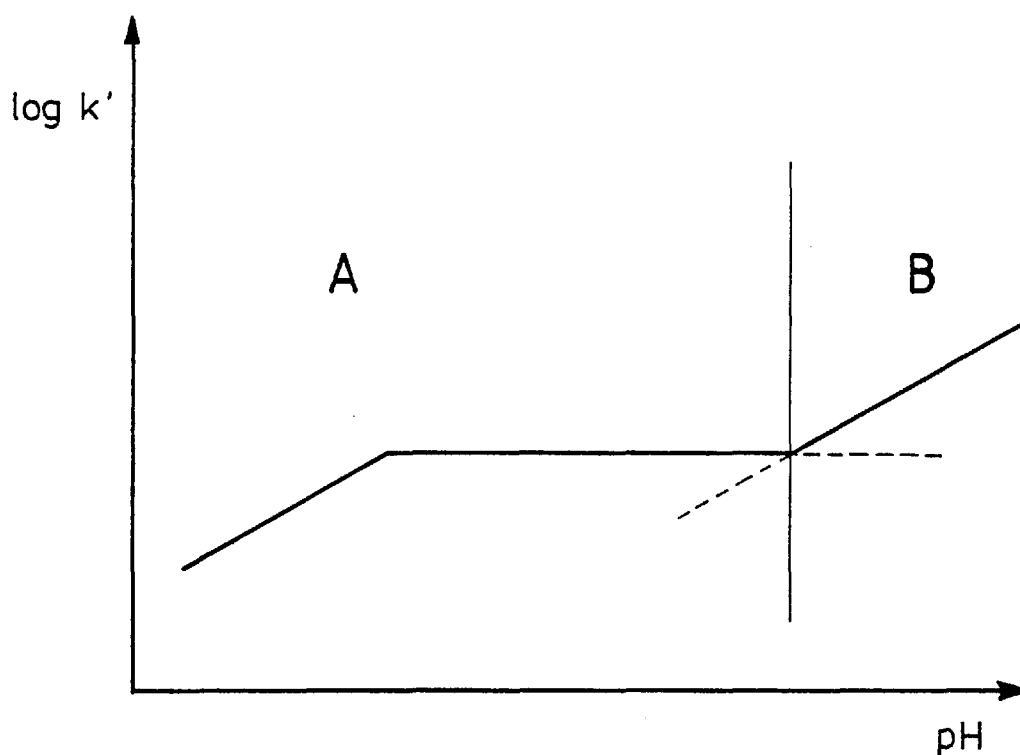


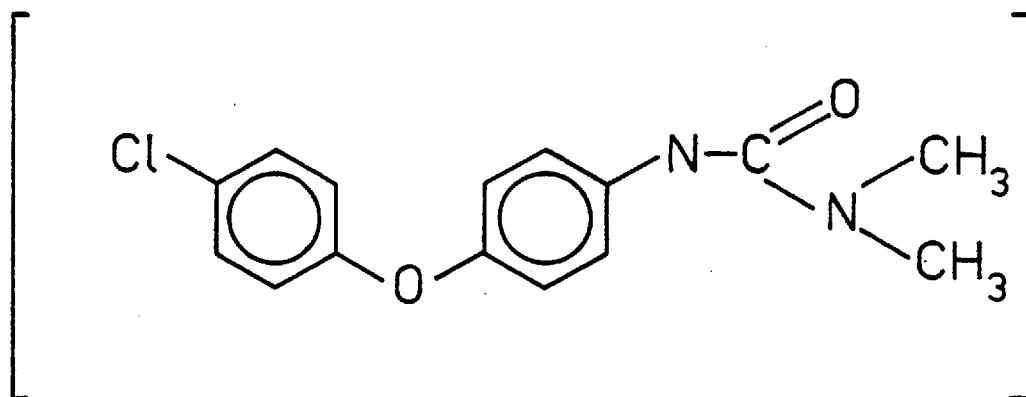
Fig. IV.6 - Plot of $\log k'$ against pH

and we can analyse the two parts A and B. In part A we have two consecutive reactions and the step with smaller rate constant is the rate determining step. Part B corresponds to parallel reactions and it is the reaction which proceeds with the greatest velocity that characterises the kinetics. We know now that the mechanism proceeds through two consecutive reactions at low pH and two parallel reactions at higher pH and we are going to interpret this using the scheme of squares.

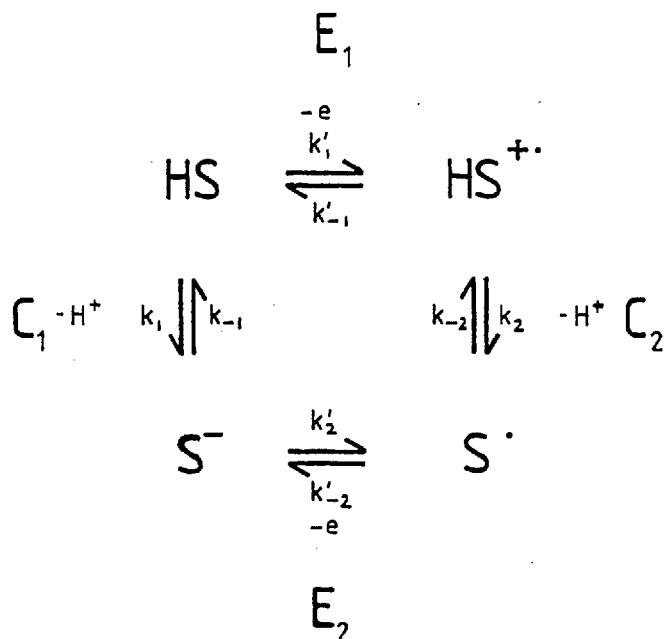
3. SCHEME OF SQUARES

The mechanism of oxidation of chloroxuron is a complex reaction with chemical step and electron transfer. In Chapter I, it was mentioned

that the scheme of squares (33) would be used to explain the electrode mechanism. Chloroxuron is going to be labelled HS, where S is



we consider that the chemical steps involved are proton transfers. A scheme of electron and proton transfers in the oxidation of chloroxuron is



The rate constant of electron transfer is given by

$$k'_{in} = k'_{\pm, E_0} \exp \left(\frac{\alpha E_1 F}{RT} \right)$$

and taking logarithms,

$$\log k'_{\pm n} = \log k'_{\pm n, E_0} + \frac{\alpha E_{\frac{1}{2}} F}{RT} \quad (\text{IV.1})$$

and

$$\log k'_{E_0} = \log (k'_{E=0})_{\text{pH}=0} \pm npH \quad (\text{IV.2})$$

Substituting (IV.2) in (IV.1) we obtain,

$$\log (k'_{E=0})_{\text{pH}=0} \pm npH + \frac{\alpha E_{\frac{1}{2}} F}{RT} = \log k'_{\pm n}$$

and

$$\frac{d E_{\frac{1}{2}}}{d \text{pH}} = \pm \frac{n}{\alpha} \left(\frac{RT}{F} \right)$$

Assuming that α , the transfer coefficient for each electron transfer, is $\frac{1}{2}$,

$$\log k'_{\pm n} = (\log k'_{\pm n, P_0}) \pm P$$

where

$$P = E_{\frac{1}{2}} F / 4.606 RT$$

and is a non-dimensional variable.

When we plot the variation of $\log k'_{\pm n}$ with P , the slope is ± 1 when the first electron transfer is rate determining, and ± 3 when there is a pre-equilibrium followed by a second rate determining electron transfer.

We now consider the complications introduced by the proton transfer. The analysis into a scheme of squares has been discussed assuming that the proton and electron transfer in it take place separately. The proton transfers between oxygen and nitrogen bases in aqueous solutions are very rapid.

In the square HS and S[•] are the more stable species and HS⁺ and S⁻ are higher energy intermediates. Each route can either have rate-determining electron or proton transfer. This depends on whether the intermediate, either HS⁺ or S⁻, is more likely to form S[•] or SH. One cannot compare directly k'₋₁, for instance, with k₂ because the former is a heterogeneous and the latter a homogeneous rate constant.

The critical condition of a CE mechanism concerns the relative sizes of k'₂ and D/μ. When the rate determining step is the electron transfer,

$$k'_2 \ll \frac{D}{\mu}$$

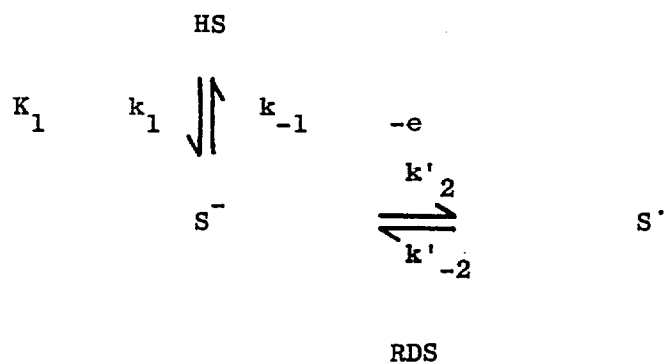
where

$$\mu = \sqrt{\frac{D}{k_1 + k_{-1}}}$$

and D is the diffusion coefficient,

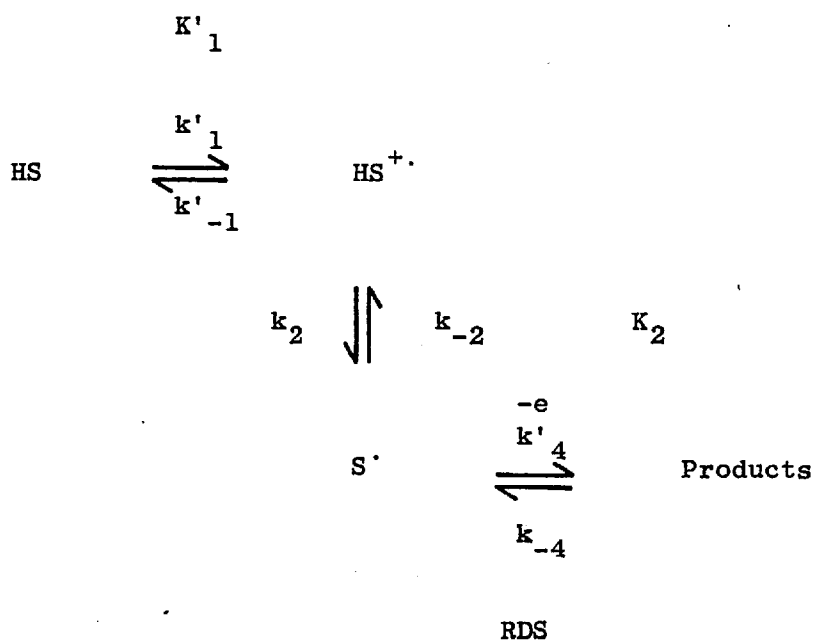
$$\text{rate} = K_1 k'_2 [\text{OH}^-] [\text{HS}]$$

where $K_1 = k_1/k_{-1}$ and the mechanism followed for higher pH is



corresponding to part B in Fig. IV.6.

For low pH a pre-equilibrium proton transfer followed by a second rate determining electron transfer is observed. The mechanism is thus,



and here

$$k'_{-4} \ll \frac{D}{\mu}$$

$$\text{rate} = k'_4 K'_1 K_2 [\text{HS}]$$

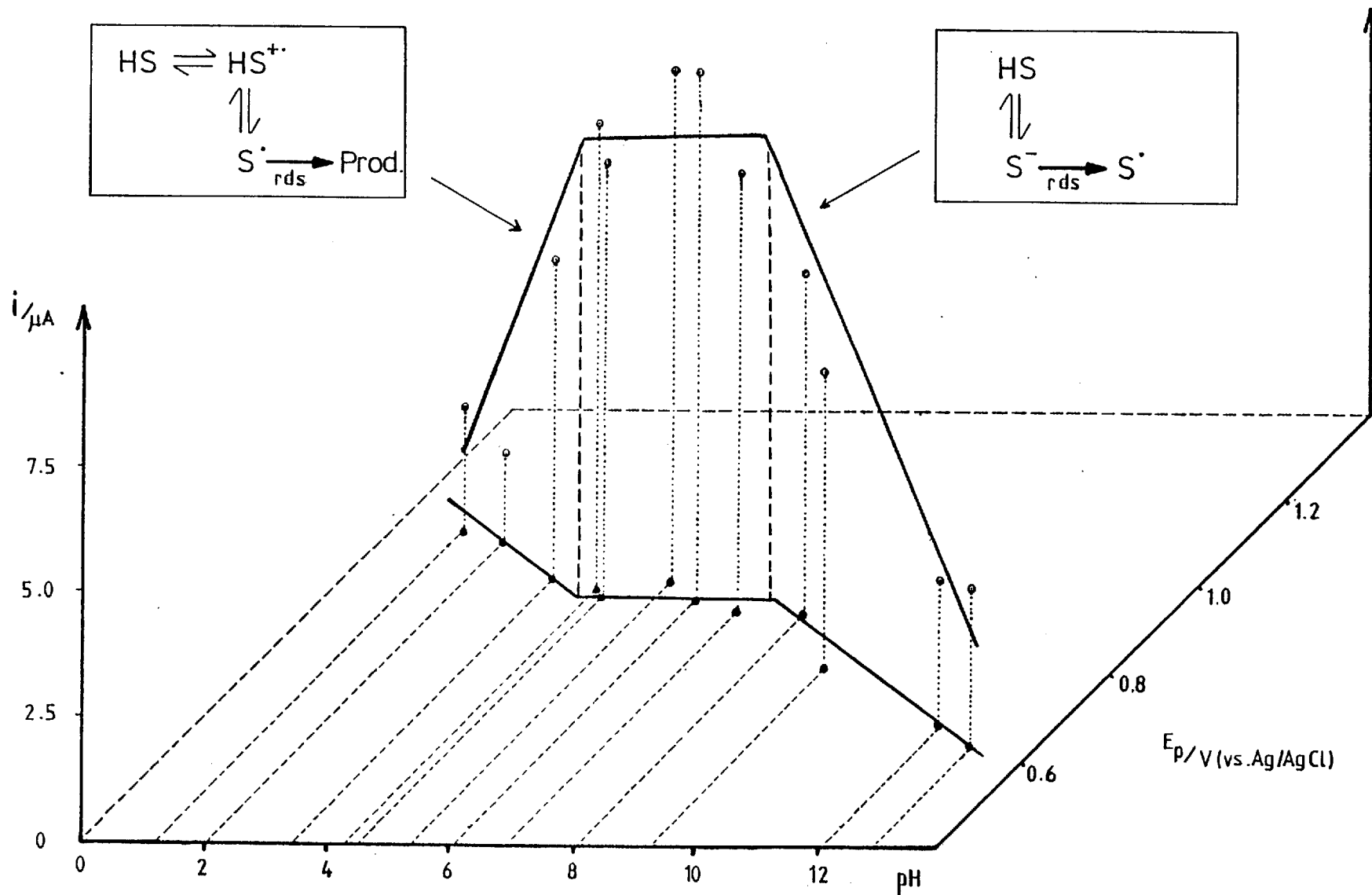


Fig. IV.7 - Variations in the oxidation of chloroxuron with pH.

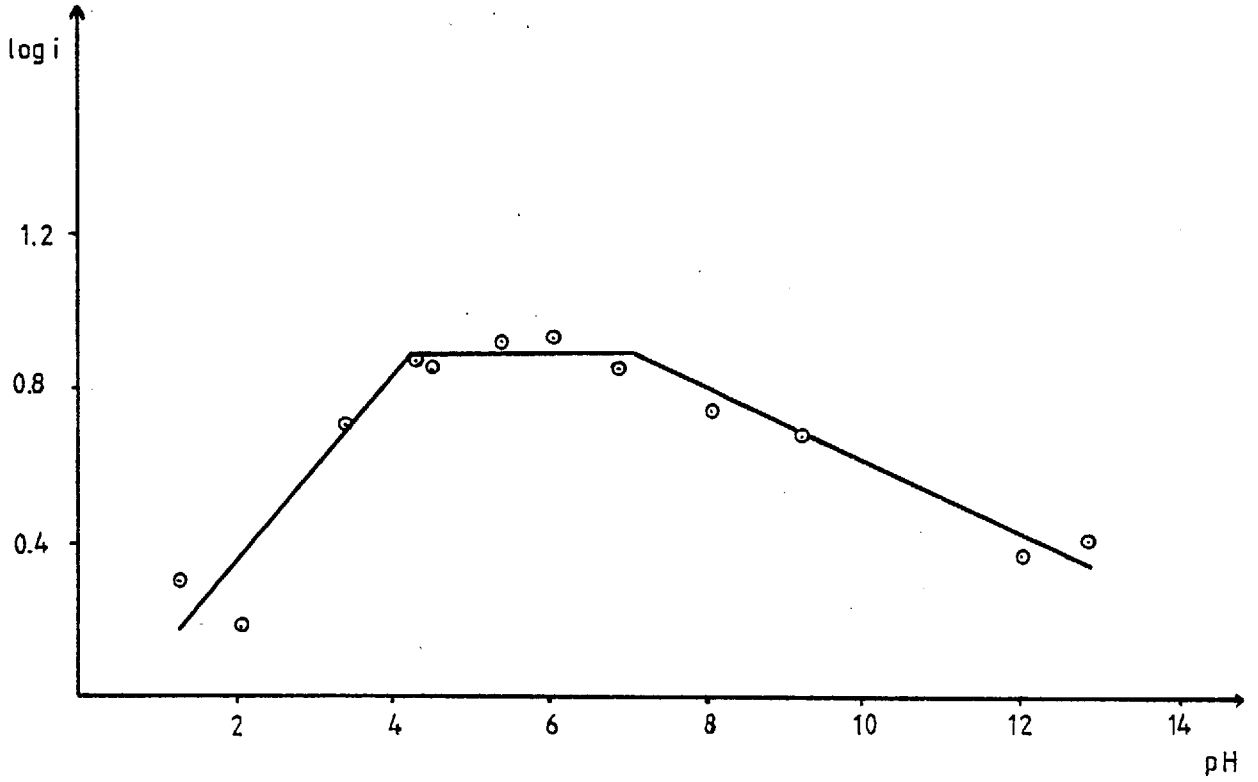


Fig. IV.8 - Plot of $\log i$ versus pH.

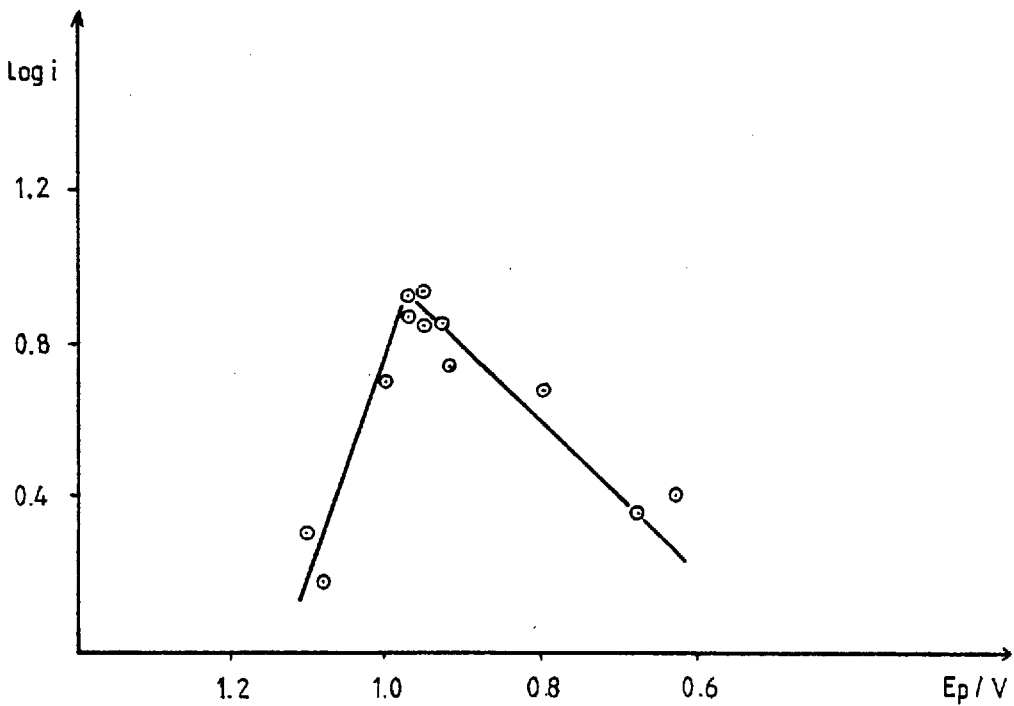


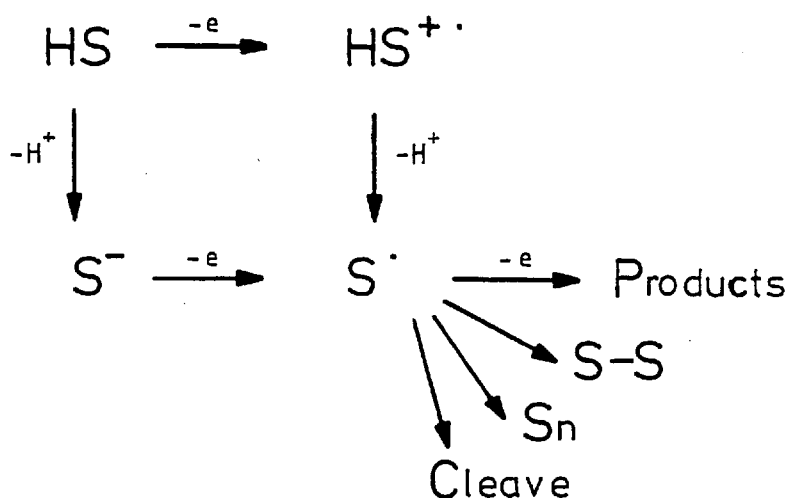
Fig. IV.9 - Plot of $\log i$ versus observed E_p .

This is the two consecutive reactions mechanism followed for low pH, corresponding to part A in Fig. IV.6.

The results shown in Figs. IV.7, IV.8 and IV.9 are plots of i and $\log i$ versus pH and observed E_p (see Appendix). These are not understood and several factors can be considered as causes for the decrease in current: the state of electrode surface; change in the number of electrons transferred due to dimerisation; the formation of a non-electroactive S; or change in the diffusion coefficient of chloroxuron at extremes of pH.

4. CONCLUSIONS

The pathways of the oxidation mechanism of chloroxuron follow different routes according to the pH of the medium.



The product S^{\cdot} may dimerize, polymerize, oxidize or cleave. From Fig. IV.1 we believe that it oxidizes and subsequently forms an unreactive film on the surface of the electrode.

CHAPTER V

FLOW SYSTEMS

1. INTRODUCTION

In this chapter we are going to deal with three different aspects of electroanalytical flow detection. We consider first the case where the electroactive compound is injected into the flow stream just before the detector and afterwards the case where several compounds are separated by High Pressure Liquid Chromatography before arriving at the detector.

2. ELECTROANALYTICAL DETECTION WITHOUT PREVIOUS SEPARATION.

The experimental technique has already been described (Chapter III, sections 2.4, 3. and 4.) and Fig. III.4 shows the experimental apparatus.

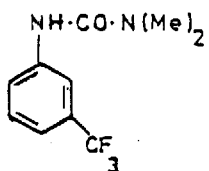
2.1 Continuous flow analysis

The objective of this analysis was to test the reproducibility of

ADSORPTION OF PRODUCTS OF ELECTRODE PROCESSES

FLUOMETURON

10^{-4} M



5% Ethanol
 10^{-2} M KOH

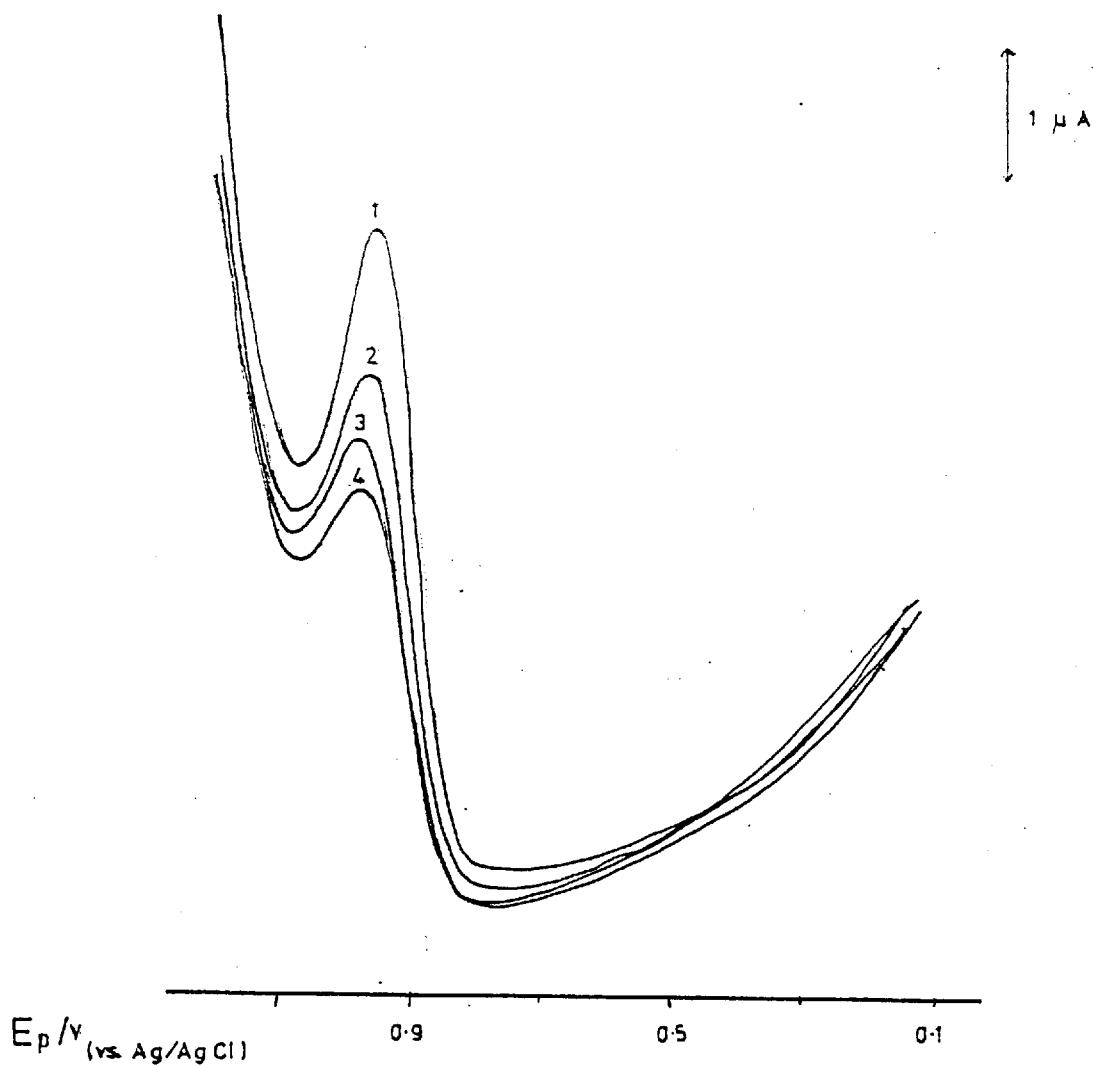


Fig. V.1 - D.P. Voltammogram of Fluometuron.

DIURON

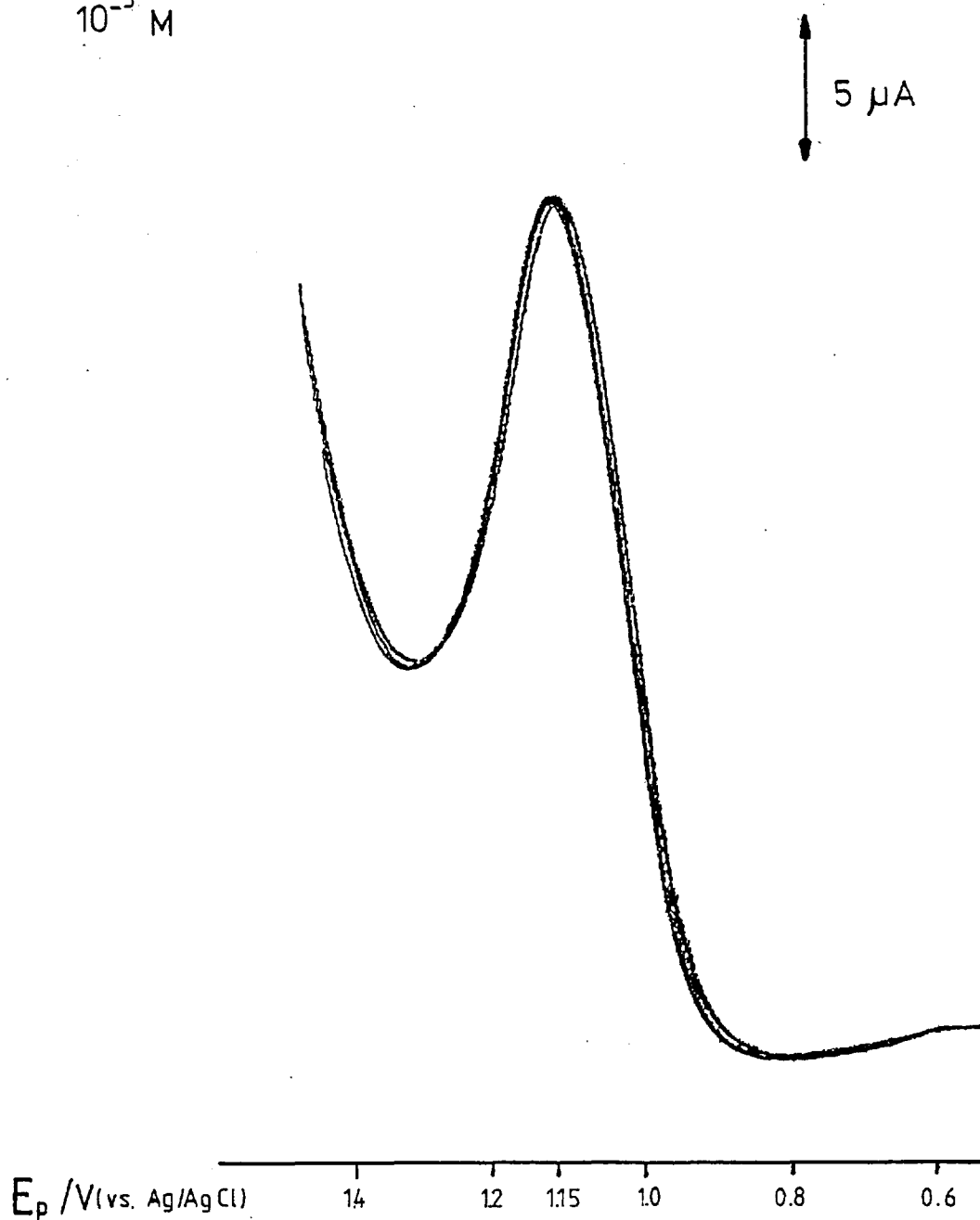
 10^{-3} M

Fig. V.2 - Continuous Flow Voltammogram of Diuron.

the wall-jet cell using differential pulse. As we have seen (Chapter IV) the urea compounds' oxidation mechanism will lead to the formation of a film on the surface of the solid electrode. In Fig. V.1 is shown the effects of the adsorption products of the electrode processes for a particular compound, fluometuron, in a stationary solution. The poisoning effects on the electrode were found for all the other compounds.

In Continuous Flow Analysis the jet impinges on the electrode and fresh solution is continuously arriving to its surface. We chose one of the compounds, diuron to do the voltammograms. It was found, Fig. V.2, that we could increase its concentration in the solution up to 10^{-3} M without poisoning the electrode. The reproducibility is very good over, at least, 17 scans. But using continuous flow it was only possible to detect concentrations as low as 10^{-4} M because the signal to noise ratio became too small.

2.2 Flow Injection Analysis

We now know that the wall-jet cell employed in this work has good reproducibility and can be used in flow systems. Continuous Flow Analysis is not a quick method as we have to clean the whole system before a new sample is put through. If we inject the sample into the carrier stream, which in electrochemistry is the supporting electrolyte, we have a higher sample through-put. In this Flow Injection Analysis (FIA), the sample is introduced as a plug via a valve, the mixing is mainly a diffusion-controlled process and the response has the form of a sharp peak.

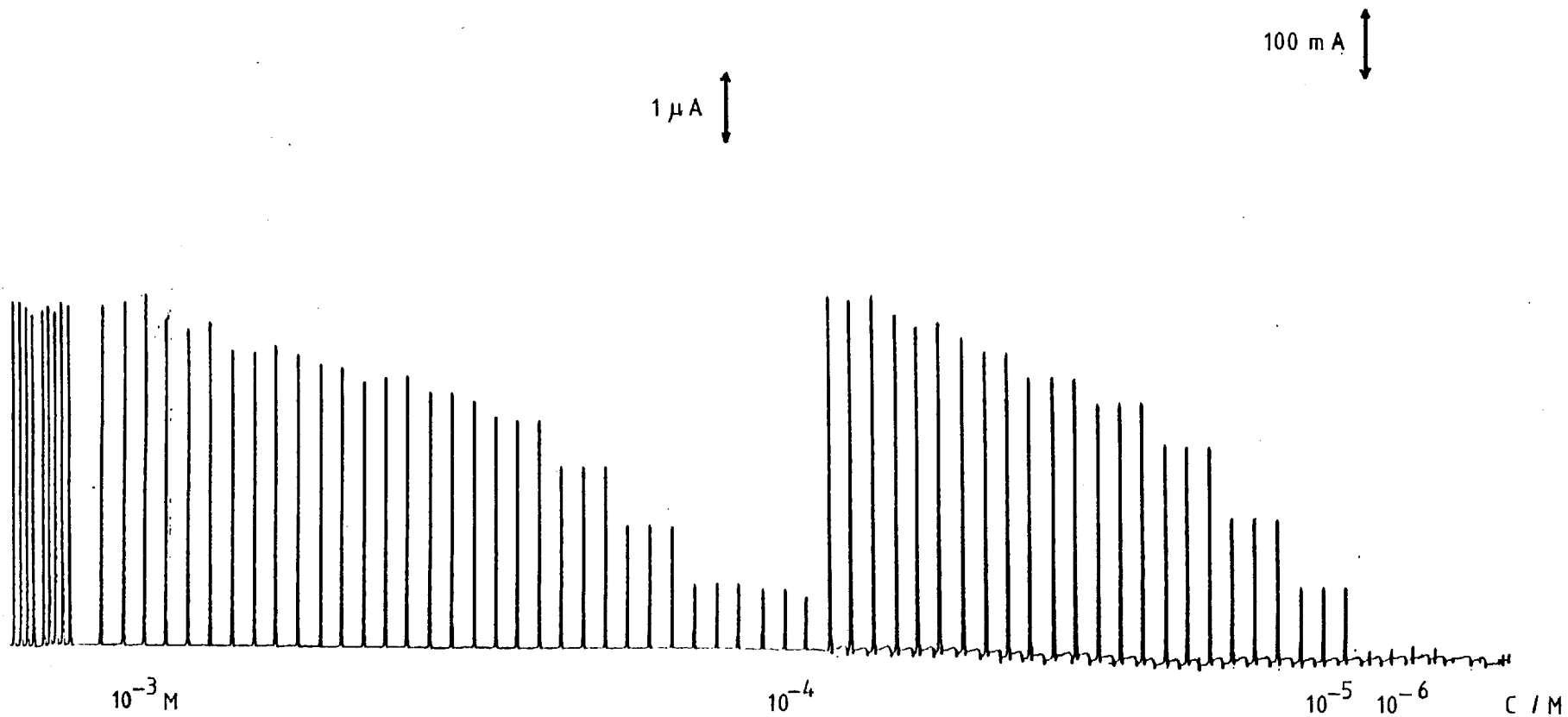


Fig. V.3 - Injection Calibration for Fluometuron.

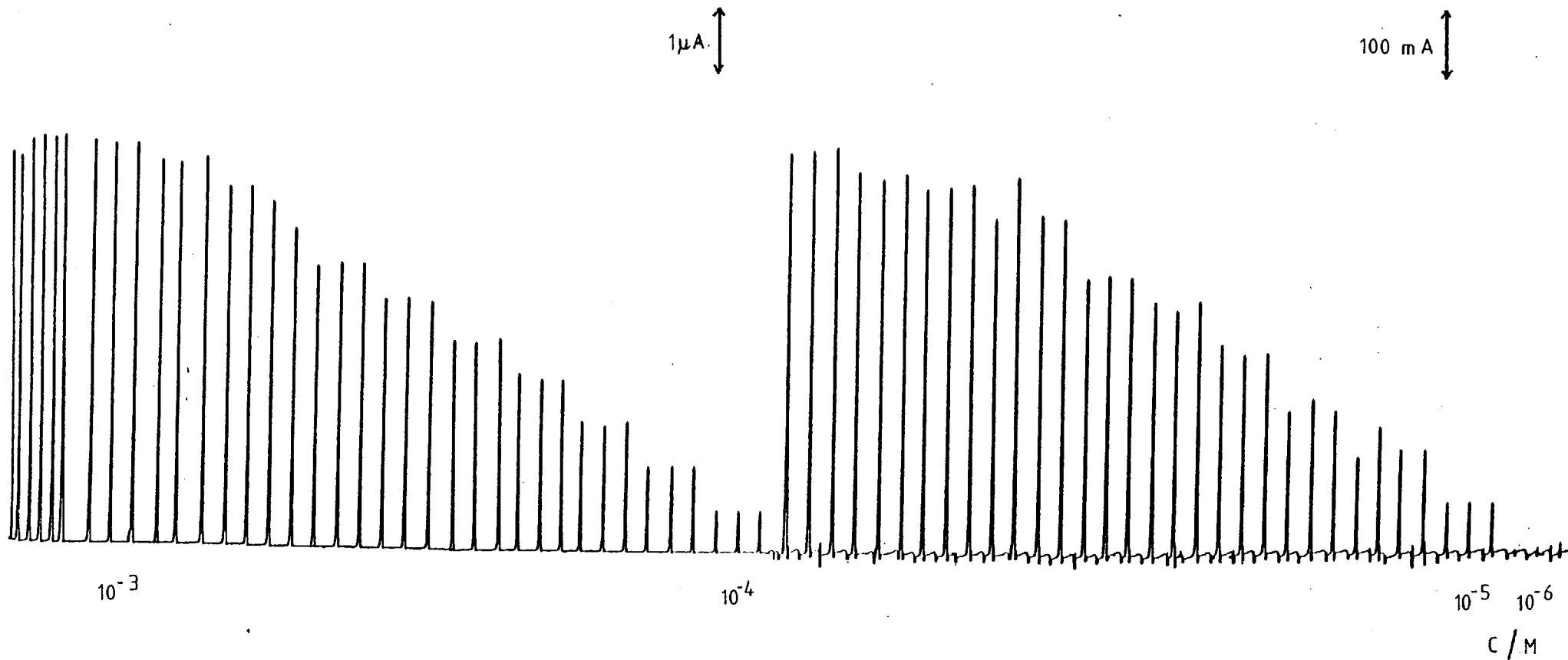


Fig. V.4 - Injection Calibration for Diuron.

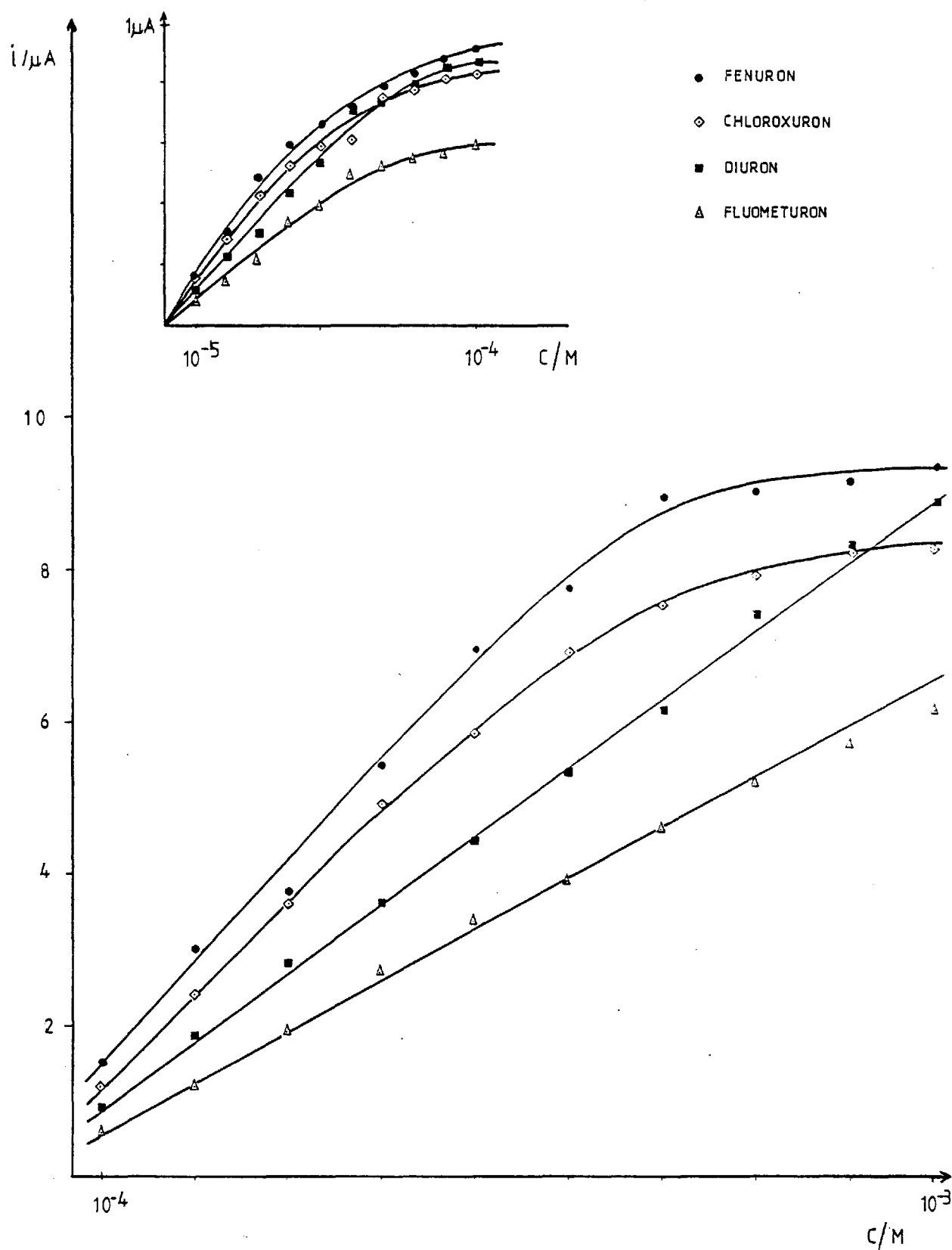


Fig. V. 5 - Flow Injection Analysis Calibration Plots.

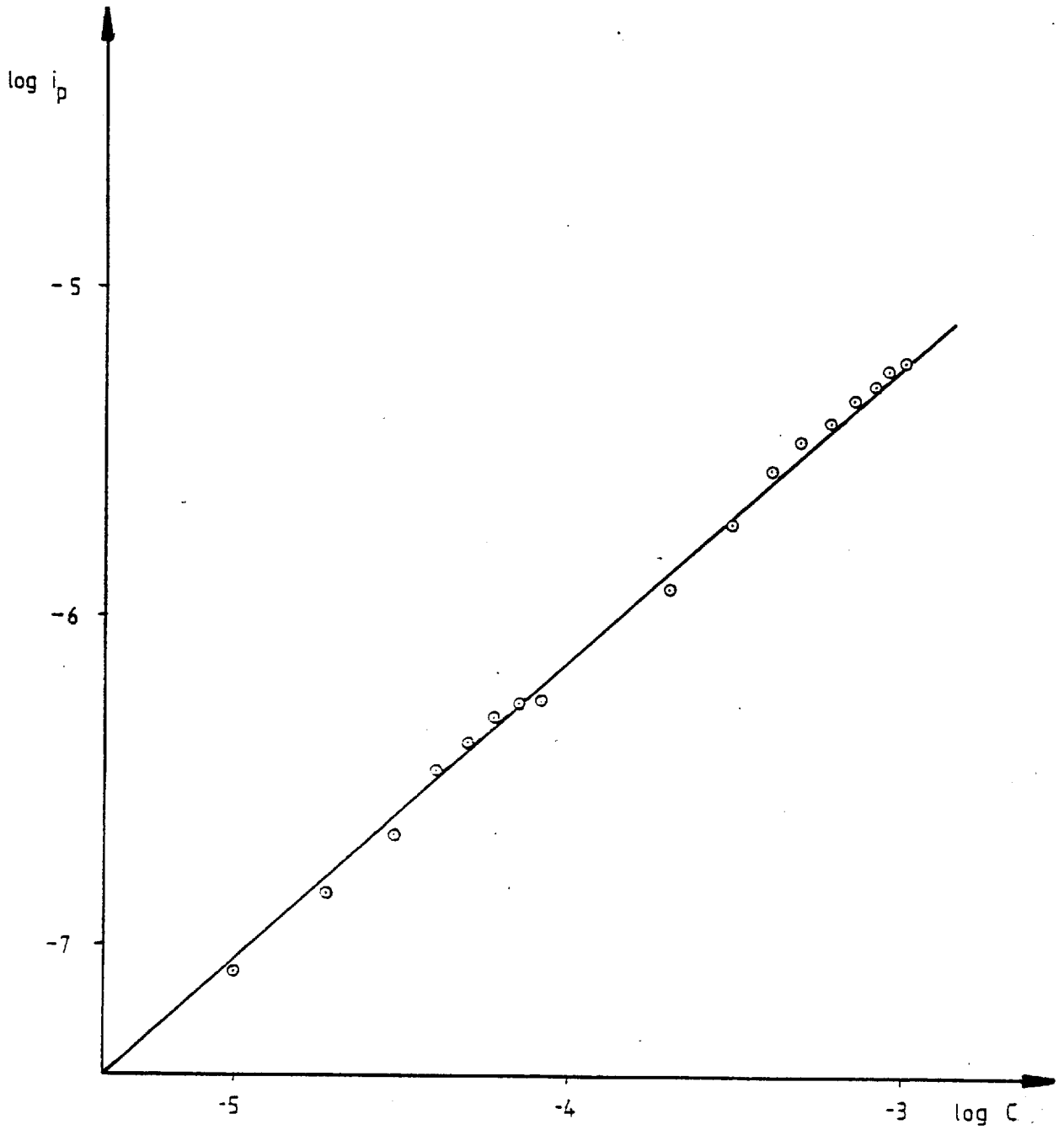


Fig. V.6 - Log-log Plot for Injection of Fluometuron.

As we want to detect very low concentrations, it is necessary to use a very precise valve and not a syringe: only using a valve could reproducible results be obtained. The stationary solution voltammograms give an indication of the oxidation potentials and the potential was set at + 1.4 V vs. Ag/AgCl to make sure all the compounds would be oxidised. The electrode was cleaned with 1 μ m alumina before each set of experiments. In Figs. V.3 and V.4 are shown the calibration injection curves for fluometuron and diuron. We have good response for injection of 20 μ l over the range 10^{-5} M to 10^{-3} M. Again the signal to noise ratio was too small to detect lower concentrations. The intercept is nearly zero showing that the current is directly proportional to concentration. The deviations in Fig. V.5 are due to electronic limitations; Fig. V.6. gives the log-log plot for fluometuron.

3. ELECTROANALYTICAL DETECTION AFTER CHROMATOGRAPHIC SEPARATION.

All these compounds are to an unknown extent pollutants. Some of the urea herbicides are recognized carcinogens and indicate a possible hazard. Flow injection analysis is a very quick method if we are looking for only one specific compound. When there are several compounds in solution that are all electroactive and with a similar structure we have to separate them first. The experimental apparatus for this is described in Chapter III, Section 2 and illustrated in Fig. III.6.

In the group of eleven ureas and carbamates we were looking at, it was possible to analyse quantitatively seven at a time, Fig. V.7. They have different times of elution and in less than 20 minutes we could detect all of them. As there were five all with the same elution

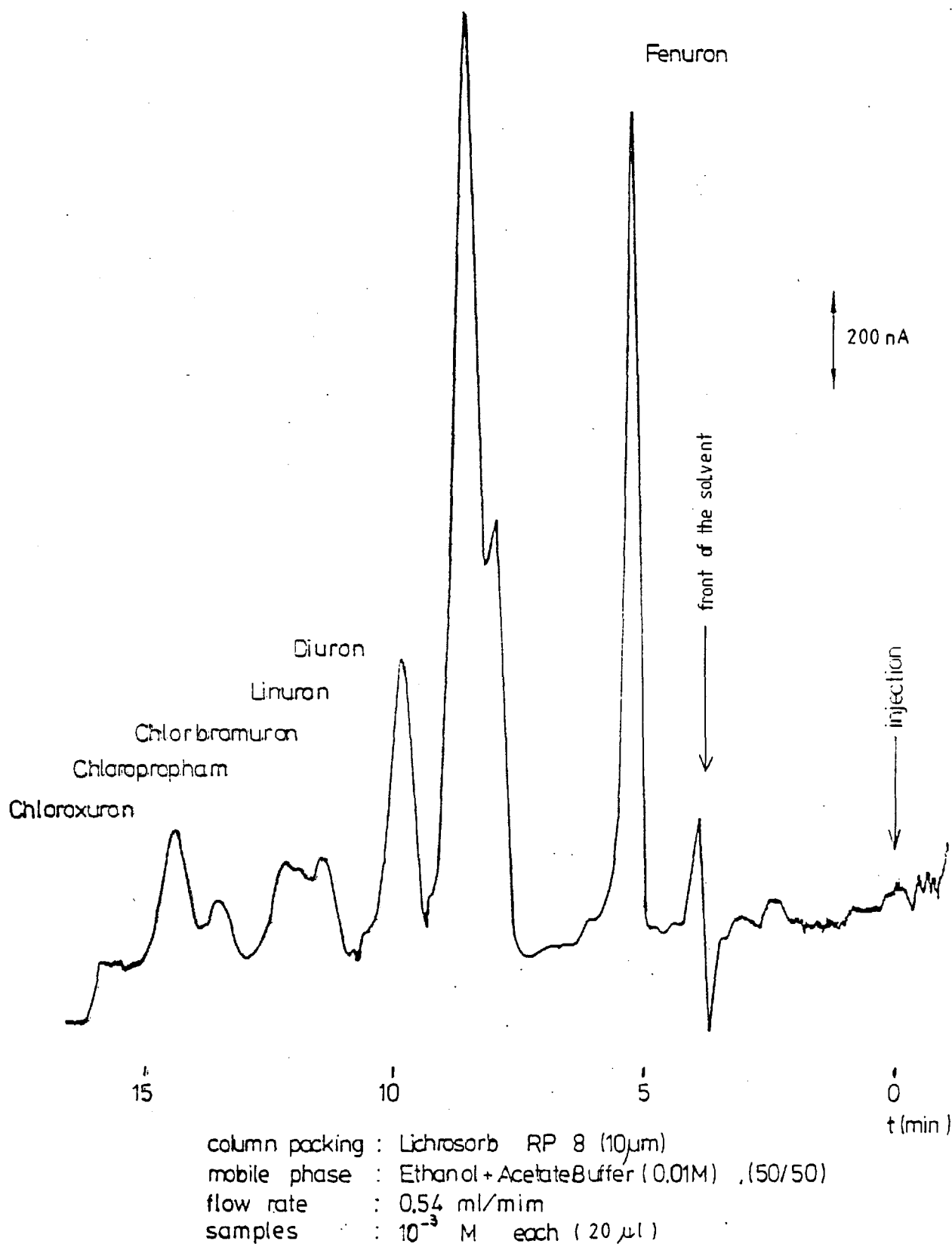


Fig. V.7 - Chromo-amperogram of the Mixture of Urea and Carbamate Herbicides.

time we decided to separate them for analysis into three groups according to the group attached to the C=O. They are one group of carbamates and two groups of different substituted ureas. Again, the potential was set at +1.4 V vs. Ag/AgCl and the electrode was cleaned with 1 μ m alumina before each set of experiments.

In Fig. V.8 and V.9 are the results obtained with the carbamates and there is good agreement between calibrations in the mixture and the compound by itself. In Figs. V.10-15 are the results for one of the urea groups and Figs. V.16-23 show the results for the other group. In table V.1 are listed the elution times, the slopes and the detection limits for all the compounds. The intercepts in all the calibration curves were nearly zero showing that the current is directly proportional to concentration. It was not possible to detect concentrations lower than 10^{-6} M because the signal to noise ratio was too small, Fig. V.24. Impurities in the compounds may cause the difference in slope between the calibrations of the compound by itself and in the mixture.

The peaks of the pair monolinuron and metabromuron interfered with each other as did linuron and chlorobromuron; they were deconvoluted before readings were taken. In the case of fluometuron, that eluted together with chlortoluron, calibration curves were done for two different mixtures, one containing fluometuron and the other not. The peak for fluometuron was determined by the difference between the two calibration curves.

We notice that the calibration curves have different slopes and as the area under the peak is proportional to the current we can work

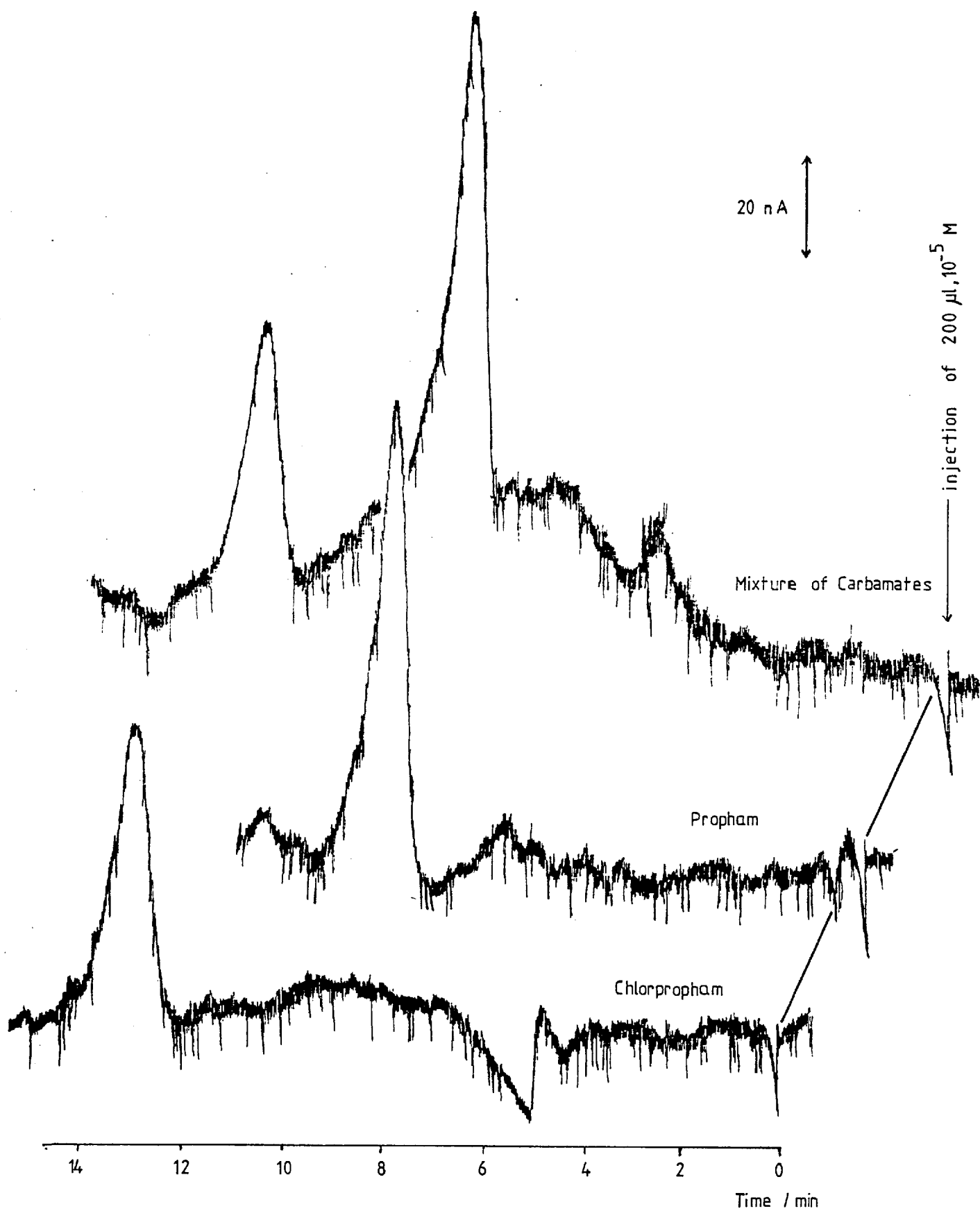


Fig. V.8 - Chromo-amperograms of the Carbamate Herbicides.

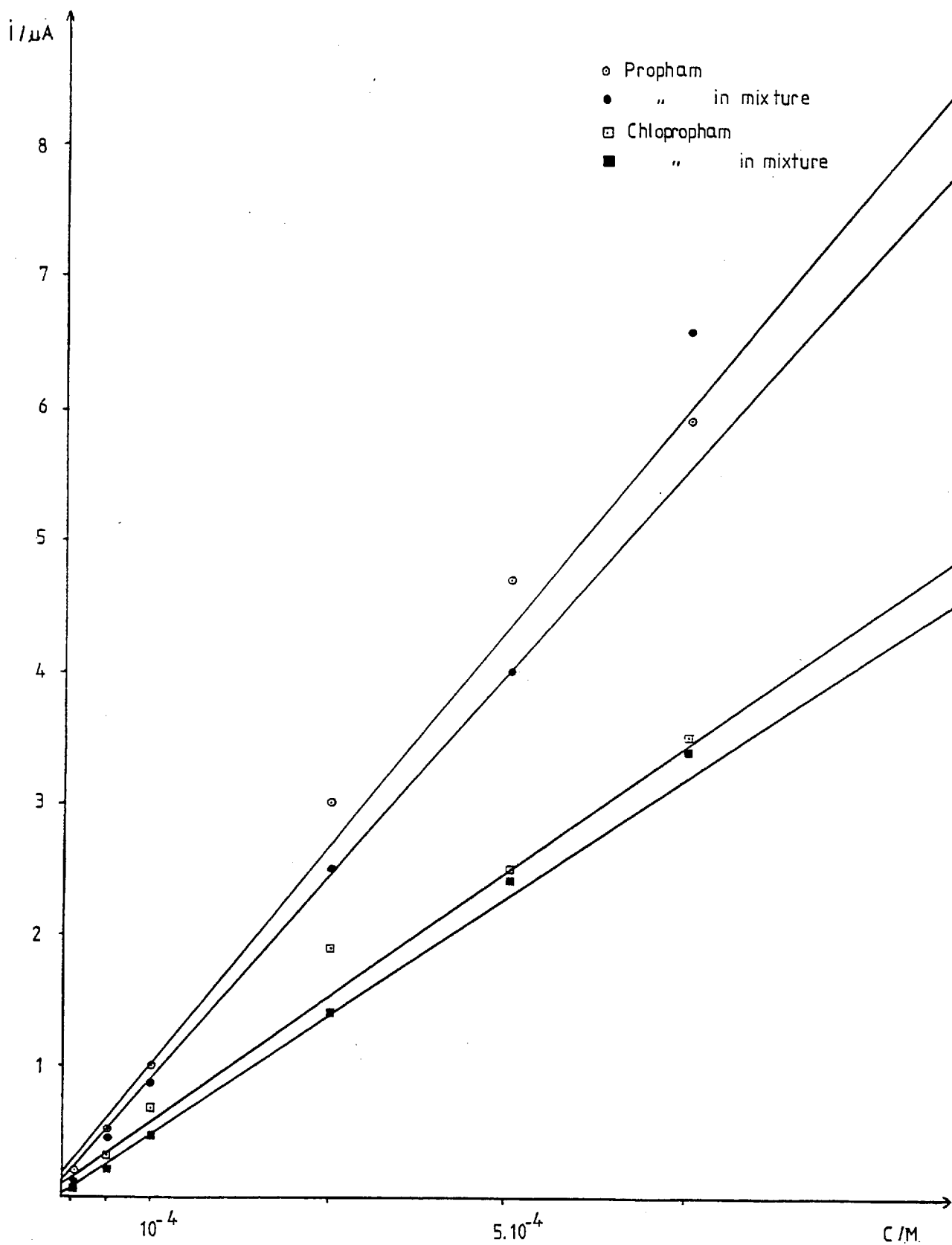


Fig. V.9 - Calibration Curves of Propnam and Chlorpropnam .

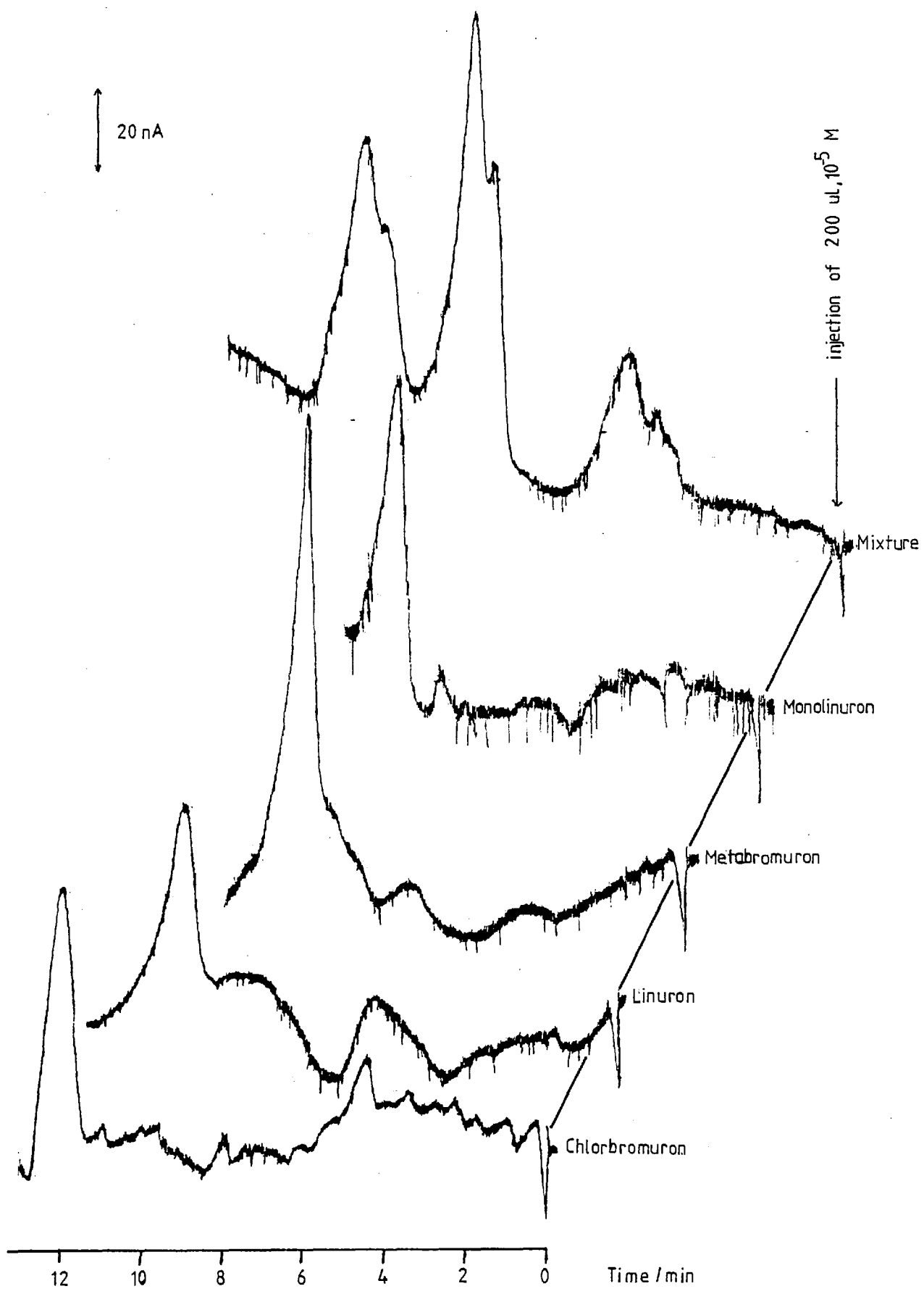


Fig. V.10 -- Chromo-amperegrams of Urea Herbicides Group I.

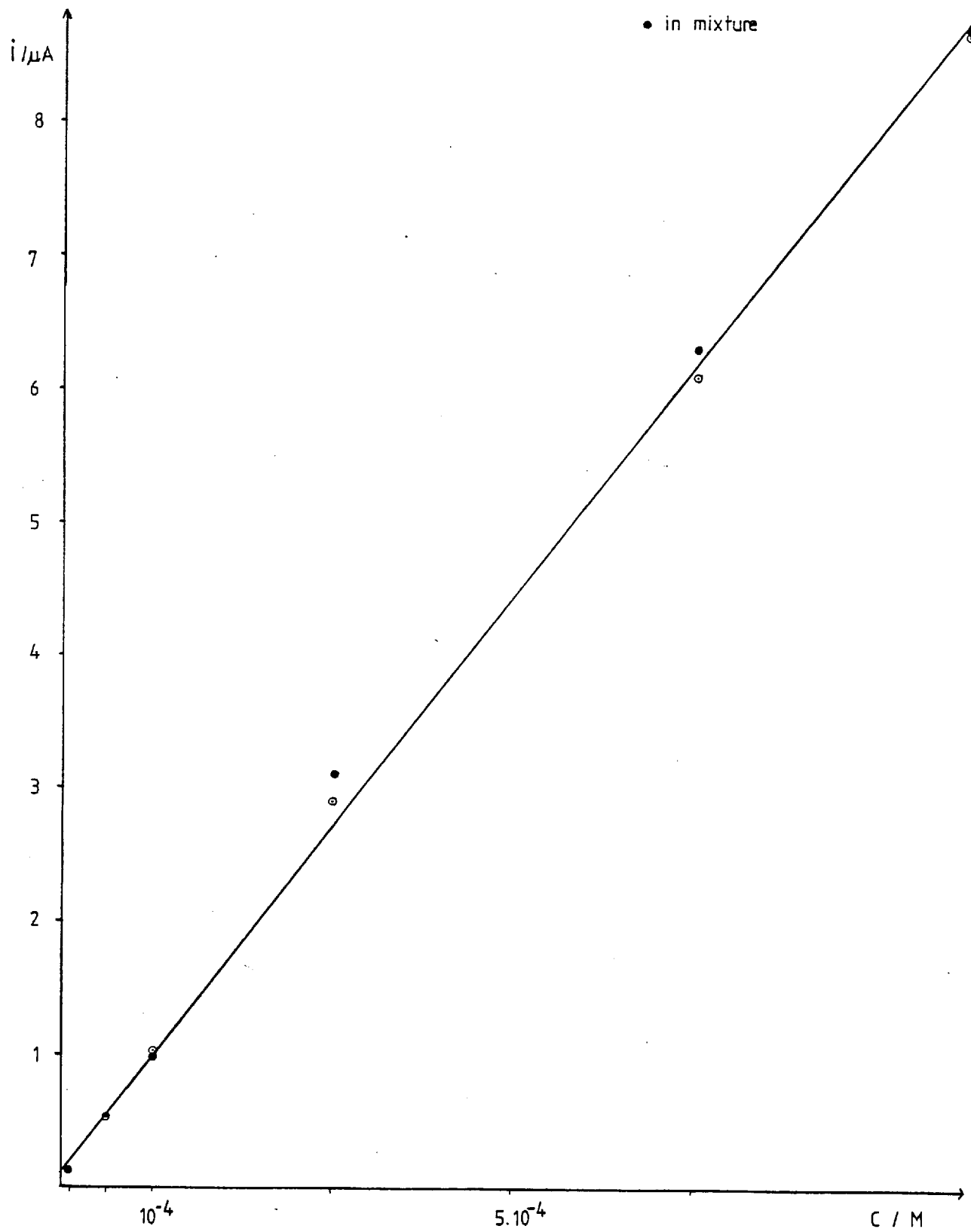


Fig. V.11 - Calibration Curve of Metabromuron.

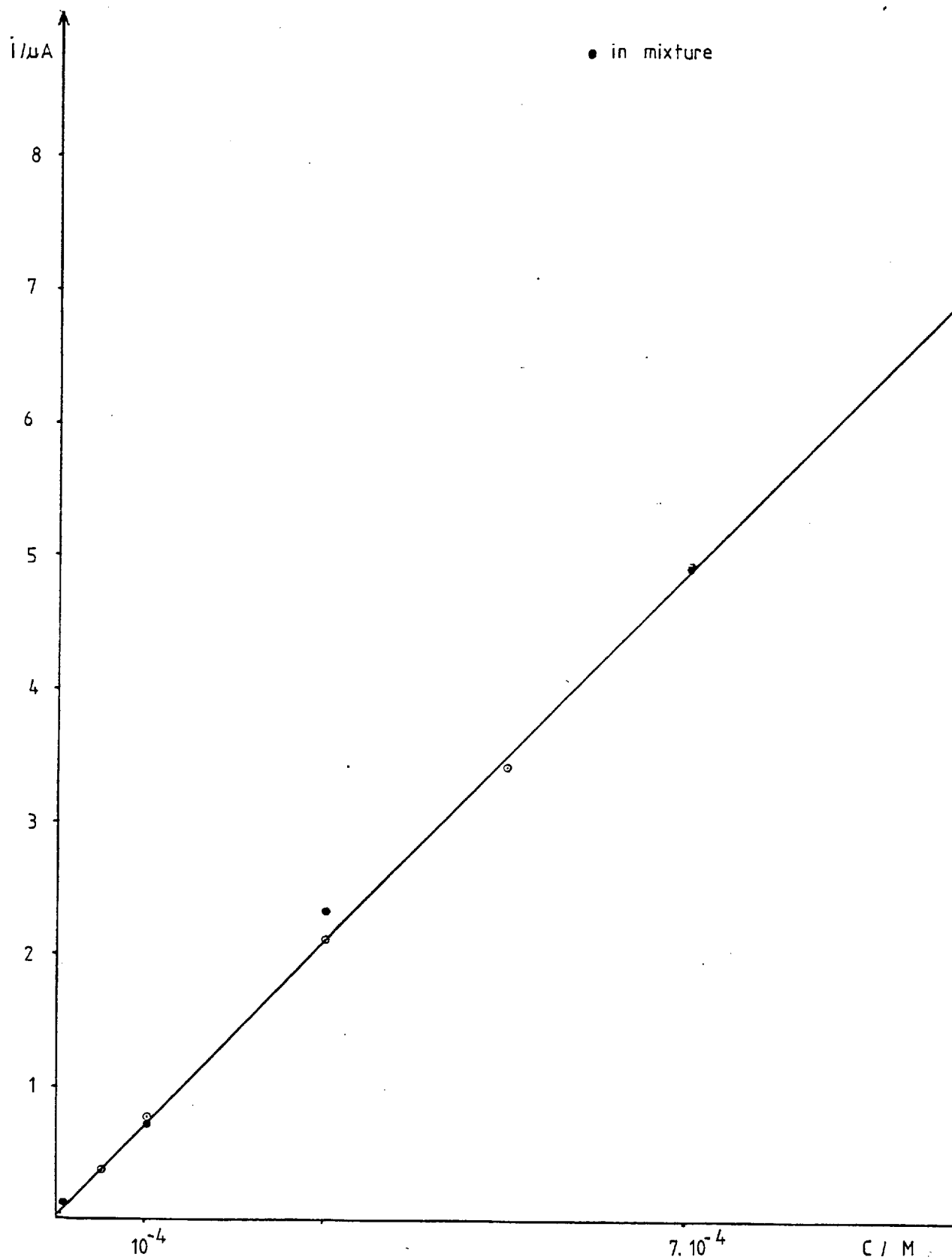


Fig. V.12 - Calibration Curve of Monolinuron.

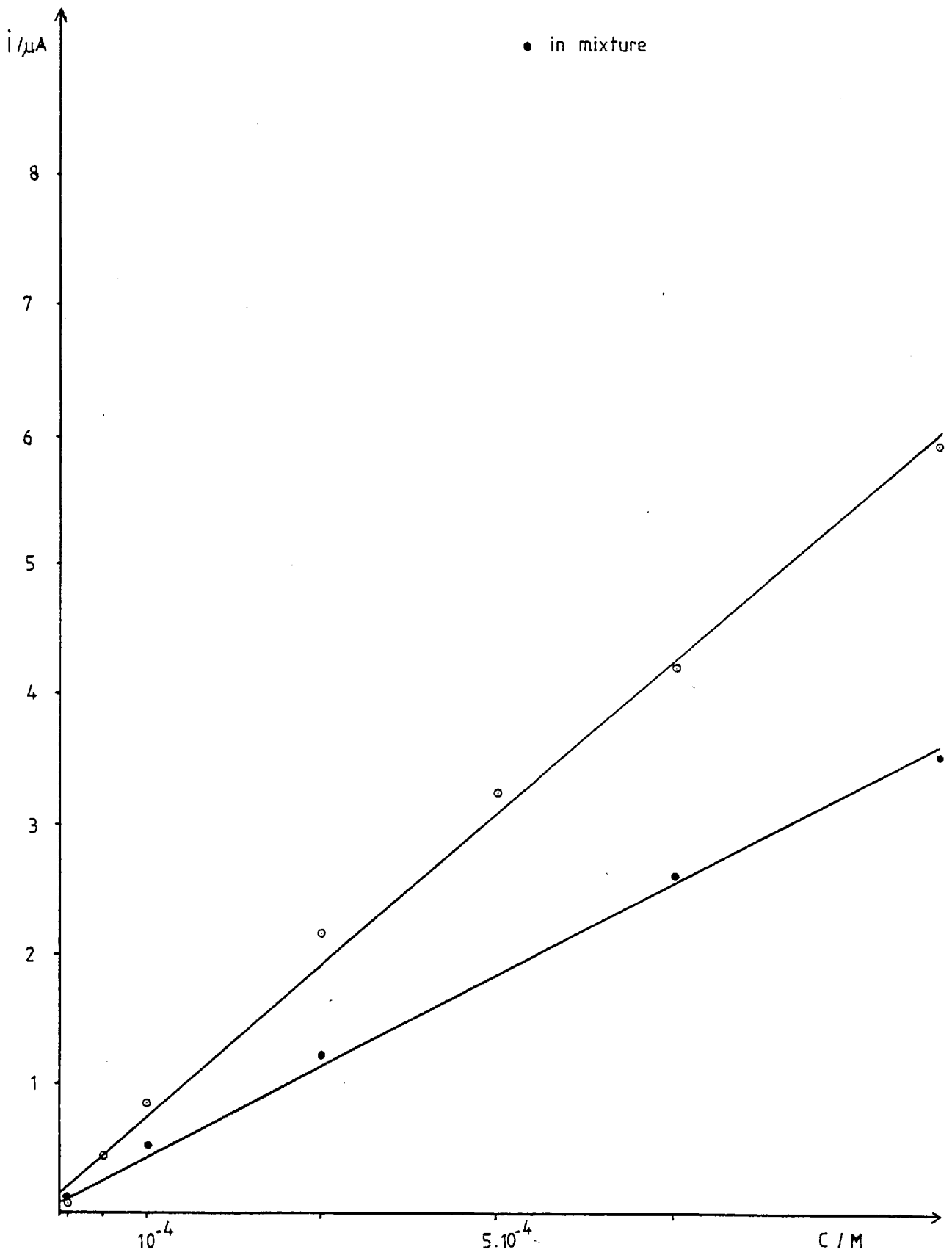


Fig. V.13 - Calibration Curve of Chlorbromuron.

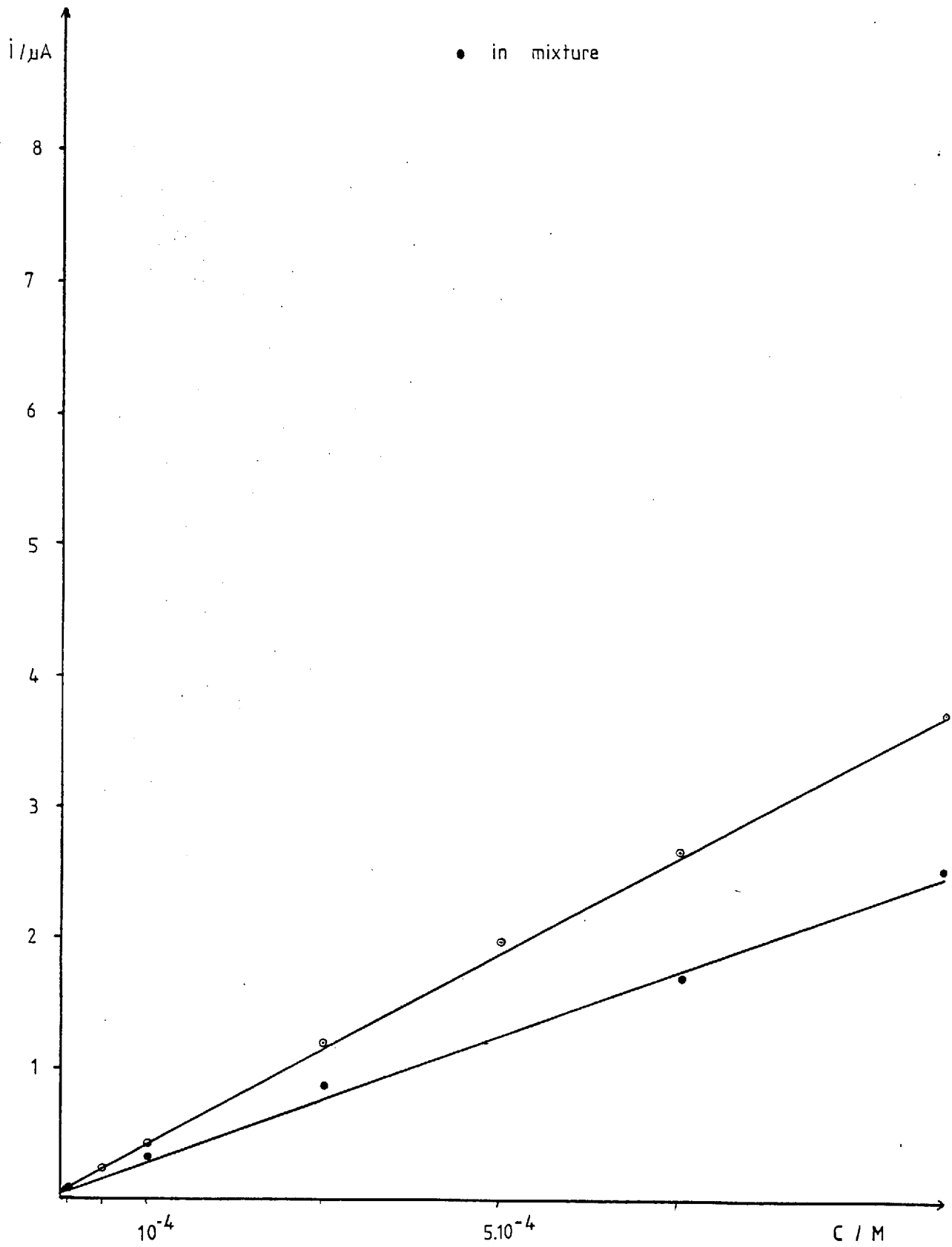


Fig. V.14 - Calibration Curve of Linuron.

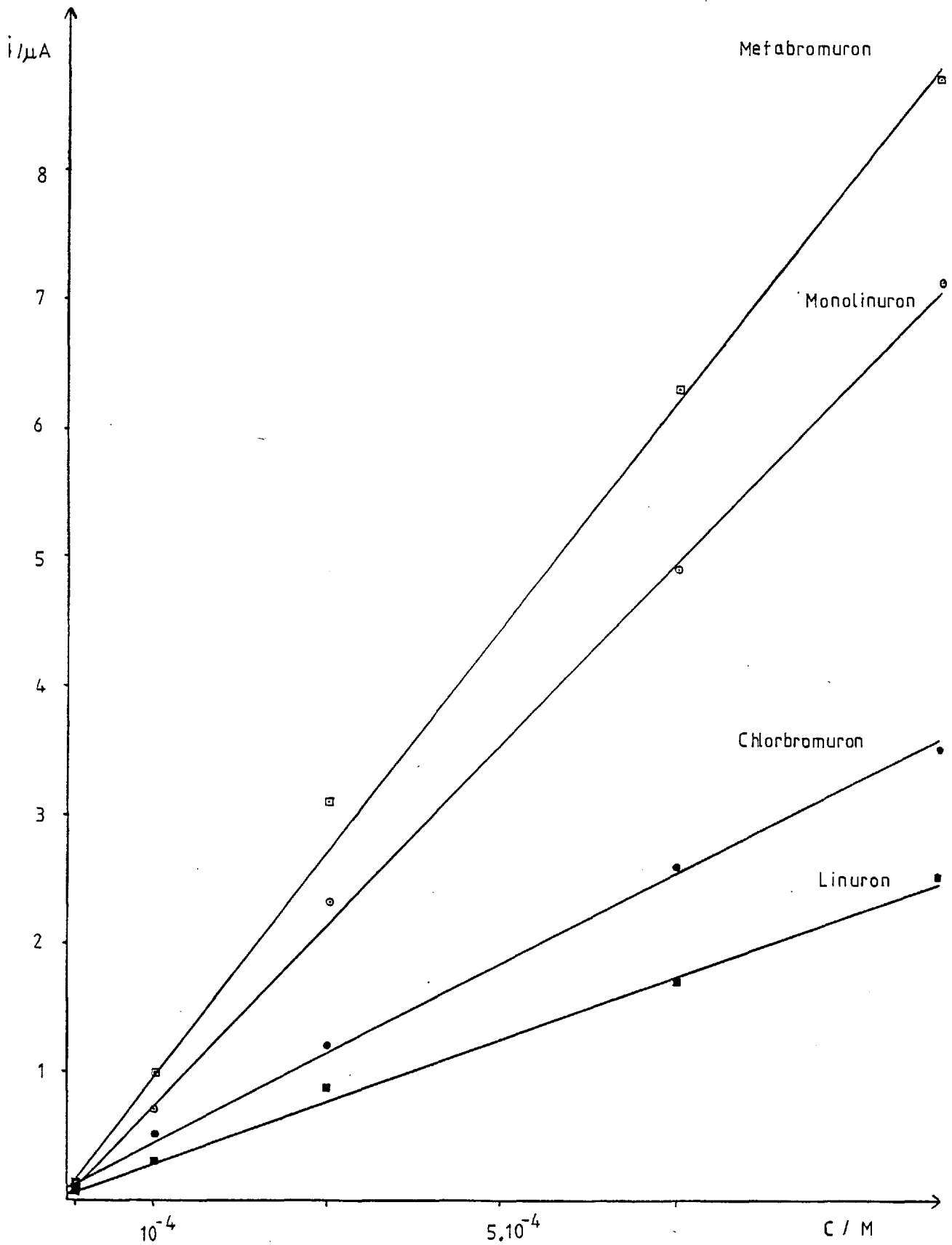


Fig. V. 15 - Calibration Curve of the mixture of Group I.

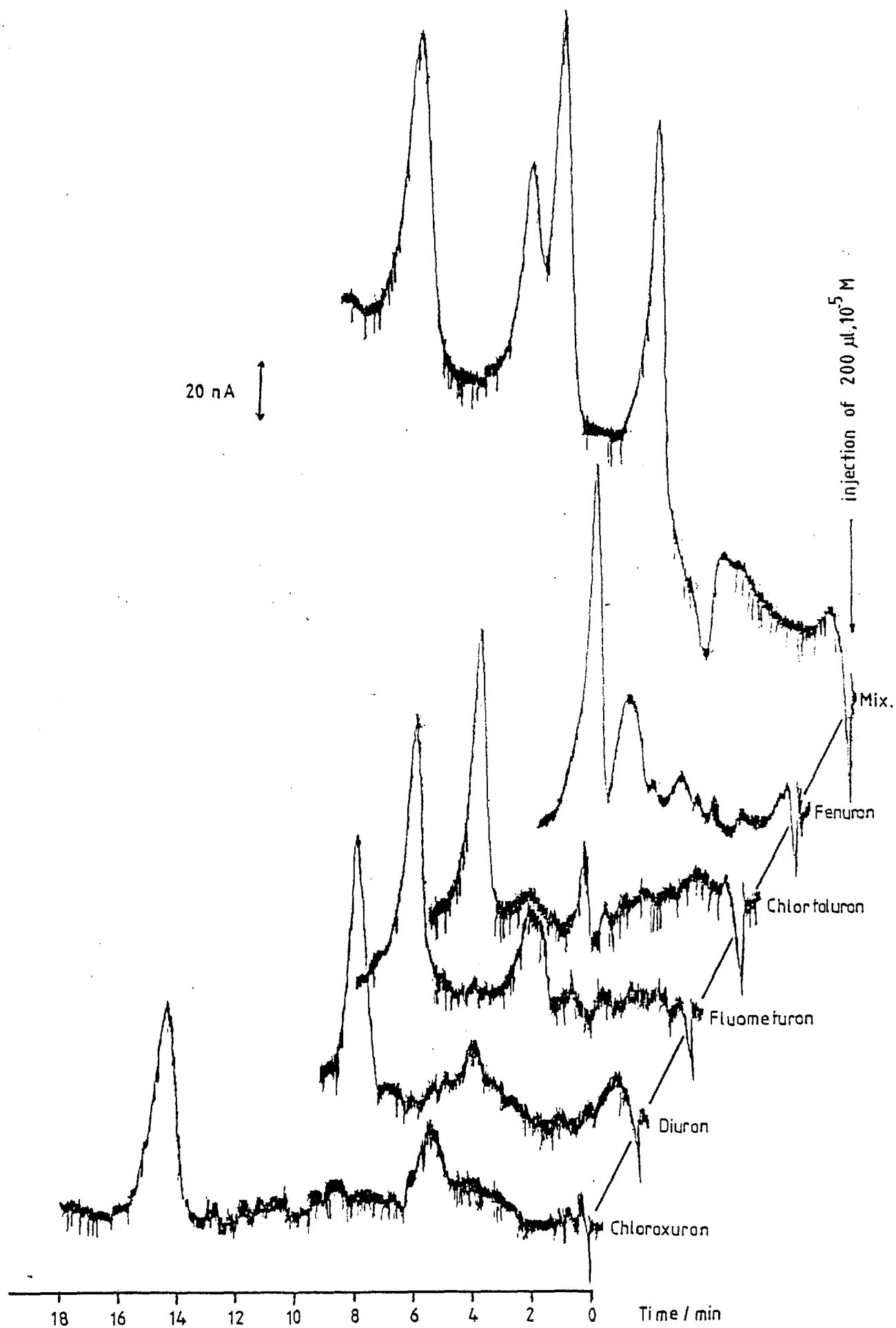


Fig. V. 16 - Chromo-amperograms of Urea Herbicides Group II

Mixture of urea herbicides:

Fenuron	328 ng
Chlortoluron	424 ng
Diuron	464 ng
Chloroxuron	580 ng

20 nA

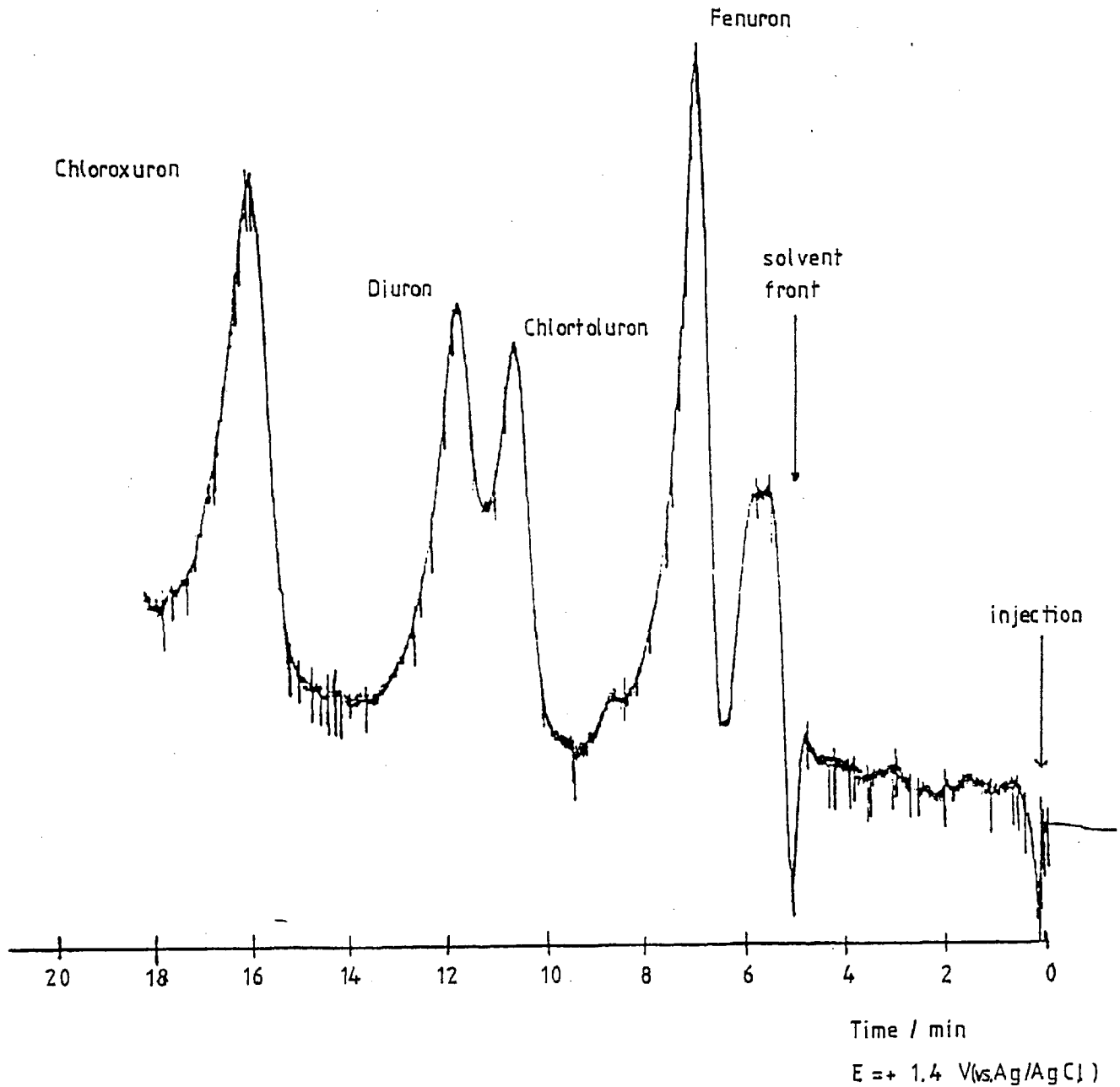


Fig. V.17 - Chromo-amperegrams of Urea Herbicides of Group II.

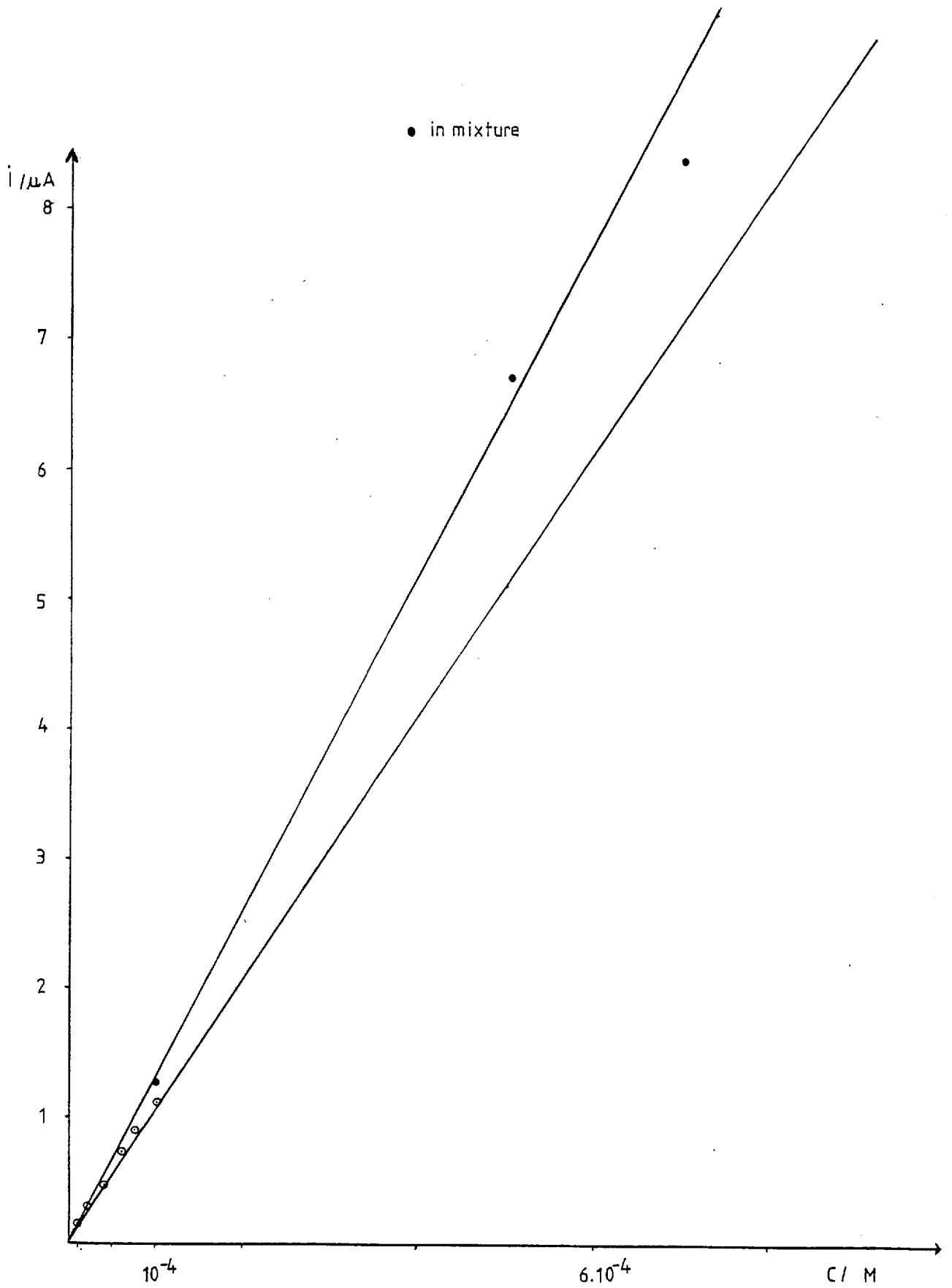


Fig. V.18 - Calibration Curve of Fenuron.

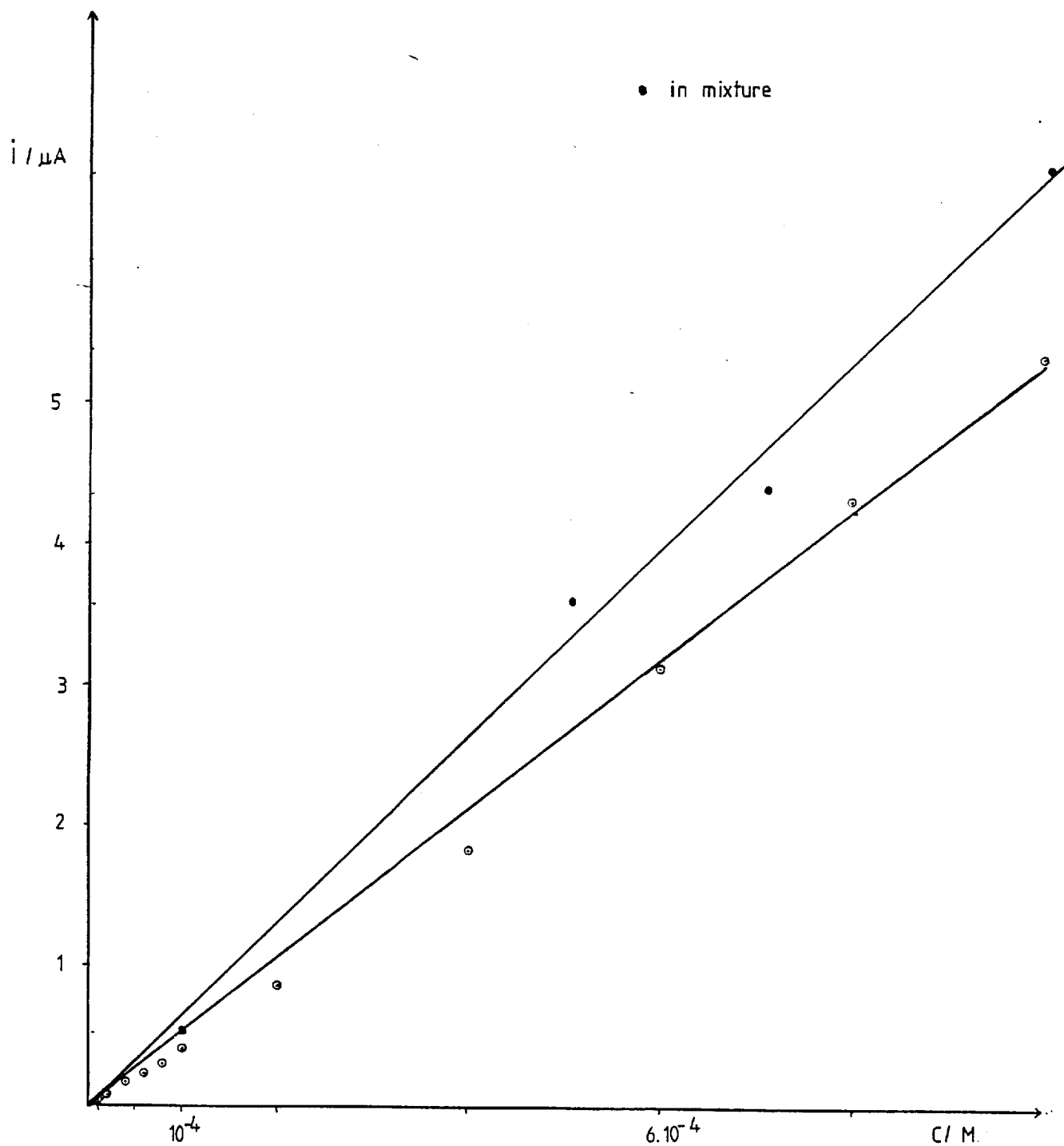


Fig. V. 19 - Calibration Curve of Fluometuron.

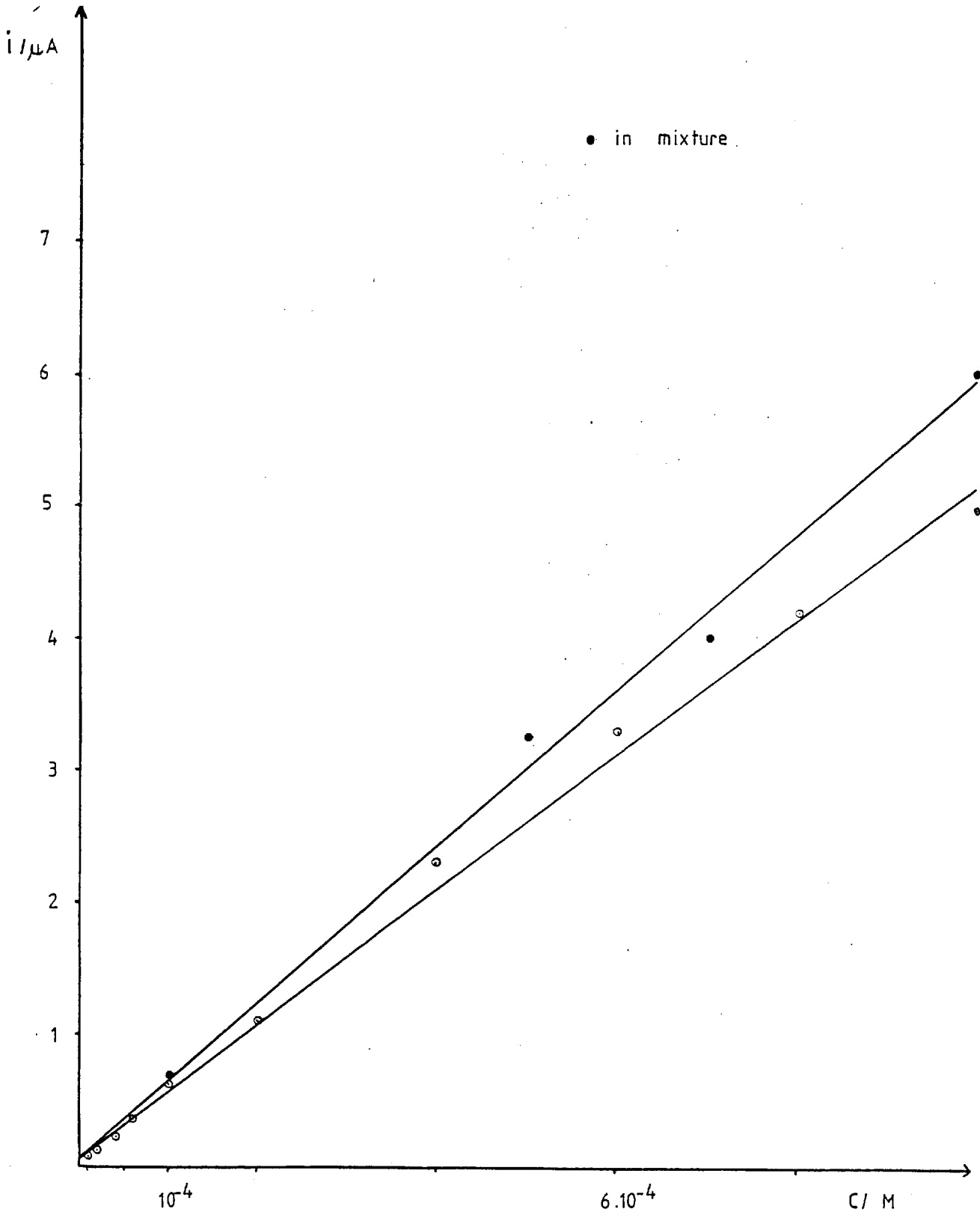


Fig. V. 20 Calibration Curve of Diuron.

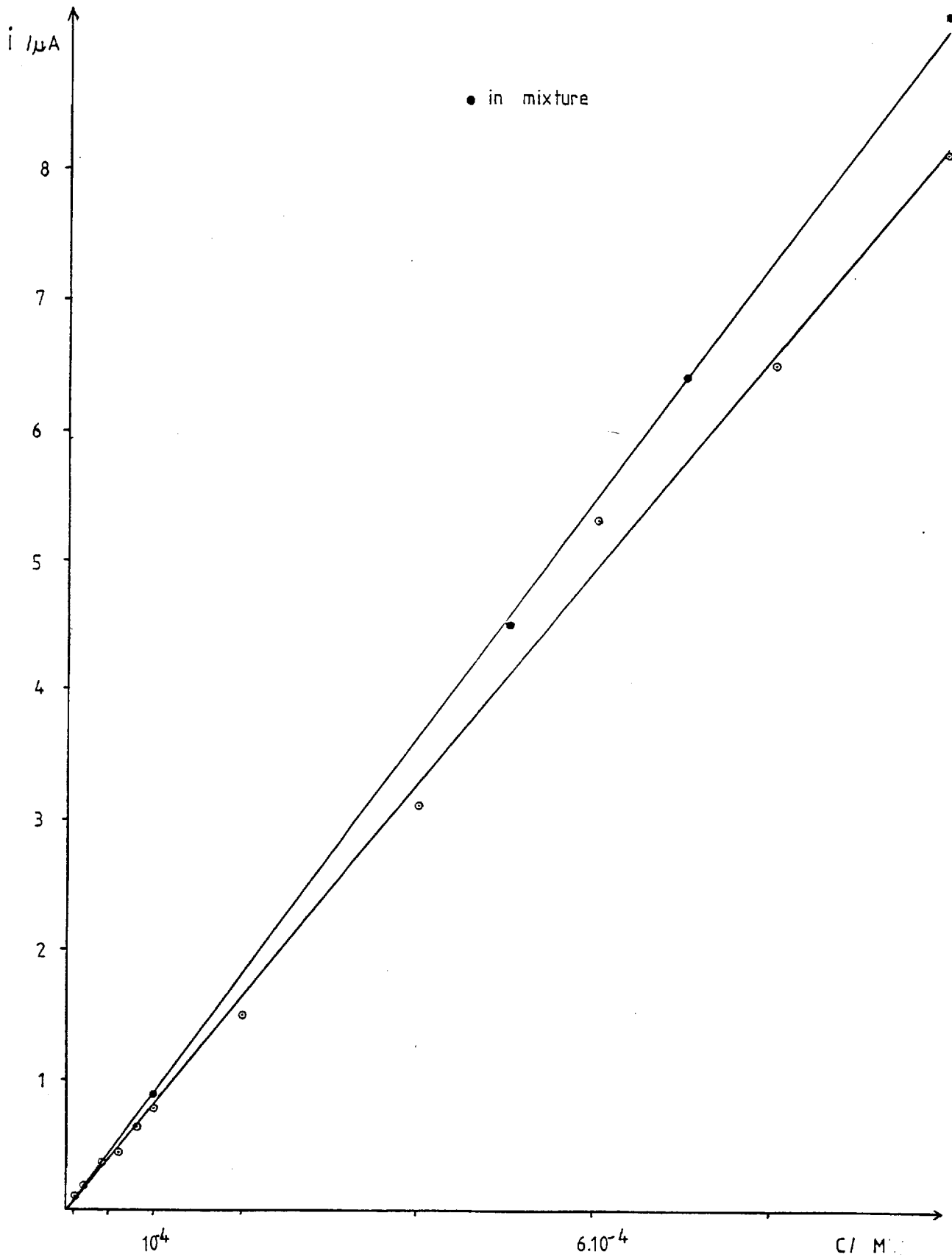


Fig. V.21 - Calibration Curve of Chloroxuron.

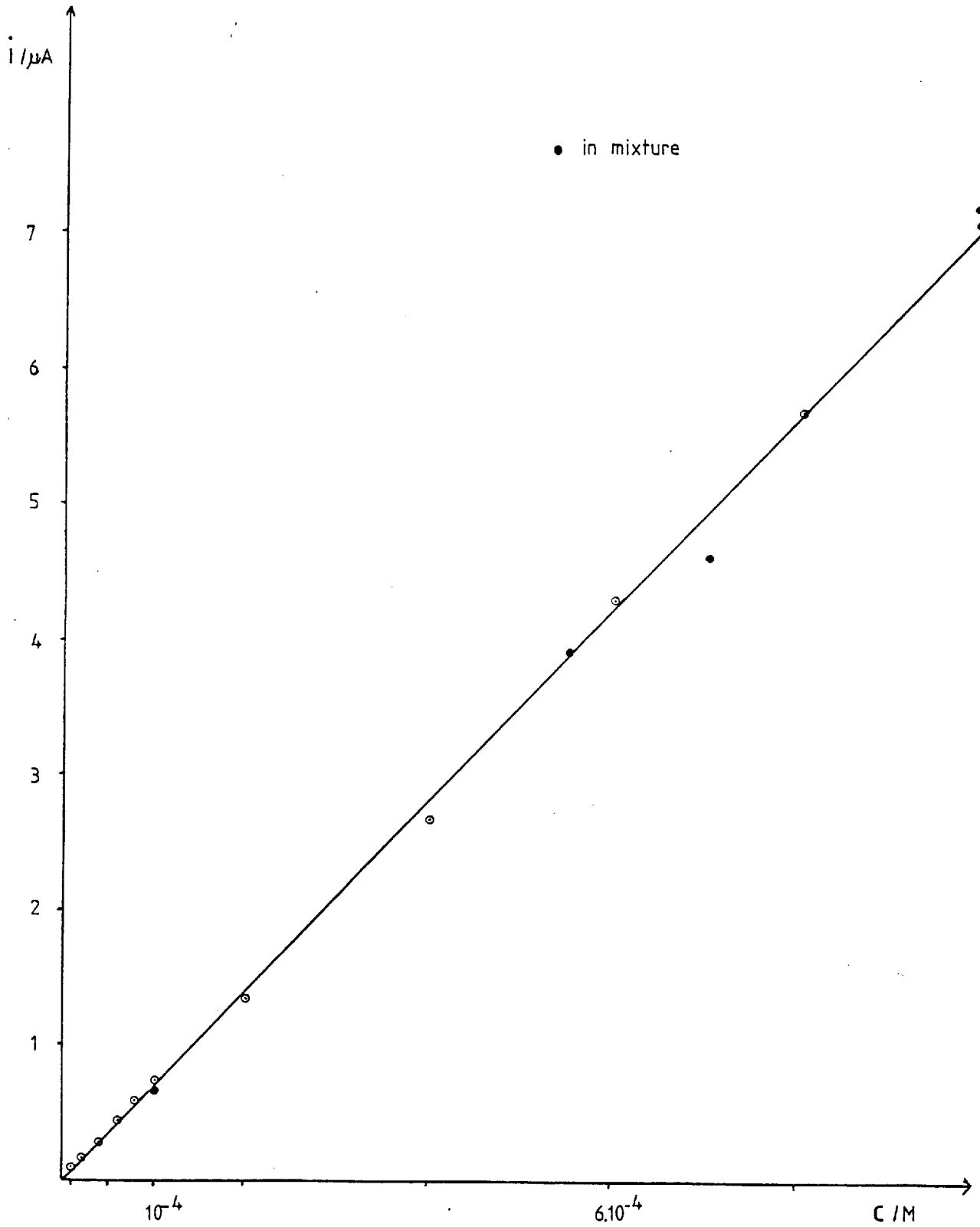


Fig. V.22 - Calibration Curve of Chlortoluron.

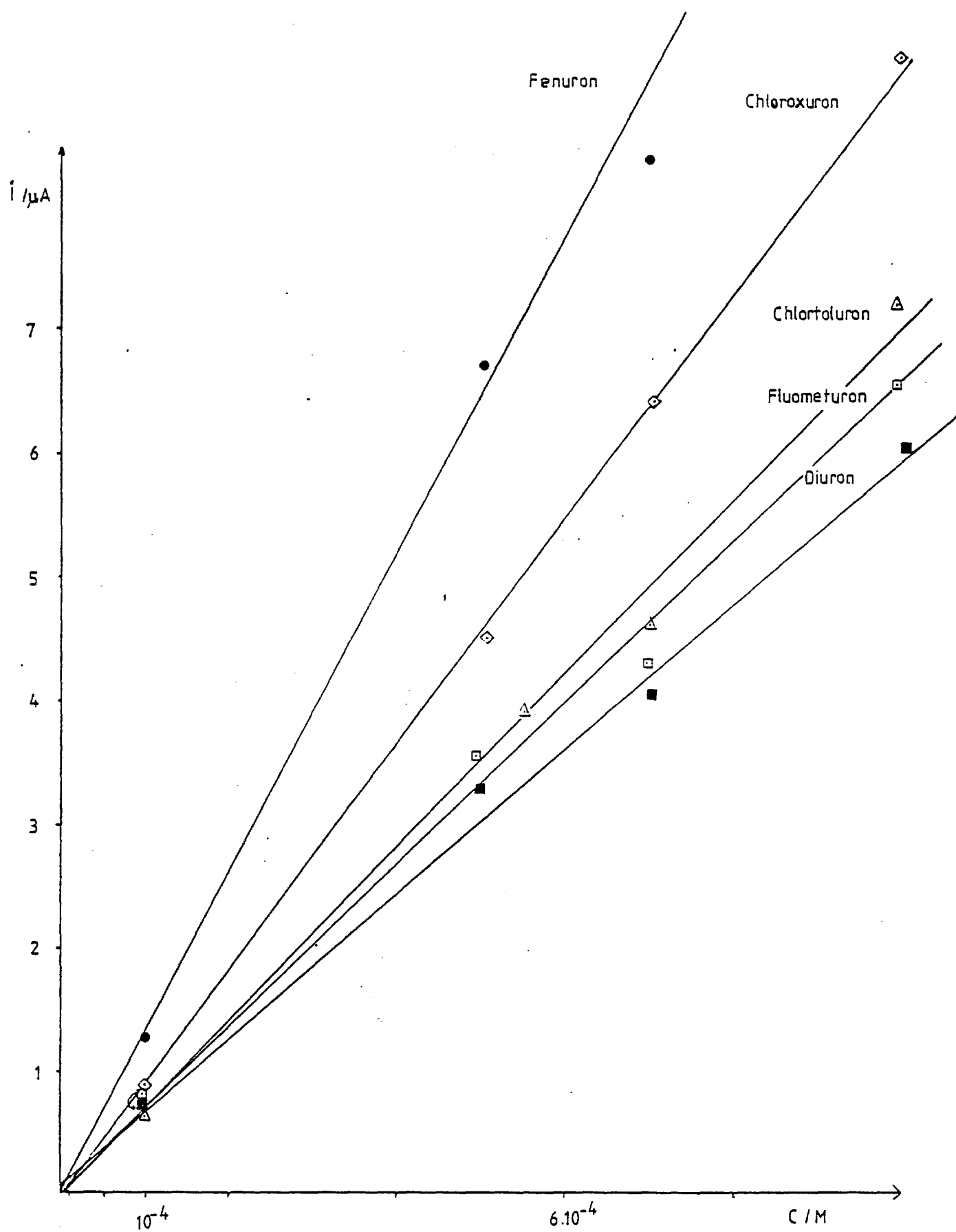


Fig. V.23 - Calibration Curve of the Mixture of Group II.

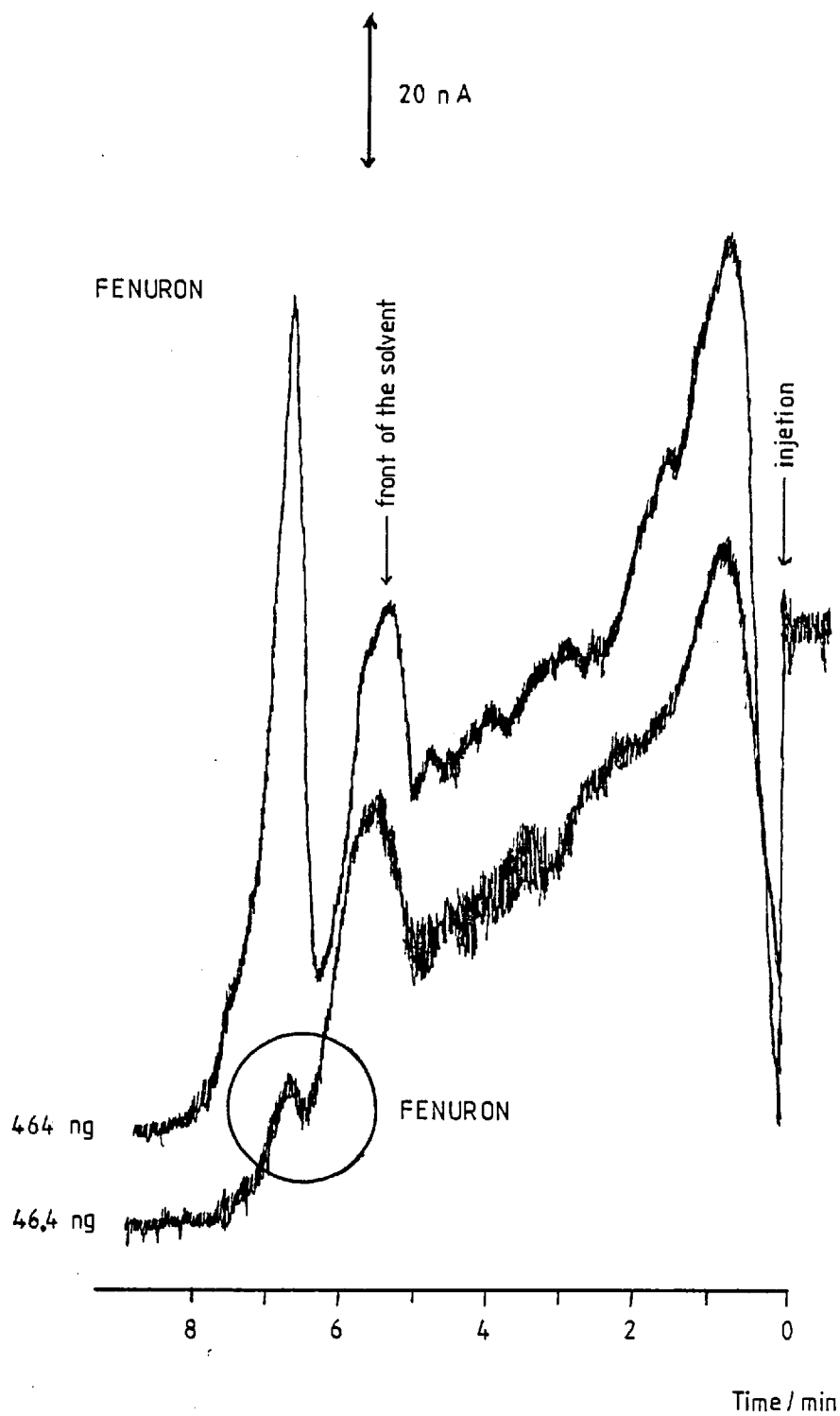


Fig. V.24 - Detection Limit Chromo-amperegram of Fenuron.

Table V.1. Results for the Electrochemical Estimation of the Herbicides.

Compound	Elution Time, min.	Slope, nA	Elution Time (in mixture) min.	Slope (in mixture) nA	Detection limit, ng	Fig. No.
Propham	9	82.6 \pm 2.7	10	76.7 \pm 2.8	35.8	V.9
Chlorpropham	12	47.2 \pm 1.8	14	44.5 \pm 1.6	42.9	V.9
Mololinuron	8.5	69.5 \pm 0.5	9	70.4 \pm 1.2	42.9	V.11
Metabromuron	9	85.6 \pm 1.2	9.5	86.4 \pm 2.8	54.8	V.12
Linuron	10.5	36.7 \pm 0.4	12	24.3 \pm 0.7	50.0	V.13
Chlorbromuron	12	57.9 \pm 1.7	13.5	34.4 \pm 1.0	58.9	V.14
Fenuron	6.5	101.6 \pm 3.4	7	135.4 \pm 0.5	32.8	V.18
Chlortoluron	8.5	70.9 \pm 0.6	10	70.9 \pm 0.4	42.5	V.19
Fluometuron	9.5	53.8 \pm 1.0	10	66.3 \pm 1.3	46.4	V.20
Diuron	11.5	50.8 \pm 0.9	12	58.7 \pm 0.2	46.6	V.21
Chloroxuron	14	82.3 \pm 1.4	16	92.0 \pm 0.6	58.1	V.22

out the number of electrons transferred assuming that the diffusion coefficient is the same for all the compounds.

Using the equation for the limiting current,

$$i_L = (1.60 k) n F C^0 D^{2/3} \nu^{-5/12} V_f^{3/4} a^{-1/2} r^{3/4}$$

and substitution the following experimental values

$$\nu^{-5/12} = 6.52 (\text{cm}^2 \text{ s}^{-1})^{-5/12}$$

$$D \approx 7 \times 10^{-6} \text{ cm}^2 \text{ s}^{-1} \text{ (90) and so}$$

$$D^{2/3} = 3.66 \times 10^{-4}$$

and for this specific glassy carbon electrode and wall jet cell,

$$a^{-1/2} = 5.13 \text{ cm}^{-1/2}$$

$$r^{3/4} = 0.356 \text{ cm}^{3/4}$$

$$V_f^{3/4} = 0.032 (\text{cm}^3 \text{ s}^{-1})^{3/4} \quad (V_f = 0.01 \text{ cm}^3 \text{ s}^{-1})$$

and as determined by Yamada and Matsuda

$$1.60 k = 1.38$$

the limiting current is

$$i_L = 18.3 C^0 \cdot n, \quad \text{where } C^0 \text{ is mol cm}^{-3} \quad (\text{V.1})$$

If all the solution reaches the electrode

$$\begin{aligned} i_L &= n F C^0 \cdot V_f \\ &= 96485 \cdot 0.01 \cdot n \cdot C^0 \\ &= 964.85 \cdot n \cdot C^0 \end{aligned}$$

but the value for the wall-jet cell is as in (V.1) so only $\sim 1.9\%$ reacts.

The area under the peak is proportional to the charge and we determine the experimental value of the ratio.

$$\frac{\text{area under the peak}}{\text{peak current}} = \text{Constant}$$

for each compound. Using the experimental result for a given concentration n was calculated.

For chloroxuron it was found $n = 1$ in good agreement with the result obtained before (Chapter IV). The same $n = 1$ was found for metabromuron, propham and chlorbromuron. For the others $n < 1$ which suggests that the compounds may be in the form of dimers.

The limit of detection is in the range of 30-50 nanograms: Fig. V.24 exemplifies this for Fenuron and Table V.1 give numerical values for all the compounds. No prior chemical treatment of the herbicide was necessary and as only 2% reacts at the electrode the method is only slightly destructive.

3. CONCLUSIONS

Electrochemical techniques prove to be very good for the detection of urea-type herbicides. It is a very quick and sensitive method. The main disadvantage is due to the fact that the column has to be cleaned with water: as a result it takes a long time for the flow system to equilibrate. The use of internal standards could

reduce the time of each experiment. The limit of detection is in the range 30-50 nanograms (injection of 200 μ l - 10^{-6} M) and it will be possible to detect lower concentrations with more sensitive electronics.

APPENDIX

In the steady state (34) the flux of material reacting at the electrode surface must equal the flux being transported through the diffusion layer and arriving on the outside of the double layer. Hence

$$j = k'C^0 \quad \text{for the electrode reaction} \quad (1)$$

and

$$j = D\left(\frac{\partial C}{\partial x}\right) = \frac{D}{x_D}(C^0 - C) \quad \text{for the transport}$$

Elimination of C gives

$$\frac{i}{j} = \frac{1}{k'C^0} + \frac{1}{DC^0/x_D} \quad (2)$$

Hence the flux is mainly determined by the smaller of the two terms in this equation. The relation between current and flux is

$$i = n F A j \quad (3)$$

where j is the flux ($\text{mol m}^{-2} \text{s}^{-1}$), A is the area of the electrode (m^2), F is the Faraday, n is the number of electrons per molecule reacting and i is the current.

When the flux is transport controlled

$$j_i = \frac{D C^0}{x_D}$$

substituting we obtain

$$\frac{i}{i_i} = \frac{1}{1 + k_D/k'}$$

where k' is the heterogeneous rate constant (m s^{-1}) and

$$k_D = \frac{D}{x_D}$$

expresses the fact that the rate constant for crossing the stagnant layer depends on D , and x_D , the thickness of the diffusion layer.

From equations (1), (3) and (IV.1)

$$\log i \propto E_p$$

REFERENCES

1. M.R. Rifi and F.H. Covitz,
Introduction to Organic Electrochemistry, Dekker, 1974.
2. S. Ross, M. Finkelstein and E. Rudd,
Anodic Oxidation, Academic Press, 1975.
3. M. Baizer,
Organic Electrochemistry, Dekker, 1973.
4. C. Mann and K. Barnes,
Electrochemical Reactions in Nonaqueous Systems, Dekker, 1970.
5. P.G. Desideri, D. Heimler and L. Lepri,
J. Electroanal. Chem., 1978, 87, 275-282.
6. M. Neptune and R.L. McCreery,
J. Med. Chem., 1978, 21, 362-368.
7. L.L. Miller, et al.,
J. Amer. Chem. Soc., 1976, 98, 8271-8272.
8. G. Matricali, M. Deing, J-F. Dufen and M. Guillon,
C.R. Acad. Sc. Paris, 1977, t-284, Série C, 301-304.
9. C.A. Chambers and J.Q. Chambers,
J. Amer. Chem. Soc., 1966, 88, 2922-2928.
10. H.K. Chan and A.G. Fogg,
Anal. Chim. Acta, 1979, 109, 341-349.
11. H.K. Chan and A.G. Fogg,
Anal. Chim. Acta, 1979, 105, 423-428.
12. J. Ballantine and A.D. Woolfson,
J. Pharm. and Pharmacol. Suppl., Brit. Pharm. Conf., 1978, Part 30, p. 46.
13. M.D. Hawley, S.V. Takwawady, S. Piekarski and R.N. Adams,
J. Amer. Chem. Soc., 1967, 89, 447-450.

14. W.J. Albery, T.W. Beck, W.N. Brooks and M. Fillenz,
J. Electroanal. Chem., in press.
15. V. Brabee and G. Dryhurst,
J. Electroanal. Chem., 1978, 91, 219-229.
16. V. Brabee and G. Dryhurst,
Studia Biophysica, Berlin, 1978, 67, 23-24.
17. J. Moiroux and P. Elving,
Anal. Chem., 1978, 50, 1056-1062.
18. T. Yao, T. Wasa and S. Musha,
Bull. Chem. Soc., Japan, 1977, 50, 2917-2920.
19. T. Yao, T. Wasa and S. Musha,
Bull. Chem. Soc., Japan, 1978, 51, 1235-1236.
20. T. Yao and S. Musha,
Bull. Chem. Soc., Japan, 1979, 52, 2307-2311.
21. W.F. Smith, ed.,
Polarography of Molecules of Biological Significance,
Academic Press, 1979.
22. S. Yamada and H. Sato,
Nature, 1962, 193, 261-262.
23. J.C. Lewis, B. Redfern and E.C. Cowland,
Solid State Electronics, 1963, 6, 251-254.
24. A. Trebest and W. Draber in
Advances in Pesticide Science, Pergamon, 1979.
25. J.C. Cowland and J.C. Lewis,
J. Mat. Sci., 1967, 2, 507-512.
26. A.A. Korobanov, V.S. Vilinskaya and R. Bueshtein,
Elektrokhimiya, 1978, 14, 101-107.
27. H.E. Zittel and E.J. Miller,
Anal. Chem., 1967, 37, 200-203.
28. R.N. Adams,
Electrochemistry of Solid Electrodes, Dekker, 1969.
29. D.T. Sawyer and J.L. Roberts Jr.,
Experimental Electrochemistry for Chemists, Wiley, 1974.
30. A.J. Bard, ed.,
Electroanalytical Chemistry: a Series of Advances,
Dekker, 1969, vol. 3.

31. Sh. Sh. Khidirov, T.I. Antonova and T.S. Shamina,
Elektrokhimiya, 1979, 15, 82-84.
32. N.L. Weinberg, ed.,
Techniques of Electroorganic Synthesis, Wiley, 1974, vol. 5.
33. W.J. Albery and M.L. Hitchman,
Ring-Disc Electrodes, Clarendon Press, Oxford, 1971.
34. W.J. Albery,
Electrode Kinetics, Clarendon Press, Oxford, 1975.
35. S. Valcher and M. Mastragostino,
Electrochim. Acta, 1972, 17, 107-117.
36. J. Ruzicka and E.H. Hansen,
Anal. Chim. Acta, 1975, 78, 145-157.
37. J. Ruzicka and J.W.B. Stewart,
Anal. Chim. Acta, 1975, 79, 79-91.
38. J.W.B. Stewart, J. Ruzicka, H.C. Fillio and E.A. Zagatto,
Anal. Chim. Acta, 1976, 81, 371-386.
39. J. Ruzicka, J.W.B. Stewart and E.A. Zagatto,
Anal. Chim. Acta, 1976, 81, 387-396.
40. J.W.B. Stewart and J. Ruzicka,
Anal. Chim. Acta, 1976, 82, 137-144.
41. J. Ruzicka and E.H. Hansen,
Anal. Chim. Acta, 1976, 87, 353-363.
42. J. Ruzicka, E.H. Hansen and E.A. Zagatto,
Anal. Chim. Acta, 1977, 88, 1-16.
43. E.H. Hansen, J. Ruzicka and B. Rietz,
Anal. Chim. Acta, 1977, 89, 241-254.
44. J. Ruzicka, E.H. Hansen and H. Mosback,
Anal. Chim. Acta, 1977, 92, 235-249.
45. J. Ruzicka and E.H. Hansen,
Anal. Chim. Acta, 1979, 106, 207-224.
46. G. Nagy, Zs. Feher and E. Pungor,
Anal. Chim. Acta, 1970, 52, 47-54.
47. D. Betteridge,
Anal. Chem., 1978, 50, 832A-841A.
48. M. Varadi, J. Balla and E. Pungor,
Pure Appl. Chem., 1979, 51, 1177-1182.
49. E. Pungor, K. Toth, Zs. Feher, G. Nagy and M. Varadi,
Anal. Lett., 1975, 8, ix-xxiii.

50. B. Fleet and C.J. Little,
J. Chromatogr. Sci., 1974, 12, 747-752.
51. P.T. Kissinger, P.J. Refschange, C. Dreiling and R.N. Adams,
Anal. Lett., 1973, 6, 465-477.
52. R.E. Skoup and P.T. Kissinger,
Chemical Instrumentation, 1976, 7, 171-177.
53. J. Laukelma and H. Poppe,
J. Chromatogr., 1976, 125, 375-388.
54. K. Brunt, and C.H.P. Bruins,
J. Chromatogr., 1978, 161, 310-314.
55. C. Bollet, P. Oliva and M. Caude,
J. Chromatogr., 1977, 149, 625-644.
56. D.G. Swartzfager,
Anal. Chem., 1976, 48, 2189-2192.
57. R.M. Wightman, E.C. Paik, S. Borman and M.A. Dayton,
Anal. Chem., 1978, 50, 1411-1414.
58. J. Takata and K. Fujita,
J. Chromatogr., 1975, 108, 255-263.
59. C.L. Blank,
J. Chromatogr., 1976, 117, 35-46.
60. K. Stulik and V. Hora,
J. Electroanal. Chem., 1976, 70, 253-263.
61. K. Stulik and V. Pakakova,
Chem. Listy, 1979, 73, 395-820.
62. L. Michel and A. Zatka,
Anal. Chim. Acta, 1979, 105, 109-117.
63. J. Yamada and H. Matsuda,
J. Electroanal. Chem., 1973, 44, 189-198.
64. P.T. Kissinger, et al.,
Clin. Chem., 1977, 23, 1449-1445.
65. P.M. Plotsky, D.M. Gibbs, and J.D. Neill,
Endocrinology, 1978, 102, 1887-1894.
66. H. Hallman, et al.,
Life Sci., 1975, 23, 1049-1052.

67. P. Hjendahl, M. Daleskog and T. Kahan,
Life Sci., 1977, 25, 131-138.
68. M.J. Cooper, R-O'Dea and B. Mirkin,
J. Chromatogr., 1979, 162, 601-604.
69. C. Hansson, et al.,
J. Chromatogr., 1979, 162, 7-22.
70. H. Hashimoto and Y. Maruyama,
J. Chromatogr., 1978, 152, 387-393.
71. S. Sasa and C.L. Blank,
Anal. Chim. Acta, 1979, 104, 29-45.
72. C. Hansson and E. Rosengren,
Anal. Lett., 1978, B11, 901-912,
73. R.J. Fenn, S. Siggia and D.J. Curran,
Anal. Chem., 1978, 50, 1067-1073.
74. Sou-Yie Chu,
J. Pharm. Sci., 1978, 68, 1623-1625.
75. M.S. Greenberg and W.J. Mayer,
J. Chromatogr., 1979, 169, 321-327.
76. E.C. Lewis and D.C. Johnson,
Chin. Chem., 1978, 24, 1711-1719.
77. D.A. Richards,
J. Chromatogr., 1979, 175, 293-299.
78. I. Mefford and R.N. Adams,
Life Sci., 1978, 23, 1167-1174.
79. J.W. Munson, R. Weierstall and H.B. Kostenbauder,
J. Chromatogr. 1978, 145, 328-331.
80. R.E. Skoup and P.T. Kissinger,
Biochem. Med., 1975, 14, 317-323.
81. D.N. Armentrout, J. McLean and M.W. Long,
Anal. Chem., 1979, 51, 1039-1049.
82. E.M. Lores, D.W. Bristol and R.F. Moseman,
J. Chromatogr. Sci., 1978, 16, 358-362.
83. J.H. Knox, ed.,
High Performance Liquid Chromatography, Edinburgh University Press, 1978.
84. C.F. Simpson, ed.,
Practical High Performance Liquid Chromatography, Heyden, 1976.

85. J.N. Done, J.H. Knox and J. Loheac,
Applications of High-Speed Liquid Chromatography, Wiley, 1974.
86. M.B. Glauert,
J. Fluid Mech., 1956, 1, 625-643.
87. W.J. Albery and C.M.A. Brett,
Unpublished work.
88. C.M.A. Brett,
Personal communication.
89. Y. Osteryoung and K. Hasebe,
Review of Polarography (Japan), 1976, 22, 1-25.
90. R.C. Weast, ed.,
Handbook of Chemistry and Physics, CRC Press, 1978-79, 59th edition.